DEVELOPMENT OF A HYBRID ION EXCHANGE-CATALYST SYSTEM TO DENITRIFY ION EXCHANGE WASTE BRINE

BY

ALLISON MACKENZIE BERGQUIST

DISSERTATION

Submitted in partial fulfillment of the requirements
for the degree of Doctor of Philosophy in Environmental Engineering in Civil Engineering
in the Graduate College of the
University of Illinois at Urbana-Champaign, 2016

Urbana, Illinois

Doctoral Committee:

Professor Charles J. Werth, Chair
Professor Timothy J. Strathmann, Co-Chair
Assistant Professor Jeremy S. Guest
Professor Desmond Lawler, University of Texas-Austin
Mr. Gary Gildert, Johnson Matthey Inc.

ABSTRACT

Nitrate is the most common groundwater contaminant in the United States and is regulated in drinking water by the EPA due to its harmful health impacts. Ion exchange (IX) is frequently used to treat nitrate and is very effective, but suffers from inefficiencies associated with the regeneration process. When the IX resin is saturated, it requires regeneration, which is accomplished through back-washing with a high-salt brine, which treatment plants use only one time prior to disposal. The cost of salt to make fresh brine and disposal requirements of waste brine are expensive processes for the water treatment plant. Additionally, this process merely transfers the nitrate to another phase (from resin to brine) rather than destroying it, leading to significant environmental impacts of the brine disposal process. Recently, a hybrid system that incorporates catalytic denitrification of IX waste brine has been shown to be technically feasible. Using a bimetallic palladium-indium on activated carbon catalyst, nitrate in waste brine can be selectively reduced to inert dinitrogen gas. This technology has the potential to significantly reduce the cost and environmental burden of the convention IX process for nitrate treatment.

In order to improve the hybrid-IX system, the following research objectives were pursued: (1) Using an experimental and modeling approach, determine whether the accumulation of bicarbonate and sulfate in reused waste brine will negatively impact the hybrid system performance and model key IX system variables using a case-study approach, (2) Evaluate reactor performance in continuously stirred and fixed bed reactors; and optimize a fixed bed reactor to reduce hydrogen mass transfer limitations to the catalyst surface, and (3) Evaluate selectivity of Pd-In/AC catalyst using different reactor types and matrix conditions.

A model of the IX-catalyst system was developed, calibrated and validated using experimental data. Results from modeling simulations show that concentrations of non-target

ions like sulfate and bicarbonate will buildup in waste brines over repeated cycles of reuse, but this buildup will not negatively impact IX performance or lead to permanent deactivation of the Pd metal catalyst. IX columns were tested experimentally to verify the modeling results. The key IX variables evaluated using the model and case study approach based on data from Chino, CA were resin regeneration length, treatment time, and addition of make-up salt. Overall, salt costs and waste brine volumes can be decreased by up to 80% with the hybrid system. A fixed-bed catalytic reactor was used to evaluate a real brine from Chino, CA and demonstrated consistent reduction, however the overall activity was very low due to hydrogen mass transfer limitations. This led to prohibitively high predicted catalyst costs for a commercial-scale hybrid system, leading to a focus on reactor design in an attempt to reduce mass transfer limitations.

Based on its significant use in industrial catalytic applications and the known ability to facilitate high mass transfer rates, a trickle bed reactor (TBR) was chosen as the new reactor design for use in the hybrid IX-catalyst system. The 2" ID TBR with two 10" beds of catalyst and recycling flow was designed in accordance with reactor design guidelines and evaluated across a range of liquid and gas superficial velocities. Synthetic waste brines were treated with two Pd-In/AC catalysts that had different support sizes. In comparison to a previously tested up-flow fixed-bed reactor, the same catalyst in the TBR demonstrated c. 300% higher activity. While the results showed a major step forward in reactor performance, the TBR activity was only 8.3% of the activity found in batch, indicating significant mass transfer limitations remained.

The impact of catalyst dilution was evaluated in the TBR and had been previously shown to improve reactor performance. The catalyst was diluted at a ratio of 1 part catalyst : 2 parts inert support. Continuous flow experiments using the diluted TBR did not demonstrate better performance and, to the contrary, showed a significant decrease in selectivity of catalyst. The

TBR with non-diluted catalyst resulted in c. 50% selectivity towards N_2, which is the desired end product due to its inert nature. The TBR with 1:2 diluted catalyst resulted in selectivity of nearly 100% towards NH_4^+. To better understand reduction mechanisms and selectivity, a series of experiments were performed and it was found the support had no direct role in selectivity. Rather, the change in selectivity was due to high hydrogen concentrations on the catalyst surface. In the diluted catalyst bed, reactive metal surfaces were geographically dispersed, allowing more time for hydrogen mass transfer from the gas to liquid phase. This led to higher hydrogen concentrations on the catalyst surface, which altered the N:H ratio and shifted selectivity towards NH_4^+. In contrast, in the non-diluted catalyst bed, reactive metal surfaces are found throughout the reactor, leaving less time for hydrogen mass transfer and resulting in a lower concentration of hydrogen on each metal surface.

Overall, this thesis advanced the state of the art for a hybrid IX-catalyst system and brought the system closer to economic feasibility. The modeling and experimental approaches served to more thoroughly evaluate the system and provide focus on the remaining barriers to increased improvement. This thesis also highlighted the critical role hydrogen mass transfer played as a barrier to a significant step forward in technology development. Reactor design contributed to improvements in the catalytic system, but were unable to completely overcome mass transfer limitations thus far. The findings from this thesis supported additional research directions regarding hydrogen delivery, reactor design and techno-economic analysis.

TABLE OF CONTENTS

CHAPTER 1

INTRODUCTION

1.1 Motivation

As population continues to increase, so will the demand for food. In order to grow sufficient quantities of food, we use fertilizers to maximize the output of farm land. Fertilizers add many important nutrients to the land and generally increase crop productivity. The nutrient that is the subject of this dissertation is nitrogen, typically applied in the form of ammonia as a fertilizer. During the last 50 years, the global nitrogen cycle has been altered by rising fertilizer use [1–4], which has increased by over 500% [5], indicating our global practices are not sustainable [6–8]. The importance of this issue is highlighted by the National Academy of Engineers, which includes global nitrogen cycle management as a "Grand Challenge" [9]. Concurrently, nitrogen use efficiency has been decreasing [10], leading to more wasted nitrogen that ends up polluting drinking water supplies [11] and altering the ecology and chemistry of natural water bodies supporting plant and animal life [12]. Though nitrogen takes the form of ammonia in fertilizers, in the environment nitrogen is readily converted to nitrate by nitrifying bacteria [13]. In addition to fertilizer runoff, other significant sources of nitrate contamination are combined animal feeding operations (CAFOs) and leaking septic tanks [14]. As an anion, nitrate is highly mobile and leads to widespread contamination of water supplies. It is the most common groundwater pollutant in the United States and the National Ground Water Association estimates 37% of Americans rely on groundwater as their drinking water source [15–19].

Nitrate is regulated by the United States Environmental Protection Agency [20] and European Union (EU) [21] for drinking water standards due to its harmful human health impacts, including "blue baby syndrome" in infants and the in vivo production of nitrosamines in adults,

which are suspected of causing cancer [15, 22–26]. The current prevalence and anticipated rise in nitrate contamination increases the importance of sustainably treating it [2, 6, 27]. When possible, non-treatment alternatives (i.e., drilling a new well, blending with a low nitrate source or connecting to an adjacent system) for eliminating nitrate contamination from drinking water are typically less costly and more reliable [28], but in the face of wide-spread contamination, treatment options must be used.

Ion exchange (IX) is the most common technology used in the US for treating nitrate, and is very effective in small to medium sized treatment plants [29]. However, the resin regeneration process with fresh brine (5 wt% - 12 wt% NaCl) and disposal of waste brine are expensive and have negative local and global environmental impacts [30]. Current practice involves using fresh brine for each regeneration cycle, leading to inefficiency and waste of expensive NaCl. A recent IX demonstration study in Vale, Oregon found the cost of salt accounted for 78% of the overall operations and maintenance (O&M) of the IX system [31]. Thus, technologies designed to reduce overall salt consumption during IX operations will have both economic and environmental benefits.

1.2 Background

1.2.1 Current Waste Brine Disposal Methods

Waste brine disposal in the United States relies on several common methods depending on geographic location and preference, including deep well injection, evaporation in aeration ponds, direct release to sanitary sewers, and piping into the ocean [32, 33]. Deep well injection is frequently used in California, where there is widespread nitrate contamination and

approximately 16,000 Class I injection wells [34]. Brine disposal can cost between $0.60 and $4.44/1,000 gal of treated drinking water, approaching the cost of water treatment itself ($4.58/1,000 gal) [35].

In Pheonix, Arizona, evaporation ponds are common but the rate of increased brine production has led to exploration of alternative methods. Building evaporation ponds for an expected future production of 30 MGD of brine (waste from 200 MGD potable water) would require 10 square miles of real estate and cost over $114M per year, whereas using an injection well would cost $44M per year [36].

Some states are tightening restrictions on surface discharge of waste brine, making that disposal method more challenging. For example, Florida regulators mandated that the addition of concentrated waste brine to a wastewater treatment stream cannot impact the treatment facility's ability to reach its treatment goals or harm vegetation in the reuse system; this resulted in the City of Arcadia, FL building holding tanks for its IX waste brine so the waste brine could be released slowly into the wastewater collection system [33].

Treating and reusing waste brine multiple times would decrease the economic cost and environmental burden of the IX process. Further, treating the waste brine would enable destruction of nitrate rather than its transfer to another phase, which is currently what happens. Efforts to treat ion exchange waste brine have been pursued for over two decades, and the main approaches leverage biological or chemical processes [37–39].

1.2.2 Biological Waste Brine Treatment

Efforts to biologically denitrify ion exchange brine have been underway for a few decades and the results are very promising. Using anaerobic bacteria in an up-flow sludge

blanket denitrification (USBR) reactor, Van der Hoek, *et al.* demonstrated a 95% reduction in waste brine volume and 80% reduction in regeneration salt requirement. This process also had high selectivity towards N_2 gas, the desired end-product for nitrate [39, 40]. Bae, *et al.* [41] improved the USBR process by adding a sulfate reduction reactor and GAC step. Using a different treatment scheme, a Dutch water company developed a multi-step treatment train for IX waste brine, which involves proprietary biological denitrification followed by nanofiltration and dynamic vapor recompression, aimed at zero liquid discharge and recovery of salt for reuse [42].

Clifford and coworkers reported on a series of efforts using an anaerobic sequencing batch reactor (SBR) for nitrate removal and waste brine regeneration. They demonstrated the efficacy of the SBR to regenerate a synthetic IX waste brine over 15 cycles in the lab, and 20 cycles in a pilot study [37, 43]. Further, they reported a 50% reduction in fresh brine consumption and a 90% reduction in discharged waste salt [44]. The SBR also proved effective and timely when tested with real brine obtained from a water treatment plant, consistently reducing nitrate to below detection limits in 24 hours [45]. Okeke *et al.* [46] performed a similar study using incubation flasks, but observed nitrate reduction took up to one week. System modifications and enhancements such as addition of cations for culture stability or incorporating inoculated GAC have been tested as well [47, 48].

Membrane biofilm reactors (MBfR) have also been used successfully to treat real IX waste brines [49]. Most recently, Ebrahimi and Roberts [50] used salt-tolerant nitrate-reducing bacteria in a novel system, submerging spent IX resin in a bacteria culture while the resin was wrapped in a membrane to provide a physical barrier; they successfully ran four reuse cycles with no IX performance degradation.

Despite these promising results, the main drawback to using biological treatment of brine is public perception and risk, which entails the perceived and actual risk of microbes contaminating the drinking water supply. Additionally, culture stability can be a challenge, particularly when treatment is performed intermittently [43]. Because nitrate contamination varies seasonally in some regions, a biological reactor would require multiple start-up and shut-down events, each of which may present challenges. Lastly, the biological brine treatment systems discussed above typically use acetate or methane as the electron donor, the use of which has great economic and environmental impacts when compared to hydrogen [51].

1.3 Catalytic Waste Brine Treatment

Research supporting the use of catalysis for IX waste brine treatment has a much shorter history, but here I propose its use due to several potential benefits over a biological approach. The potential advantages of catalytic treatment are lower cost and environmental impact of the electron donor (i.e., hydrogen), and a smaller reactor footprint relative to biological treatment. The main drawback is the initial cost of the catalyst, and the risk of catalyst deactivation and associated lower reactions rates due to the presence of non-target constituents in water.

Pintar *et al.* proposed and later modified a closed loop IX-catalyst system for brine reuse, in which a 1 wt% NaCl brine was continually recirculated through both the catalyst column and IX resin until all nitrate was removed [38, 52]. In contrast to Pintar *et al.*, Choe *et al.* [51] proposed a hybrid IX-catalyst system that used either a single fixed bed reactor (FBR) or sequencing batch reactor (SBR) for denitrification, which treated IX brine in a single pass. Most recently, Yang *et al.* [53] proposed the use of photocatalysis as an additional option for catalytic

waste brine treatment. Though their results were promising, the photocatalyst suffered the same reaction rate setbacks as other studies in the presence of brine-level NaCl levels and high sulfate.

Recent results and analysis of the hybrid system indicated a catalytic system in an SBR design provides sufficient catalytic activity to meet target cost requirements; a concurrent Life Cycle Assessment (LCA) showed the hybrid system had lower environmental impacts than the conventional IX system [51]. However, an SBR was impractical for full scale use due to catalyst handling challenges and particle breakup with long-term mixing, leading to further exploration of FBR options. Choe, *et al.* [51] showed the catalytic activity in a co-current up-flow fixed bed reactor with low liquid and gas superficial velocities was not adequate to meet target cost requirements, and resulted in higher environmental impacts for the hybrid system when compared to conventional IX, due to the need for a larger reactor with more Pd catalyst. The difference in performance and feasibility for full-scale implementation of SBR versus FBR was largely due to hydrogen mass transfer limitations in the FBR.

1.3.1 Hydrogen Mass Transfer

In the catalytic reactor, hydrogen was used as an electron donor to reduce nitrate over a bimetallic catalyst, destroying the nitrate and converting it primarily to inert dinitrogen gas, with some ammonium. The two hydrogen mass transfer processes of interest in this reaction were gas-liquid and liquid-solid, which were modeled as:

$$H_{2(g)} \xrightarrow{k_L} H_{2(l)} \xrightarrow{k_S} H^{\bullet} - Pd - H^{\bullet}$$

First, the hydrogen gas must cross the gas-liquid interface and dissolve into the liquid phase, which was limited by the low solubility of hydrogen in water (~0.8 mM in equilibrium with 1 bar H_2(g) at 25 °C). Next, the dissolved hydrogen must diffuse through the boundary layer around

the catalyst particle and hydrogenate palladium. In this reaction, $k_L << k_S$, so overall mass transfer was limited by the gas-liquid transfer step [54].

1.3.2 Bimetallic Catalysts for Waste Brine Denitrification

The bimetallic catalyst consisted of a hydrogenation plus promoter metal, both loaded onto a porous support (see Figure 1.1). Among the materials tested, the hydrogenation metal palladium and the promoter metal indium on an activated carbon support (Pd-In/AC) have shown the highest activity for nitrate reduction and selectivity for dinitrogen gas [55–58]. Copper and indium have emerged as the most active and selective promoter metals, but there were no direct comparisons of their effect on nitrate reduction activity and selectivity for dinitrogen gas in a waste brine, and/or with an activated carbon support [59–61]. Using an alumina support with 5 wt%Pd, Chaplin *et al.* found that activity and selectivity were similar using indium or copper, but that only In (not Cu) was stable during periodic oxidative catalyst regeneration to reverse sulfide fouling [62, 63]. Oxidative regeneration stability might be an important catalyst attribute required when waste brine treatment was considered, due to the potential for high sulfate concentrations in re-used brine and subsequent production of Pd-poisoning sulfide species by sulfate reducing bacteria [38, 53, 64].

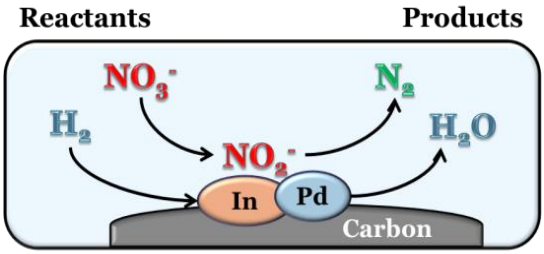

Figure 1.1: Catalyst mechanism for nitrate reduction

1.3.3 Catalytic Reactor Design

To achieve high enough catalytic activity to support commercialization, reactor design was critical. Previously, my advisor's research group used a fixed bed reactor that demonstrated poor hydrogen mass transfer to the catalyst surface [51, 65]. Hydrogen has a very low solubility in water (~0.8 mM in equilibrium with 1 bar $H_{2(g)}$ at 25 °C), while nitrate could be present in brine at up to 15,000 mg/L (~180 mM). Thus, only a very small fraction of the stoichiometric requirement of hydrogen can be dissolved in water at any given time. This required designing a reactor with a fast hydrogen mass transfer rate.

Among the possible reactors, two commercially-proven systems were known for fast gas to liquid mass transfer rates: a fluidized bed reactor (Flu-BR) and trickle bed reactor (TBR) (see Figure 1.2). Catalytic Flu-BRs have been used in industry for many years, predominantly in the hydrocarbon/petrochemical sectors [66, 67], and also in limited water treatment applications [48, 68, 69]. Turbulent mixing in a Flu-BR was known to increase mass transfer rates and therefore apparent catalyst activity [70], making it an attractive alternate reactor configuration for this application. The primary drawback of the Flu-BR was destruction of many catalysts due to abrasion between grains during the turbulent mixing [71]; therefore, this reactor configuration was bypassed in the current effort because the activated carbon used in this study was a brittle support.

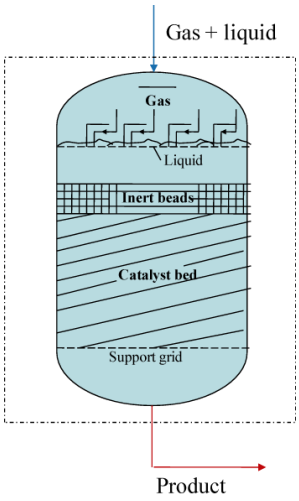

Figure 1.2: Simple schematic of a trickle bed reactor

Catalytic TBRs are also commonly used in industry for hydrocarbon/ petrochemical refinement and conversion, as well as pharmaceuticals and fine chemical production [72–79]. This reactor design incorporated a fixed catalyst bed (or multiple beds) and was not fluidized, so catalyst destruction via abrasion was not an issue. Mederos *et al.* [80] outlined the three key challenges for successful TBR operation as: 1) deviation from plug flow, 2) external wetting efficiency, and 3) reactor wall effects. Each of these challenges could be address through reactor design and optimization.

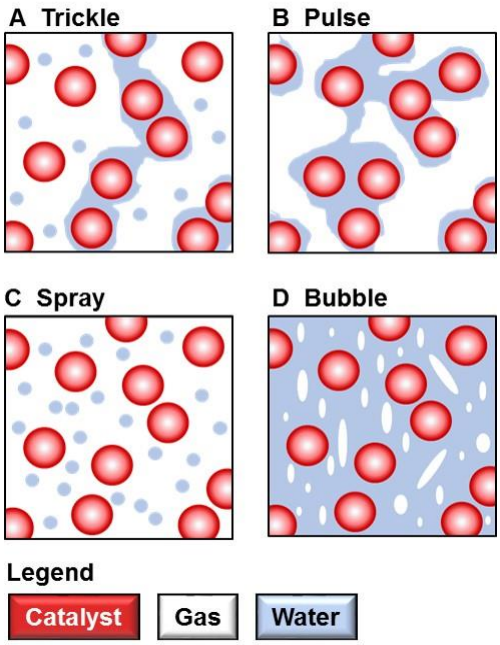

Figure 1.3: Diagram of the four primary flow regimes in a TMR, adapted from [81]

A TBR can be operated in multiple flow regimes (trickle, pulse, spray and bubble flow), which differ primarily according to the ratio of gas-liquid superficial velocities, and co-current down flow operation (versus counter-current flow) was preferred because of increased particle stability [81, 82]. A graphic of the different TBR flow regimes can be seen in Figure 1.3. Extensive literature exists regarding trickle flow (continuous gas phase) and the transition area between trickle-pulse flow, as these were common flow regimes used in industry, particularly for hydrocarbon reactions [83]. The trickle flow regime was often used for industrial catalytic applications because high gas superficial velocities were needed to meet or exceed stoichiometric needs, helped control reactor temperature, and improved mass transfer rates [79, 84]. The pulse flow regime occurred with higher liquid superficial velocities and provided high mass transfer rates due to increased turbulence within the bed and thinner stagnant liquid films

around catalyst particles [85, 86]. Pintar and Batista [87] briefly experimented with a bench-scale TBR for drinking water treatment, but continued research using an up-flow fixed bed reactor due to higher nitrate conversion and higher selectivity for dinitrogen when compared to the TBR. A TBR for waste brine denitrification in the trickle and pulse flow regimes has not been evaluated.

1.3.4 Modeling Approaches and Their Relevance

Modeling the hybrid IX-catalytic system involved two different components: the IX system and the catalyst system. Several ion exchange models exist, but there were no published models that assessed the impacts of multi-cycle waste brine reuse in a hybrid ion exchange-catalyst system. Hekmatzadeh, *et al.* [88] developed and validated a rigorous ion exchange model, based on the Langmiur isotherm and mono-layer theory, using the classic advection-dispersion-retardation equation. However, this model only predicted ion exchange performance during the feed cycle, or treatment phase, and did not address regeneration considerations; they further concluded a simple mass-action model was sufficient for ion exchange modeling.

For a brine re-use system, accurately modeling the regeneration cycle was critical. In high ionic strengths solutions, selectivity reversal occurred and necessitated a separate set of selectivity constants for the model to simulate the IX processes accurately [89, 90]. Valverda, *et al.* [91] reported the influence of ion concentration on resin selectivity during their study of heavy metal remediation using ion exchange, but did not quantify or focus on the issue. Kim and Benjamin [92] modeled a three-step ion exchange process involving regeneration and sulfate precipitation, but did not incorporate nitrate reduction or use the model for a real world scenario. Their study specifically quantified a change in selectivity constants under low (0.003 M) and

high (3.0 M) ionic strength conditions and found that sulfate-nitrate selectivity constant ($K_{sel,S/N}$) increased by an order of magnitude from low to high ionic strength solutions [92]. Flodman and Dvorak [93] also quantified the selectivity reversal, though they focused on mass transfer coefficients rather than selectivity constants, as it related to water softening and cation exchange resins.

Modeling catalytic applications was often used in industry to help optimize variables related to reactor performance and selectivity, which were critical to the economics of the system [94–98]. There were fewer examples of denitrification models for packed bed reactors and those focused primarily on electrochemical-biological denitrification in fixed and fluidized beds [99–101]. Important variables in model development for catalytic denitrification were volumetric gas and liquid superficial velocities, bed porosity, catalyst metal content, catalytic reaction rates and hydrogen mass transfer rates. While these variables were represented in most of the efforts cited above, I am not aware of a bimetallic catalyst denitrification model in a packed bed reactor.

1.4 Research Goals and Objectives

The overall goal of my research was to advance the state of the art regarding catalytic denitrification of ion exchange waste brine to support a hybrid IX/catalyst treatment system. My research plan was designed to: (1) Evaluate the hybrid system using a modeling and experimental approach, assessing the impact of key variables, (2) Compare catalytic performance in batch, fixed bed and trickle bed reactors, (3) Design and operate a laboratory-based pilot scale reactor to improve mass transfer rates and reactor performance and (4) Evaluate selectivity of the

Pd-In/AC catalyst in different matrices and reactors. With this goal in mind, I proposed the following research objectives and hypotheses:

Objective 1: ***Using an experimental and modeling approach, determine whether the accumulation of bicarbonate and sulfate in reused waste brine will negatively impact the hybrid system performance and model key IX system variables using a case-study approach.*** An important distinction between the hybrid system and conventional IX treatment was the reuse of waste brine. When waste brine was reused, bicarbonate and sulfate ions (and other minor anions) would accumulate over repeated resin regeneration cycles since these ions were not removed during catalytic denitrification. I hypothesized this accumulation would have no impact on the IX component performance for nitrate treatment because I was using a nitrate-selective resin. To test this hypothesis, a modeling and experimental approach was used. An analytic model based on the one presented by Gerald Guter [102], which used mass balance and mass action relationships to describe multi-component equilibrium conditions in an ideal plug-flow IX system, was used to explore key variables in the hybrid system using a case-study from Chino, CA. Experiments using fix-bed flow through reactors tested multiple synthetic brines with varying levels of bicarbonate and sulfate.

Objective 2: ***Evaluate reactor performance in continuously stirred batch reactors and fixed bed reactors; and optimize a fixed bed reactor to reduce hydrogen mass transfer limitations to the catalyst surface.*** Continuously-stirred reactors with excess hydrogen gas eliminated external mass transfer limitations and demonstrated the intrinsic activity of a catalyst, which provided a bench-mark for comparing the performance of fixed bed reactors. An up-flow, co-current flooded fixed bed reactor (FBR) and a down-flow, co-current trickle bed reactor (TBR) were used to denitrify waste brine. Because TBRs have been used for decades in

commercial applications and were known for their high mass transfer rates, I hypothesized the TBR would demonstrate higher catalytic activity than the up-flow FBR. Experiments using the TBR evaluated a range of liquid and gas superficial velocities using two different catalyst support sizes. A numerical model of the system was developed to evaluate hydrogen mass transfer rate coefficients at the range of operating conditions tested.

Objective 3: ***Evaluate selectivity of Pd-In/AC catalyst using different reactor types and matrix conditions***. The two end-products of nitrate reduction were dinitrogen gas (N_2) and ammonium (NH_4^+), with N_2 generally preferred because of its inert nature. Reduction to N_2 required less hydrogen than reduction to NH_4^+ (2.5 mol/mol vs 4.0 mol)/mol, which meant hydrogen mass transfer had an impact on selectivity. A TBR and continuously stirred batch reactor were be tested under different conditions. I hypothesized that while the selectivity of the reactors would not be directly comparable, the underlying mechanism of competitive sorption would dominate selectivity results and be consistent between reactors.

1.5 Dissertation Outline

- Chapter 2 contains a manuscript published in *Water Research*, entitled "Evaluation of a hybrid ion exchange-catalyst treatment Technology for Nitrate Removal from drinking water" with co-authors J.K. Choe, T.J. Strathmann and C.J. Werth. This work addressed research objective 1, evaluating the hybrid system using a modeling and experimental approach. The impact of sulfate and bicarbonate build-up on the hybrid system was evaluated. A case study approach was used to model the impact of

key variables in the IX system, such as resin regeneration length and catalytic nitrate reduction level.

- Chapter 3 contains a manuscript submitted to *J. AWWA*, entitled "Catalytic denitrification in a trickle bed reactor: Ion exchange waste brine treatment" with co-authors M. Bertoch, G. Gildert, T.J. Strathmann and C.J. Werth. This work addressed objective 2, comparing nitrate reduction in multiple reactor configurations. A trickle bed reactor was designed and then evaluated under a range of liquid and gas superficial velocities. The model was used to calculate hydrogen mass transfer rate coefficients and predict the effect of different intrinsic activity rates.
- Chapter 4 contains results addressing objective 3. Experiments in the trickle bed reactor and continuously stirred batch reactor were performed with diluted and non-diluted catalyst. The impact on selectivity of hydrogen concentration, nitrite concentration, chloride concentration and catalyst dilution was tested. A model of competitive sorption on the catalyst surface was proposed to describe selectivity.
- Chapter 5 contains a final summary of the work conducted in this dissertation, as well as major conclusions and future research directions.
- Appendix A contains supplementary information that supported Chapter 2.

CHAPTER 2

EVALUATION OF A HYBRID ION EXCHANGE-CATALYST TREATMENT TECHNOLOGY FOR NITRATE REMOVAL FROM DRINKING WATER

2.1 Abstract

Ion exchange (IX) is the most common approach to treating nitrate-contaminated drinking water sources, but the cost of salt to make regeneration brine, as well as the cost and environmental burden of waste brine disposal, are major disadvantages. A hybrid ion exchange-catalyst treatment system, in which waste brine is catalytically treated for reuse, shows promise for reducing costs and environmental burdens of the conventional IX system. An IX model with separate treatment and regeneration cycles was developed, and ion selectivity coefficients for each cycle were separately calibrated by fitting experimental data. Of note, selectivity coefficients for the regeneration cycle required fitting the second treatment cycle after incomplete resin regeneration. The calibrated and validated model was used to simulate many cycles of treatment and regeneration using the hybrid system. Simulated waste brines and a real brine obtained from a California utility were also evaluated for catalytic nitrate treatment in a packed-bed, flow-through column with 0.5wt%Pd-0.05wt%In on an activated carbon support (Pd-In/C). Consistent nitrate removal and no apparent catalyst deactivation were observed over 23 d (synthetic brine) and 45 d (real waste brine) of continuous-flow treatment. Ion exchange and catalyst results were used to evaluate treatment of 1 billion gallons of nitrate-contaminated source water at a 0.5 MGD water treatment plant. Switching from a conventional IX system with a two bed volume regeneration to a hybrid system with the same regeneration length and sequencing batch catalytic reactor treatment

would save 76% in salt cost. The results suggest the hybrid system has the potential to address the disadvantages of a conventional IX treatment systems.

2.2 Introduction

Sustainably addressing nitrate-contaminated groundwater sources is a serious and growing issue due to nitrate's well-documented health effects [15, 20–26] and ever increasing use in agriculture [2, 6, 27]. Ion exchange (IX) is the predominant technology used in the U.S. for removing nitrate from drinking water sources, and has proven very effective in small to medium sized treatment plants [29]. However, when the IX resin is exhausted, regeneration is accomplished by flushing a concentrated salt brine (5 - 12 wt% NaCl) through the resin bed. The purchase of salt used for this regeneration step and disposal of the resulting nitrate-contaminated waste brines is expensive and leads to negative environmental impacts [29, 31]. Current treatment practices involve using fresh brine for each regeneration cycle, leading to inefficiency in the use of NaCl. The results of a 2011 study found that salt costs accounted for 78% of the overall operations and maintenance (O&M) at an IX treatment demonstration plant in Vale, OR [31]. Thus, treating waste brine to enable reuse could decrease both the economic costs and environmental burdens of IX treatment processes.

Biological denitrification of ion exchange waste brine has been extensively studied and is a viable option for waste brine treatment [37, 39, 40, 43]. However, biological treatment is sensitive to influent nitrate loading, and raises concerns over pathogens in drinking water. Results from a recent life cycle assessment suggest that a hybrid IX-catalyst system, in which waste brine reuse is enabled by catalytic denitrification, is another promising option for addressing IX inefficiencies [51]. In the proposed catalytic reactor, hydrogen is supplied as an

electron donor to reduce nitrate over a bimetallic catalyst, converting the toxic oxyanion primarily to inert dinitrogen gas ($NO_3^- + 2.5H_2 \rightarrow 0.5N_2 + OH^- + 2H_2O$). Among the materials tested, the combination of the hydrogenation metal palladium and the promoter metal indium immobilized on an activated carbon support (Pd-In/AC) has shown both high activity and selectivity for dinitrogen gas [55–58]. In addition, unlike Pd-Cu catalysts, the Pd-In catalysts are stable during oxidative regeneration processes that could be periodically required to reverse sulfide poisoning [63].

Pintar *et al.* [103] proposed and later modified [52] a closed loop hybrid IX-catalyst system for brine reuse, in which a 1 wt% NaCl brine was continually recirculated through both the catalyst column and IX resin until all nitrate was removed. In contrast, Choe *et al.*, [51] proposed a 2-stage hybrid treatment system using IX for treatment of the contaminated source water followed by resin regeneration using waste brine that is catalytically treated in a separate reactor (either packed bed or sequencing batch catalyst reactor) between regeneration cycles. One concern, though, is that IX model simulations predicted buildup of unreactive bicarbonate and sulfate ions in waste brines over repeated catalyst treatment and reuse cycles, and previous experiments in batch reactor systems suggest that elevated levels of these non-target ions may inhibit catalyst reactions with nitrate [51, 53, 64, 103]. It is not clear how these findings translate to continuous flow reactors, whether the reduction in catalyst activity is simply competitive inhibition or leads to more progressive loss in activity (i.e., deactivation), and how residual nitrate levels remaining after catalytic treatment affects IX performance. Prior work indicates that the elevated levels of bicarbonate and sulfate in waste brine will have minimal effect on IX performance during treatment with nitrate-selective resins [37, 39] because a selectivity reversal at high ionic strength favors chloride sorption over bicarbonate or sulfate during resin

regeneration [93, 104]. However, the effects of very high sulfate and bicarbonate levels expected for repeated reuse cycles (e.g., 8,000 – 30,000 mg/L) have not been experimentally evaluated, and prior IX model simulations [51] that considered this scenario used literature values for selectivity coefficients that did not consider selectivity reversal during regeneration.

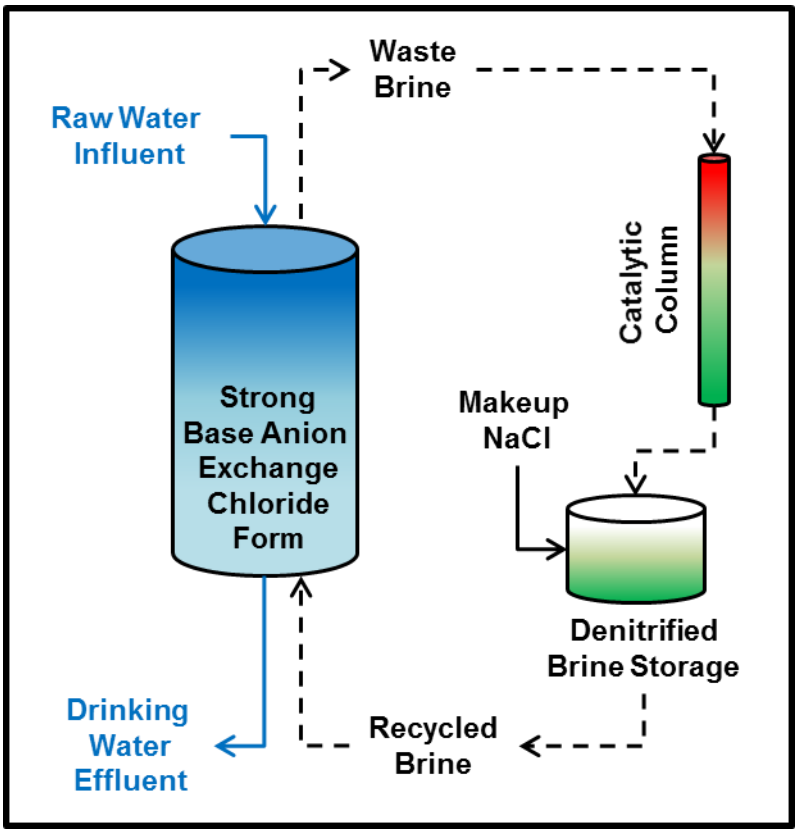

Figure 2.1: Flow diagram of the hybrid ion exchange-catalyst treatment system

The goal of this chapter is to employ a combination of process modeling and experimentation to evaluate the technical feasibility of the hybrid IX-catalyst technology for treatment of nitrate-contaminated drinking water (see Figure 2.1 for diagram). My specific objectives are to: 1) Calibrate and validate an ion exchange model for treating nitrate-contaminated water that includes repeated treatment and regeneration cycles using treated waste

brine; 2) Use the calibrated model to simulate multiple treatment/regeneration cycles to predict the buildup of bicarbonate and sulfate ions in waste brine that occurs with brine reuse and the impact of these ions on IX performance for nitrate removal; 3) Evaluate the effects of elevated levels of bicarbonate and sulfate in synthetic and real waste brines on long-term catalyst performance in a continuous-flow packed-bed reactor; and 4) Estimate input salt and catalyst metal requirements for the conventional versus hybrid IX systems as a function of regeneration bed volumes. Results are used to recommend an optimum hybrid treatment strategy, and the use of separate selectivity coefficients for IX treatment and IX regeneration steps yields new insights into how the IX system must be operated to maintain performance. In addition, long-term catalyst tests with synthetic and real brines provide important performance data needed to advance the development of a practical hybrid system.

2.3 Methods

2.3.1 Materials

Reagent-grade sodium salts (≥99% purity) of nitrate, chloride, bicarbonate, and sulfate were obtained from Fisher or Sigma-Aldrich. All synthetic brines were prepared with either deionized (DI) water or Nanopure water (18.2 MΩ-cm resistivity, Millipore system). A nitrate selective ion exchange resin (CalRes 2105) was supplied by the Calgon Carbon Corporation with a reported resin capacity of 1,000 meq/L. A 0.5wt%Pd-0.05wt%In/C was provided by Johnson Matthey.

2.3.2 IX and Catalyst Experimental Setups

IX columns were constructed from 101.6 cm (40”) long sections of 1.9 cm (0.75”) OD, 1.27 cm (0.5”) ID UV-stabilized acrylic tubing and filled with 116 mL resin. A Masterflex peristaltic pump with three pump-heads was used to deliver all solutions, and up to three IX columns were run in parallel. More details and a simple diagram are shown in Figure A1.

The packed bed catalyst reactor column was constructed from 50.8 cm (20”) of 2.54 cm (1”) OD, 1.9 cm (0.75”) ID UV-stabilized acrylic tubing and packed with 80.7 g of Pd-In/AC catalyst. It was equipped with stainless steel Swagelok fittings and PTFE tubing. More details and a simple diagram are shown in Figure A2.

All fresh brines and simulated waste brines were prepared with Nanopure water. Solutions for IX treatment cycle experiments (150-210 L feeds) were prepared with deionized (DI) water using a high pressure DI faucet to ensure proper mixing of the large volumes required (150-210 L). All experiments were conducted at ambient laboratory temperatures. IX experiments were conducted at 27°C +/- 5°C, and catalyst experiments were conducted at 20°C +/- 2°C. Previous reports indicate that IX performance varies little with temperature. In one study, anion selectivity coefficients were not significantly impacted between 5 and 25 °C [105]. In another study, there was no change in the nitrate-bromide selectivity coefficient between 0 and 50 °C [106]. Hence, the +/- 5 °C temperature variation in my runs had little effect on the results.

2.3.3 IX Experiment Protocol

IX experiments were conducted with alternating treatment and regeneration cycles. During treatment cycles, feed was pumped down-flow at 80 mL/min (EBCT=1.45 min); during regeneration cycles, brine was pumped up-flow at 3.3 mL/min (EBCT=35.15 min). Experiments

used for model calibration also included an intermediate DI water flush cycle before each treatment cycle and each regeneration cycle; this was pumped at 19 mL/min (EBCT=6.1 min) for 5 BV (empty bed volumes) in the same direction as the subsequent cycle (i.e., down-flow if preceding the treatment cycle). These BV and hydraulic retention times (based on superficial velocities) were selected in consultation with personnel from Calgon Carbon Corporation and are representative of those used in practice [107].

Table 2.1 summarizes the three sets of IX experiments performed: one set of four experiments for treatment cycle model calibration (labeled Model Treatment Exp. 1 – 4), one set of four experiments for brine cycle model parameterization (labeled Model Brine Exp. 1 – 4), and one set of six experiments for testing 2-cycle IX performance for model refinement and validation (labeled 2-Cycle Exp. 1 – 6). Further protocol details and diagrams are provided in Appendix A. Three different bed volumes of brine regeneration were considered in experiments (2, 5 and 10 BV); partial resin regeneration is expected with 2 BV and nearly complete regeneration (i.e., return resin to fully chloride-loaded state) with 10 BV.

Table 2.1: Summary of IX experiments used for model calibration and validation

Experiment Number	Water Composition				BV of Brine	# Feed Cycles	Brine Composition			
	[Cl^-]	[NO_3^-]	[HCO_3^-]	[SO_4^{2-}]			[NaCl]	[NO_3^-]	[HCO_3^-]	[SO_4^{2-}]
	mg/L	mg/L	mg/L	mg/L			mg/L	mg/L	mg/L	mg/L
Experiments used to parameterize the model during the Feed Cycle										
Model Treatment Exp. 1	0	0	0	200	NA	1	NA	NA	NA	NA
Model Treatment Exp. 2	0	0	200	0	NA	1	NA	NA	NA	NA
Model Treatment Exp. 3	0	200	0	0	NA	1	NA	NA	NA	NA
Model Treatment Exp. 4	0	200	200	200	NA	1	NA	NA	NA	NA
Experiments used to parameterize the model during the Regeneration Cycle										
Model Brine Exp. 1	0	200	0	0	9BV	1	100,000	0	0	0
Model Brine Exp. 2	0	200	0	0	9BV	1	100,000	1,500	30,000	0
Model Brine Exp. 3	0	200	0	0	9BV	1	100,000	1,500	0	30,000
Model Brine Exp. 4	0	200	0	0	9BV	1	100,000	1,500	30,000	30,000
Experiments used to refine regeneration parameters and validate model										
2-Cycle Exp. 1	70	200	131	48	2BV	2	100,000	0	0	0
2-Cycle Exp. 2	70	200	131	48	5BV	2	100,000	0	0	0
2-Cycle Exp. 3	70	200	131	48	10BV	2	100,000	0	0	0
2-Cycle Exp. 4	70	200	131	48	2BV	2	100,000	1,500	30,000	30,000
2-Cycle Exp. 5	70	200	131	48	5BV	2	100,000	1,500	30,000	30,000
2-Cycle Exp. 6	70	200	131	48	10BV	2	100,000	1,500	30,000	30,000
NA = Not Applicable										

2.3.4 Catalyst Experimental Protocol

Continuous catalytic nitrate treatment experiments were performed for 23 – 45 d to evaluate catalyst activity and longevity. A two-phase flow packed-bed reactor was used because sufficient hydrogen for stoichiometric nitrate reduction could not be delivered in the liquid phase alone. The brine superficial velocity was 0.2 mL/min (0.24 m/hr), the hydrogen gas superficial velocity was 6.8 mL/min (0.81 m/hr), and the carbon dioxide gas (pH buffer) superficial velocity was 1.6 mL/min (0.19 m/hr). At the column inlet, the H•/N molar ratio was ca. 7.5. The minimum required stoichiometric molar ratio for nitrate reduction to dinitrogen gas is 2.5, and for nitrate reduction to ammonium is 4.0. Two experiments were performed: one with a series of synthetic brines and one with a real waste brine obtained from a California utility (see Table A1). Further details concerning the protocols and brines are available in Appendix A.

Batch experiments were also performed to evaluate catalyst activity in a rapidly mixed (800 rpm) and vigorously H_2 sparged (250 mL/min) solution using a system described previously [51]. A synthetic waste brine containing 11,500 mg/L nitrate and 4.5 wt% NaCl was introduced to a 250 mL, round bottom, five-neck reaction flask containing 40 g/L catalyst. Solution pH was maintained at 5.0 with HCl addition by an automatic pH stat during reactions. Suspension samples were periodically collected for analysis and immediately filtered (0.45 μm) to quench further reaction.

2.3.5 Analytical Methods

Aqueous chloride, nitrate and sulfate concentrations were quantified using ion chromatography with conductivity detection (Dionex ICS-2000/2100, 4×250 mm IonPac AS-19). A superficial velocity of 1.0 mL/min, 32 mM KOH eluent concentration and 96 mA suppressor current were used. Internal and external standards were used to calibrate the results. All brine samples and reference standards were diluted 50-fold prior to IC analysis. Bicarbonate concentrations were estimated by alkalinity pH titration using reference 0.1 N, 0.01 N and 0.001 N HCl solutions. Inductively coupled plasma-optical emission spectrometry (ICP-OES) analysis was used to quantify total calcium, magnesium, phosphorous, iron and manganese in the real waste brine obtained from the California utility.

2.3.6 IX Model Development

An IX model was developed using the three mass action and five mass balance relationships listed in Table 2.2, which have eight unknown variables (RCl, RNO_3, $RHCO_3$, R_2SO_4, $[Cl^-]$, $[NO_3^-]$, $[HCO_3^-]$, $[SO_4^{2-}]$) evaluated in meq/L, and seven model parameters (i.e., $K_C^N, K_C^S, K_C^H, rK_C^N, r\,K_C^S, rK_C^H$ Resin Capacity). The IX column was discretized spatially into a series of theoretical "plates". The eight equations and eight unknown variables were solved at each plate as a system of non-linear equations in MATLAB assuming instantaneous equilibrium. The mathematical solution of the eight unknown variables from one plate became the initial conditions for the next plate. The number of plates required for model simulations was increased until model output was constant and a mass balance was obtained; 25 plates were determined to be sufficient to meet these criteria. The supplier-provided resin capacity of 1,000 meq/L was used as an initial guess during parameter fitting. The model code was validated by matching simulated nitrate breakthrough results provided in [102] using the same initial conditions, treatment selectivity coefficients and resin capacity.

Table 2.2: Ion exchange model equations and variables

Equations	Unknowns	Definitions
(1) $Cl_{tot} = [Cl^-] + RCl$	$[Cl^-], RCl$	$[Cl^-]$ = chloride aqueous conc RCl = chloride resin conc. Cl_{tot} = total chloride
(2) $NO_{3,tot} = [NO_3^-] + RNO_3$	$[NO_3^-], RNO_3$	$[NO_3^-]$ = nitrate aqueous conc RNO_3 = nitrate resin conc. $NO_{3,tot}$ = total nitrate
(3) $HCO_{3,tot} = [HCO_3^-] + RHCO_3$	$[HCO_3^-], RHCO_3$	$[HCO_3^-]$ = bicarbonate aqueous conc $RHCO_3$ = bicarbonate resin conc. $HCO_{3,tot}$ = total bicarbonate
(4) $SO_{4,tot} = [SO_4^{2-}] + R_2SO_4$	$[SO_4^{2-}], R_2SO_4$	$[SO_4^{2-}]$ = sulfate aqueous conc R_2SO_4 = sulfate resin conc. $SO_{4,tot}$ = total sulfate
(5) $K_C^N = \frac{[Cl^-]\ RNO_3}{[NO_3^-]\ RCl}$	$[Cl^-], RCl$ $[NO_3^-], RNO_3$	K_C^N = resin nitrate-chloride selectivity, different for feed and regeneration
(6) $K_C^S = \frac{[Cl^-]^2\ R_2SO_4}{[SO_4^{2-}]\ RCl^2}$	$[Cl^-], RCl$ $[SO_4^{2-}], R_2SO_4$	K_C^S = resin sulfate-chloride selectivity, different for feed and regeneration
(7) $K_C^H = \frac{[Cl^-]\ RHCO_3}{[HCO_3^-]\ RCl}$	$[Cl^-], RCl$ $[HCO_3^-], RHCO_3$	K_C^H = resin bicarb-chloride selectivity, different for feed and regeneration
(8) Resin Capacity = RCl + RNO_3 + $RHCO_3$ + R_2SO_4	RCl, RNO_3, $RHCO_3$, R_2SO_4	Resin Capacity = total equivalence that can be absorbed onto the resin

Ion selectivity coefficients vary depending on solution ionic strength [108, 109]. Hence, breakthrough of ions during the IX treatment (i.e., low ionic strength feed) and resin regeneration (i.e., high ionic strength brine feed) stages were modeled separately, resulting in the two different sets of selectivity coefficients (a single resin capacity value was optimized). Optimization was conducted in three distinct stages by minimizing the relative least square error between model and experimental results using a genetic algorithm (details provided in Appendix A). First, treatment cycle parameters were determined by fitting Model Treatment Exp. 1-4 data (see Appendix A for details). This resulted in an optimized set of treatment cycle selectivity coefficients. Second, regeneration cycle parameters were initially determined by fitting Model Brine Exp. 1-4 data (see Appendix A for details), and the challenges encountered are discussed in Section 2.3.1. Finally, regeneration cycle parameters were optimized by fitting 2-Cycle Exp. 1 data. The best-fit regeneration parameters were then validated by predicting nitrate breakthrough curves for 2-Cycle Exp. 2-6 experiments (see Table 2.3). The 95% confidence intervals were calculated for the best-fit parameters (see Appendix A for parameter optimization details).

Catalytic denitrification was incorporated into the IX model by (numerically) reducing the level of nitrate to 1,500 mg/L in the composite waste brine collected during a regeneration cycle. A nitrate level of 1,500 mg/L was chosen to balance subsequent treatment length with catalyst reactor requirements. Treating to a lower nitrate level would allow longer treatment time in the subsequent IX cycle (as model results will indicate), but would also require more catalyst and increase the price of the reactor. With the loss of nitrate ions from the treated brine, electroneutrality was maintained by assuming an equivalent addition of bicarbonate anions resulting from the carbon dioxide buffering agent used. Since chloride is lost from brine to the

resin during IX regeneration, makeup NaCl was (numerically) added to the composite waste brine to maintain a constant chloride level during each regeneration cycle. The modified composite waste brine (with reduced nitrate level and constant chloride level) was used in the next simulated regeneration cycle.

I note that my modeling approach assumes ideal plug flow through the IX column, i.e., dispersion is ignored. There are examples of IX models in the literature that have considered [88, 93] and neglected dispersion [51, 88, 92]. I note that Hekmatzadeh *et al.* [88] compared IX model results for nitrate breakthrough with and without dispersion for a nitrate-selective resin, and determined that models neglecting dispersion were sufficient for modeling dynamic systems for diverse operating conditions.

2.3.7 IX Model Application

After calibration and validation, the IX model was applied to simulate a range of scenarios with multiple cycles of regeneration and treatment as a function of two important design considerations, the BV used for resin regeneration and addition (or no addition) of NaCl makeup (see Table A3). Water containing 10 wt% NaCl only was used for the first regeneration cycle of all scenarios. Regeneration waste brines from this and later cycles were used for all subsequent regeneration cycles, after adjustment to reduce nitrate to 1,500 mg/L, and increase chloride to the original level via numerical NaCl addition. Each treatment cycle was modeled until nitrate breakthrough reached 44 mg/L as nitrate. A full list of the scenarios considered is provided in Table A3.

2.4 Results and Discussion

2.4.1 IX Model Calibration and Validation

Data from selected treatment (Model Treatment Exp. 4) and resin regeneration (Model Brine Exp. 4) experiments, along with model fits, are shown in Figure 2.2. The simulated treatment profiles (Figure 2.2a) and regeneration profiles (Figure 2.2b) appear to adequately match the measured profiles, with the exception of a discrepancy at early time during regeneration when experimental breakthrough is observed before 1 BV (model breakthrough starts at exactly 1 BV). This offset likely results from the assumption of ideal plug flow without dispersion (dispersion is required for breakthrough before 1 BV). Preferential flow through channels or near sidewalls could also have caused early breakthrough. Another discrepancy occurs at the beginning of treatment when model predictions of bicarbonate breakthrough (using treatment selectivity coefficients) lag behind the measured breakthrough by roughly 25 BV. This likely results from a combination of the high treatment superficial velocity preventing full equilibration time and the very low bicarbonate selectivity.

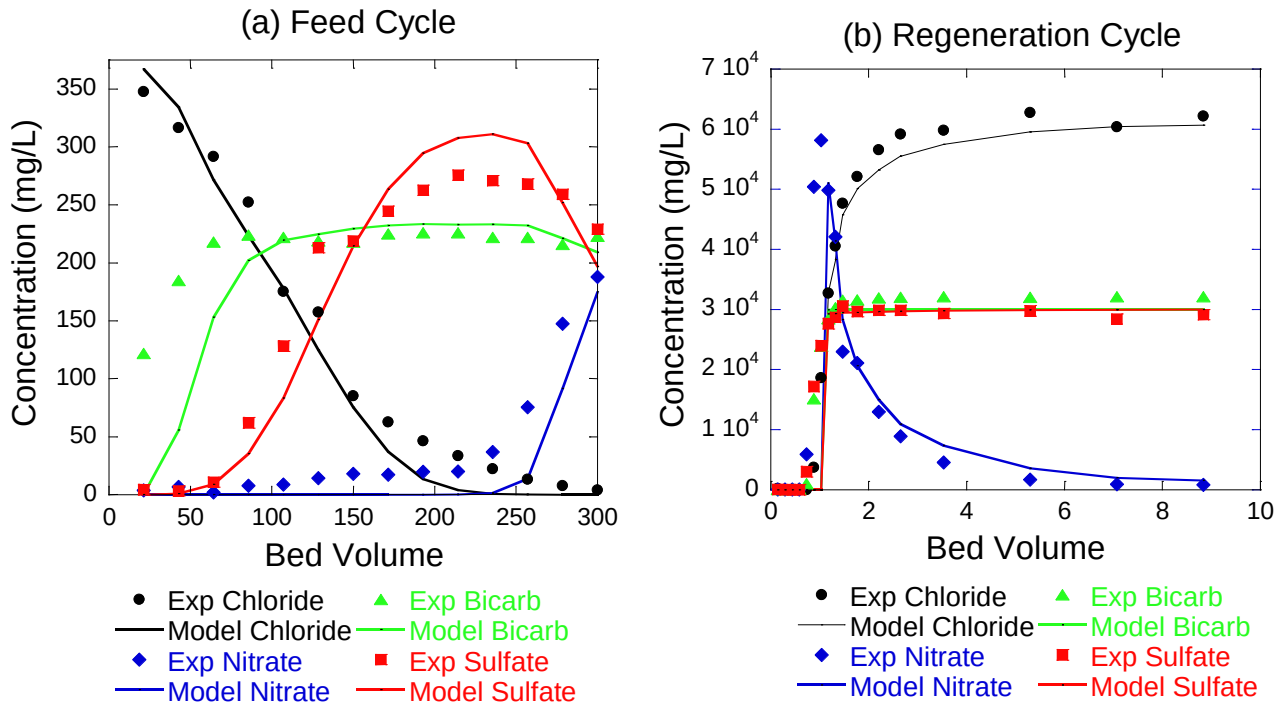

Figure 2.2: IX measurements and model fits of (a) nitrate treatment cycle and (b) resin regeneration cycle. Experiments used for model calibration are listed in Table 2.2.

The initial best-fit resin capacity parameters and selectivity coefficients for the one cycle treatment and regeneration experiments (see Table A2) were used to model the 2-Cycle Exp. 1, which was characterized by two treatment cycles separated by a regeneration cycle. This resulted in inaccurate prediction of nitrate breakthrough during the second treatment cycle (see Figure A6a), indicating model calibration using only one treatment cycle is not adequate to predict multi-cycle treatment breakthrough. A model sensitivity analysis (see Figure A5) indicated that the spatial distribution of sorbed anions in the IX column at the end of the regeneration cycle has a large effect on nitrate breakthrough during the subsequent treatment cycle. Therefore, the selectivity coefficients during brine regeneration and the resin capacity initially estimated from fits of one cycle regeneration experiments were further adjusted to

optimize model fits of nitrate breakthrough during the second cycle of the 2-Cycle Exp. 1; the treatment cycle selectivity coefficients were held constant at values determined above. Results are shown in Figure 2.3a, and the best-fit resin capacity and selectivity coefficients are listed in Table 2.3. While the fit is not exact, the simulated time to breakthrough (i.e., time when nitrate reaches the MCL of 44 mg/L) is within 17% of that measured experimentally, and major features of the breakthrough profiles (i.e., shape, plateau) are matched. The 95% confidence intervals for treatment parameters are less than 10% of fit-derived values. However, the 95% confidence interval values for regeneration parameters are up to 60% of fit-derived values. A model sensitivity analysis suggests this level of uncertainty can lead to a deviation in the cycle 2 breakthrough time of up to 22%, so the best fit parameters were further tested by using them to predict nitrate breakthrough profiles of the remaining 2-Cycle (i.e., 2-6) experiments.

Treatment results for 2-Cycle Exp. 2-3 are shown in Figure 2.3b-c. Here, regeneration was performed with a 10 wt% NaCl brine. The predicted breakthrough times in Figure 3b-c are within 2% and 0.8%, respectively, of experimental breakthrough times, and the profiles are well matched. In addition, the match improves with increasing BV used for regeneration, which is not surprising given that the IX bed becomes more uniformly chloride-saturated (i.e., closer to the initial state of the virgin resin). The results suggest the separate selectivity coefficients listed in Table 2.3 for the treatment and regeneration cycles allow adequate determination of sulfate, bicarbonate, and nitrate breakthrough in treatment and waste brines for multiple cycles of reuse under a variety of conditions, and that model accuracy improves when using greater BV for regeneration. The relatively large differences in treatment and regeneration selectivity coefficients for the same anion also call into question results from prior work [51] that used the same selectivity coefficients for both stages of the IX process.

Treatment results for 2-Cycle Exp. 4-6 are shown in Figure 2.3d-f. Here, regeneration was performed with a synthetic "treated waste brine" containing 10 wt% NaCl, 1,500 mg/L nitrate, 30,000 mg/L bicarbonate, and 30,000 mg/L sulfate. Predicted breakthrough profiles accurately simulate the earlier breakthrough of the second IX treatment cycle, resulting primarily from lower regeneration efficiency (i.e., mass of nitrate removed per mass of sodium chloride used in the brine) due to nitrate left in the brine. A comparison of Figure 2.3c and 2.3f provide the most noticeable example, as even a 10 BV regeneration with the synthetic treated brine (Fig 2.3f) does not provide full resin regeneration. A similar comparison between Fig 2.3b and 2.3e reveals a similar result.

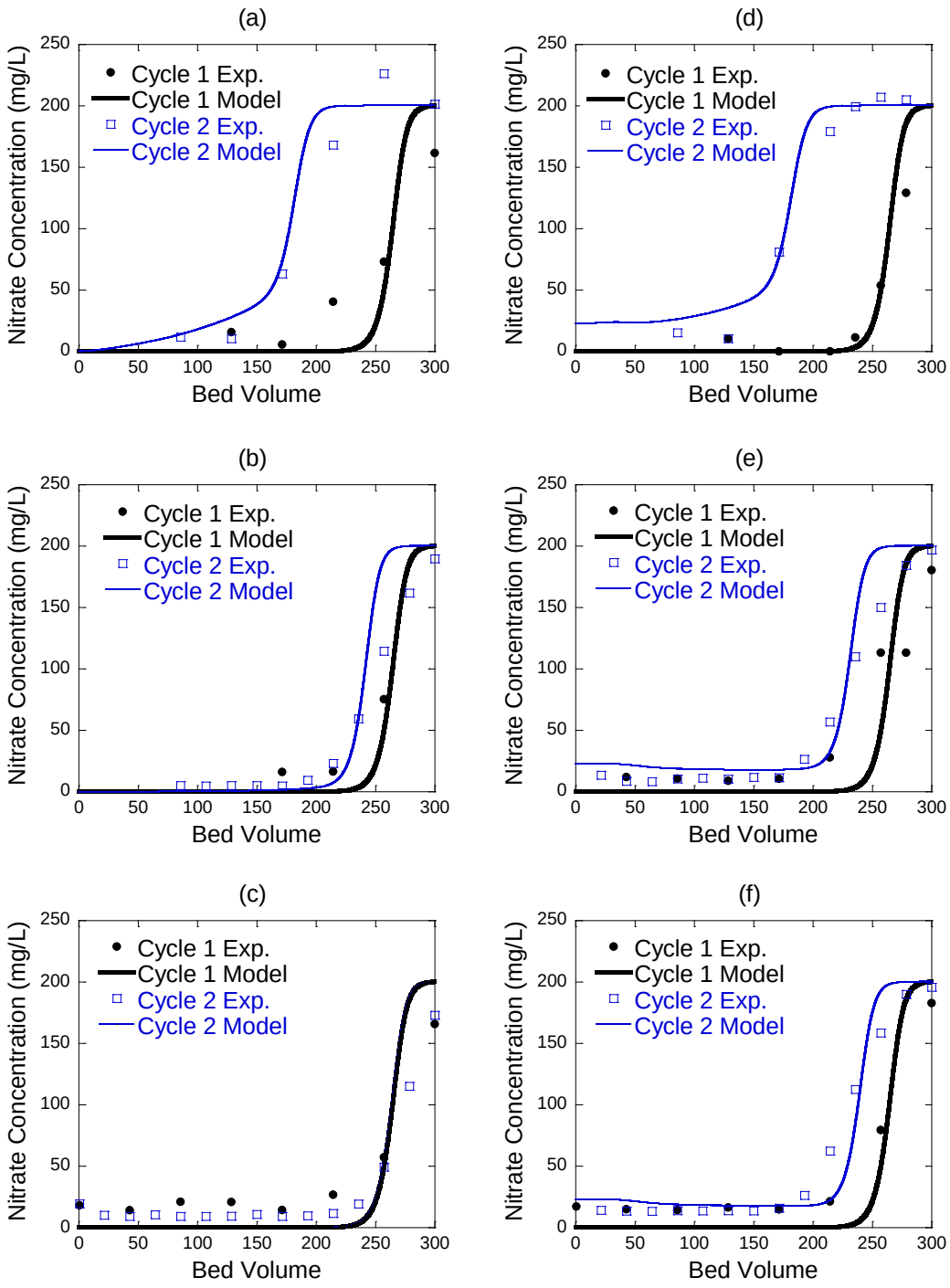

Figure 2.3: Measured versus predicted nitrate breakthrough curves during two sequential treatment cycles separated by a resin regeneration cycle using two different brines for regeneration: (a) Experimental data used to refine the regeneration selectivity parameters with 2

BV of regeneration (2-Cycle Exp. 1), and model validation (b) – (c) for 2-cycle experiments with 5 BV and 10 BV of regeneration with 10 wt% NaCl brine, (d) – (f) for 2-cycle experiments with 2 BV, 5 BV, and 10 BV regeneration with synthetic "treated waste brine" contained 10 wt% NaCl, 1,500 mg/L nitrate, 30,000 mg/L bicarbonate, and 30,000 mg/L sulfate.

Table 2.3: Best fit IX model parameters.

Ion Exchange Resin Characteristics	
Resin Name: CalRes 2105	
Resin Type: SBA Cl^- form	
Resin Selectivity: nitrate selective	
Resin Capacity: 1,096 meq/L	
Treatment Parameters	**Regeneration Parameters**
$K_C^N = 3.52 \pm 0.11$	$rK_C^N = 12.0 \pm 5.8$
$K_C^S = 0.0056 \pm 0.0002$	$rK_C^S = 0.15 \pm 0.09$
$K_C^H = 0.41 \pm 0.04$	$rK_C^H = 0.002 \pm 0.001$

2.4.2 Multi-Cycle IX Model Scenarios

The calibrated and validated IX model was then used to simulate multiple cycles of alternating IX treatment and regeneration for different brine reuse scenarios, with an assumed treatment of the waste brine nitrate down to a residual concentration of 1,500 mg/L after each regeneration cycle (to simulate catalytic treatment where ~90% of 15,000 mg/L is removed before reusing). The model runs are listed in Table A3, and allowed me to determine realistic operating conditions that would result in the most efficient design of the hybrid IX-catalyst treatment system. The buildup of unreactive bicarbonate and sulfate ions in the reused waste brine over ten cycles of treatment/regeneration is shown in Figure 2.4a for scenarios where 2 BV and 10 BV of denitrified waste brine are used for regeneration each cycle. The simulated source water was modeled after that used by a participating utility in California, 10 wt% NaCl brine was used for the first regeneration cycle, and used brine was amended with NaCl to maintain 10 wt% NaCl. As expected, the sulfate and bicarbonate concentrations buildup occurs more rapidly when using 2 BV of regeneration compared to 10 BV because more waste brine volume is required for the latter, resulting in dilution of the non-target ions removed from the resin. Bicarbonate and sulfate both reach or exceed 30,000 mg/L by the tenth cycle when using 2 BV for regeneration, which led me to use 30,000 mg/L of bicarbonate and sulfate in synthetic brines for IX experiments.

The corresponding BV of feedwater treated before nitrate breakthrough is shown in Figure 2.4b (solid lines) for cycles 1 through 10, with 5 BV of regeneration also included. Also shown is the case with no makeup NaCl addition to the denitrified brines (dashed lines). As expected, the BV treated are less for the tenth cycle than the first cycle with makeup NaCl addition, and they increase with BV of resin regeneration. Only 274 BV are treated in the tenth

cycle with 2 BV of regeneration compared to 470 BV for the first cycle; breakthrough during the tenth cycle increases to 402 BV and 420 BV, respectively when 5 BV and 10 BV of treated waste brine are used for regeneration, respectively. Despite 10 BV providing complete regeneration, the expected presence of residual nitrate in the treated waste brine (1,500 mg/L) degrades the regeneration cycle slightly and results in less nitrate treatment before breakthrough (420 BV versus 470 BV for virgin resin). Results from earlier cycles indicate that the decrease in BV of treatment before nitrate breakthrough occurs mainly between cycles 1 and 2 for all scenarios, and then levels off. This indicates that the 1,500 mg/L residual nitrate in the treated waste brine is principally responsible for the lower regeneration efficiency and reduced number of BV for breakthrough in the subsequent cycle rather than the buildup of sulfate or bicarbonate in the waste brine.

Model simulations show that without addition of makeup NaCl to the brine following each regeneration cycle, the salt's concentration will eventually be depleted and no resin regeneration can occur. Not adding makeup NaCl to the brine limited the number of times it could be reused before failing to regenerate the resin, due to the loss in NaCl during each cycle. As shown in Figure 2.4b, longer regeneration time extends the number of brine reuse opportunities, with 2 BV being reused five times, while 5 BV and 10 BV can be reused for all ten cycles, but to different levels of success. The increased reuse capability without makeup NaCl between 2 BV and 10 BV is simply a byproduct of the larger initial volume of brine used and the relatively small fraction of total chloride lost from brine during each resin regeneration cycle (3.2% for 10 BV versus 11.5% for 2 BV). Hence, makeup salt addition is very important for all regeneration BV below 10 for up to 10 cycles of treatment/regeneration before brine

replacement. It is important to note that makeup NaCl has only a marginal effect when using a 10 BV regeneration, given the small fraction chloride lost each cycle.

The total number of treatment BV after 10 cycles is shown in Figure 2.4c (red line boxes), along with NaCl requirements with reuse (solid green). Also shown are the NaCl requirements for IX treatment when brine reuse is not considered (blue diagonal lines). As expected, more regeneration BV allow for more BV of nitrate treatment over 10 cycles, and more regeneration BV incur higher NaCl requirements. However, the increase in NaCl with more regeneration BV is only a small fraction of the NaCl required when reuse is not considered, regardless of the number of regeneration BV used. These results suggest that there is a tradeoff between more treatment and higher NaCl demands with or without brine reuse.

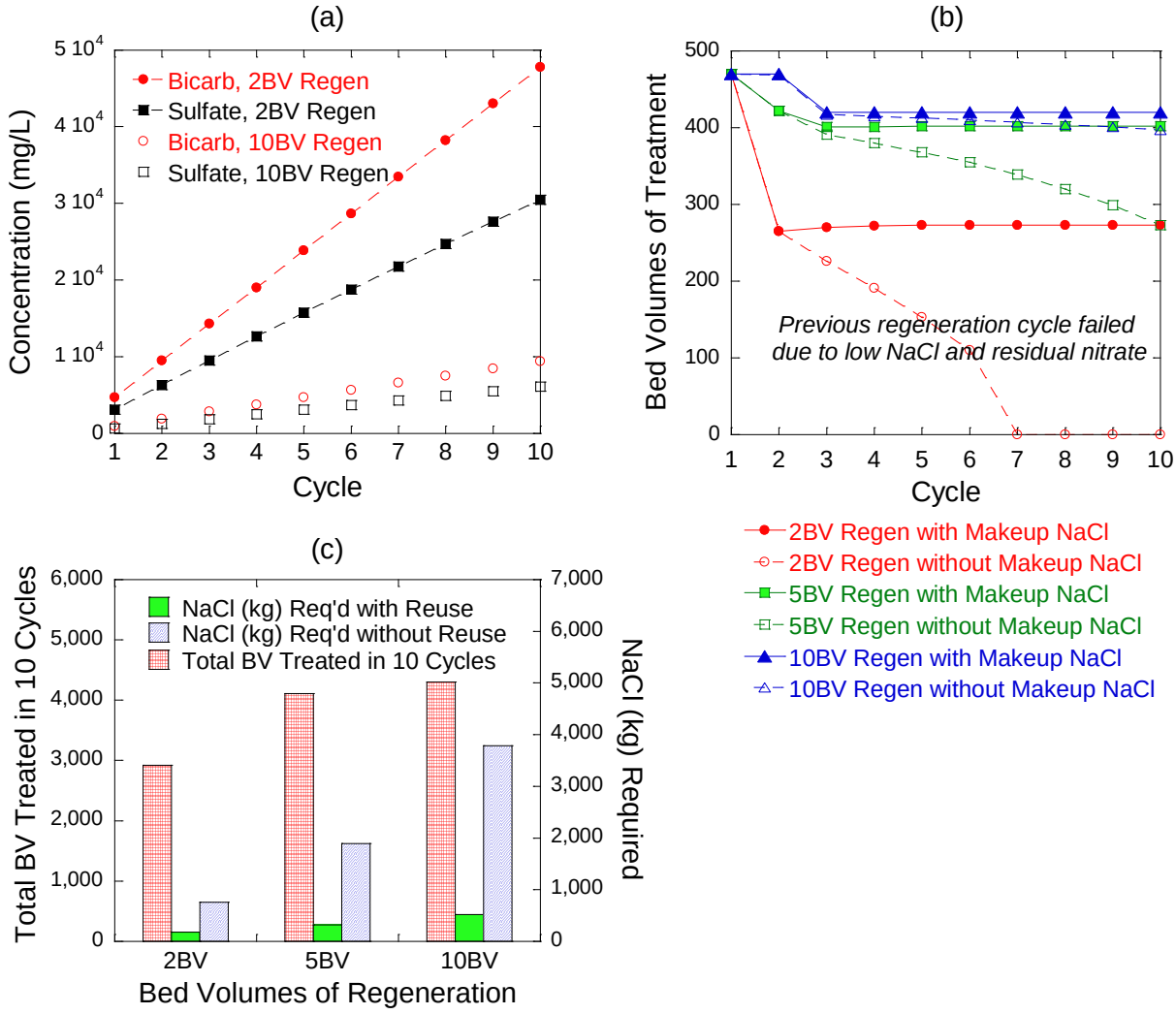

Figure 2.4: Model simulation results showing (a) buildup of bicarbonate and sulfate in waste brine when using 2 BV and 10 BV regeneration scenarios, (b) impact of the number of regeneration BVs and NaCl makeup addition on the number of BV before nitrate breakthrough during the next treatment cycle, (c) total bed volumes of groundwater treated over ten treatment/regeneration cycles as a function of the number of BV used for regeneration, and total mass of NaCl required for resin regeneration with and without brine reuse.

2.4.3 Packed Bed Catalytic Reactor Experiments

Continuous nitrate reduction in both synthetic and real waste brines was evaluated in a packed bed, flow-through catalytic column reactor (see Table A1). A schematic of the experimental set-up is shown in Figure A2. The NaCl and nitrate levels in the synthetic brine mimicked those obtained from a real waste brine sent to my laboratory in 2011. The synthetic brine was amended with elevated concentrations of bicarbonate and sulfate to mimic concentrations produced in model simulations where waste brine was subjected to many cycles of reuse (see previous sections).

The results of nitrate reduction in synthetic brines are shown in Figure 2.5. For all synthetic brine formulations, the reactor effluent nitrate concentrations were relatively constant, with fluctuations ranging between 40 - 60% of the influent concentration that did not trend with time. At least some of the fluctuations are related to the superficial velocity, i.e., when the superficial velocity decreases slightly, so does the effluent nitrate concentration (due to a longer retention time). Apparent zero order rate constants were calculated for each day based on the retention time plus influent and effluent measurements; an average value of 13.35 ± 3.27 mg NO_3^- min^{-1} L^{-1} was obtained. The corresponding Pd-mass normalized rate constant was 2.07 ± 0.26 mgNO_3^- g_{Pd}^{-1} min^{-1}. The selectivity for dinitrogen gas ranged between 73-87% for the samples tested (see Table A1). I note that the column reactor could have been designed with a longer retention time to achieve a higher level of nitrate reduction, but the intermediate level achieved was targeted to evaluate potential inhibitory effects of sulfate and bicarbonate. Zero order kinetics were assumed based on batch results that showed this behavior when treating elevated nitrate concentrations. The lack of any notable effect of either high concentrations of

sulfate or bicarbonate contrasts with results reported previously in completely mixed batch experiments [51].

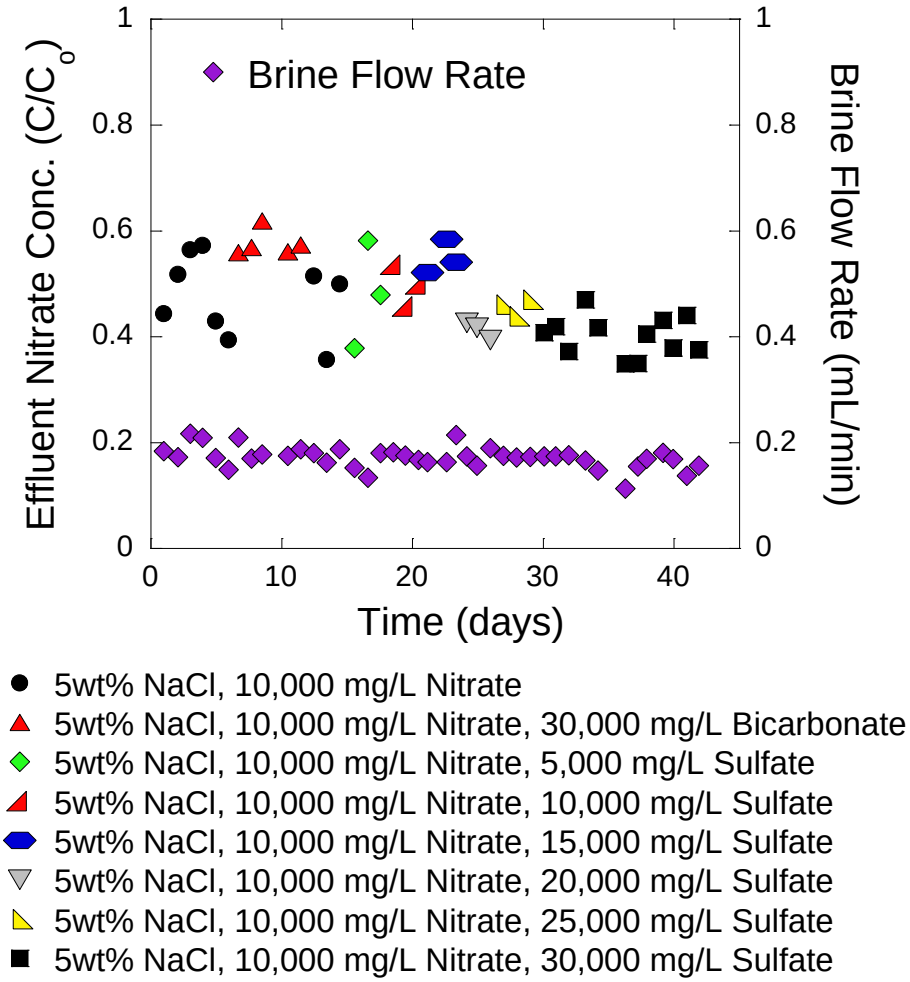

Figure 2.5: Nitrate reduction in synthetic brines by treatment in a continuous flow fix-bed catalytic reactor for 45 d with 0.5 wt% Pd-0.05 wt% In/C catalyst. NaCl concentration was fixed at 5 wt% and nitrate at 10,000 mg/L.

The results of nitrate reduction in the real brine are shown in Figure 2.6. The real brine was not recycled and contained the same anions as the synthetic brine plus lesser concentrations of other constituents (ICP analysis showed 11.1 mg/L calcium, 3.14 mg/L magnesium, 2.94 mg/L phosphorous, 0.09 mg/L iron, and 0.014 mg/L manganese). Over the 23-day study period, no change in activity for nitrate reduction was observed, with an average mass-normalized rate constant of 2.24 ± 0.22 $mgNO_3^-\ g_{Pd}^{-1}\ min^{-1}$, and 81 ± 11% selectivity for the dinitrogen product (see Table A1). Thus, results with the real waste brine are consistent with experiments conducted in the synthetic brines.

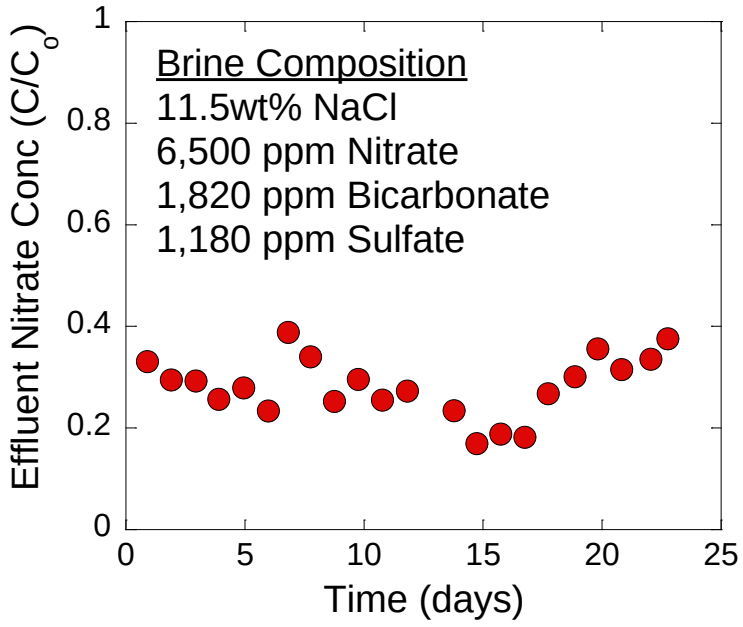

Figure 2.6: Nitrate reduction in a real waste IX brine from a California utility in a continuous flow fix-bed catalytic reactor for 23 d with 0.5 wt% Pd-0.05 wt% In/C catalyst.

The same catalyst packed into the column reactor (0.5%Pd-0.05%In/AC) was also tested in a batch reactor, where rapid mixing and excess hydrogen addition minimize mass transfer

limitations. Under these conditions, an apparent zero order rate constant of 57.32 ± 6.31 $mgNO_3^- g_{Pd}^{-1} min^{-1}$ was obtained, approximately 25 times greater than the corresponding rate constant obtained from data collected in the continuous-flow column reactor experiments. Based on the superficial velocities of hydrogen gas (0.81 m/hr (6.8 mL/min)) and brine (10,000 mg/L nitrate at 0.024 m/hr (0.2 mL/min)) in the column reactor, the stoichiometric ratio of hydrogen to nitrate-N entering the column was 8.6H:1N, a value more than three times the minimum stoichiometric ratio required for nitrate reduction to dinitrogen gas. Since H_2 was present in excess, the low column reaction rates indicate hydrogen mass transfer is likely limiting nitrate reduction. This is not surprising given the low aqueous solubility of hydrogen (0.8 mM at ambient temperature in equilibrium with 1 atm P_{H2}), which at saturation provides only 0.4-1% of the stoichiometric hydrogen needs for reduction of aqueous nitrate in the waste brine (80 mM-160 mM). The H_2 mass transfer limitations may also explain why no apparent loss in nitrate reduction activity was observed in the presence of elevated bicarbonate and sulfate in the packed bed reactor experiments. Although these ions might lower the intrinsic rate of nitrate reduction on the catalyst surface [51], this effect would be masked by the fact that the overall rate is limited by the much lower rate of H_2 mass transfer in the column reactor, rather than the surface reactions in the well-mixed batch system.

Although H_2 mass transfer limitations appear to affect apparent nitrate reduction rates, the results suggest that elevated sulfate and bicarbonate in the synthetic brine, and the many constituents present in real brine, do not progressively degrade catalyst performance over time. However, further experiments are required to confirm these results, as longer times need to be evaluated to ensure that any progressive losses are not being masked by H_2 mass transfer limitations.

Pintar, *et al.* [38] tested Pd-Cu/γ-Al_2O_3 in a column system and experienced a loss in catalytic activity after many cycles. They ruled out copper leaching as an explanation, and instead postulated that the loss in activity occurred as a result of the build-up of chloride in their brine, or hydroxide ions as nitrate reduction proceeds. Prior work [51] indicates high chloride levels may lower Pd-In/C activity, but chloride levels are maintained constant in the hybrid system proposed here and pH is buffered by CO_2 addition to the feed gas..

2.4.4 Hybrid IX-Catalyst System Considerations

The IX and catalyst results described above suggest that the choice of brine regeneration BV affects the economics and environmental impact of the hybrid system. It affects not only total salt use and BV treated, but also the amount of catalyst required in the reactor design. The effects of the number of BV used for regeneration on the treatment of one billion gallons of water with the hybrid system was simulated (Figure 2.7) and compared to simulations for conventional IX treatment without brine reuse. Calculations were based on multi-cycle model simulations and IX system information from the Vale, OR demonstration plant study (0.5 MGD), which had a single-pass IX configuration that treated water at 540 gpm [31]. The IX bed volume size at the Vale, OR site is 5,266 L (1,391 gal), and the cost of NaCl was $0.076/lb [31], and waste brines were disposed and replaced with fresh brine after every 10 treatment/regeneration cycles. Catalyst requirements for denitrifying the simulated waste brine to a level of 1,500 mg/L NO_3^- were estimated using the zero-order rate constants from the fixed-bed reactor (2.24 $mgNO_3^- g_{Pd}^{-1} min^{-1}$) and sequencing batch reactor (57 $mgNO_3^- g_{Pd}^{-1} min^{-1}$), which both used the same 0.5 wt%Pd-0.05wt%In/C catalyst. The catalyst reactors were sized according to the need to treat the generated waste brine volume before nitrate breakthrough from the IX reactor occurs. For

example, 2 BV of waste brine required a superficial velocity through the catalyst reactor of 15 L/min in order to complete waste brine treatment in 11.7 h, the time corresponding to breakthrough at 274 BV of IX run time. The price of palladium was assumed to be $800/oz, taken from a one year average between May 6, 2014 and May 6, 2015 [110]. The price of In is small compared to Pd (ca. $21/oz [111]) and was neglected.

The cost of NaCl with and without brine reuse with respect to different regeneration volume is shown in Figure 2.7a. When brine is not reused, a 10 BV regeneration strategy requires more than three times as much NaCl as a 2 BV regeneration strategy (2,591 ton vs 8,793 ton). Alternately, when brine is reused, the quantities are much lower and the difference is much smaller (612 ton vs 1,204 ton). Thus, by switching from 2 BV regen without brine reuse to 10 BV regen with brine reuse, the plant operator would see a 53% reduction in total NaCl required and 150% increase in treatment length each cycle (274 BV to 420 BV).

The efficiency of NaCl use as a ratio of BV of water treated per kilogram of NaCl used is shown in Figure 2.7b. The results show a clear benefit to brine reuse (solid red), which leads to an increase in the volume of water treated per unit mass of NaCl used by a factor ranging between 4.2 and 7.3. The results also show a clear benefit in reduced salt costs when regenerating resins with only 2 BV compared to 5 or 10 BV.

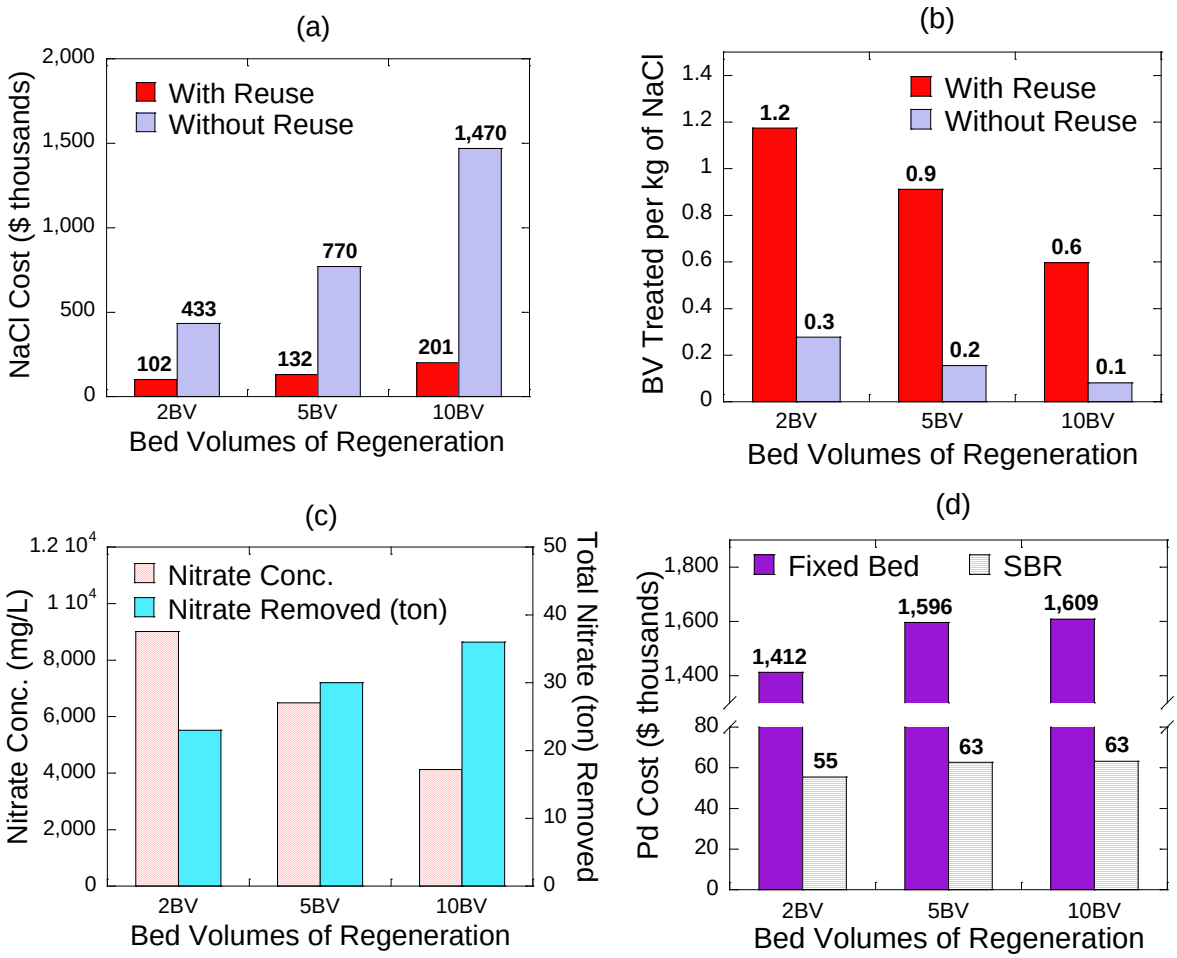

Figure 2.7: Analysis of hybrid system requirements to treat one billion gallons of water using different BV for regeneration between each nitrate treatment cycle with and without brine reuse. (a) Cost of NaCl required. (b) Efficiency of NaCl use – defined as BV water treated per kilogram of NaCl required. (c) Nitrate concentration in the waste brine before catalytic reduction and total mass of nitrate removed from waste brine when treating 1 billion gallons of water. Higher concentrations require more reduction to reach the desired 1,500 mg/L level, which impacts the catalyst required. (d) Catalyst cost as a function of regeneration BV for fixed bed and sequencing batch reactor configurations.

The average nitrate concentration in the waste brine prior to catalytic treatment (diagonal red lines), as well as the total mass of nitrate removed from the waste brine to treat 1B gallons (solid blue), are shown in Figure 2.7c. Nitrate concentration in the waste brine, as well as volume of waste brine to be treated and time available for treatment, are all impacted by the volume of brine used for regeneration. Together, these variables impact one of the most expensive parts of the hybrid system capital costs, which is palladium metal for the catalyst reactor. These estimated costs are shown in Figure 2.7d for 2, 5, and 10 BV of regeneration. A 2 BV regeneration produces a smaller volume of waste brine with a higher nitrate concentration compared to a 5 or 10 BV regeneration. Treating a smaller volume of waste brine requires a smaller catalyst reactor (and hence less Pd mass), while a higher nitrate concentration requires more catalyst. The simulation indicates the former factor dominates overall Pd metal costs, so Pd metal costs tend to decrease with decreasing BV used for resin regeneration.

Catalyst costs are also influenced directly by catalyst activity level. The anticipated costs of Pd required to reduce nitrate in the waste brine to 1,500 mg/L nitrate using the mass normalized zero order rate constant for both the fixed bed system and sequencing batch reactor are also shown in Figure 2.7d. As discussed above, catalyst activity in the fixed bed is relatively low compared to the batch system due to hydrogen mass transfer limitations, resulting in prohibitively high palladium costs (solid purple), i.e., costs that far exceed the savings associated with reduced salt usage. However, costs for Pd are much lower when the catalyst activity from the SBR is used to estimate Pd mass requirements (horizontal red lines). Considering the SBR activity, a 2 BV regeneration leads to nitrate concentrations around 9,000 mg/L and an anticipated reactor palladium cost of $55.5k; whereas 10 BV regeneration leads to nitrate concentrations around 4,100 mg/L and a palladium cost of about $63.2k. These capital costs are

50% or lower than the savings resulting from reduced salt requirements when treating 1 billion gallons of sourcewater, and highlight the promise of the hybrid system. Also important to note is that the savings from brine reuse would increase, while catalyst costs would remain unchanged, if a larger volume of sourcewater was considered (i.e., more than 1 billion gallons) or waste brine were reused for more than ten treatment/regeneration cycles before replacing with fresh brine. The actual volume treated with the same catalyst depends on catalyst longevity, and results from this study suggest the catalyst is stable over at least 45 days of continuous treatment.

Activity differences between the batch and fix bed reactors, and their resulting impact on catalyst costs, highlight limitations of the latter. Improved fixed-bed reactor design is crucial in order to minimize hydrogen mass transfer limitations. This would decrease both the amount of excess hydrogen and the amount of Pd metal required. Minimizing both hydrogen and Pd usage are critical for reducing costs and the environmental impact of the hybrid system [51].

Several factors associated with the hybrid system may necessitate re-thinking IX operations to maximize benefits. Longer regeneration times increase the number of BV treated during each cycle and decrease the nitrate concentration reduction required via catalytic treatment. However, longer regeneration times also increase the salt required for regeneration and the amount of Pd metal needed for nitrate reduction. Hence, a 2 BV regeneration length results in the lowest IX and catalytic treatment costs in the hybrid system compared to 5 and 10 BV. These results may change if brines can be reused more than the assumed 10 treatment/regeneration cycles before disposing and replacing with a fresh regenerant brine. Other salt-related factors such as unit price, delivery frequency, delivery size, plant storage capacity and use rate are important in determining plant operations and may constrain the hybrid system.

Larger regeneration brine BV would also require larger volume storage tanks with associated higher capital costs.

Near-complete nitrate removal from the waste brine would be ideal, particularly given the results discussed above. Regardless of IX configuration and regeneration strategy, the nitrate level remaining in the waste brine has an impact on future treatment length. Research focused on biological denitrification of waste brine achieved near-complete removal of nitrate in the waste brine [37, 43], which undoubtedly aided in the hybrid process's successful results. Near-complete nitrate removal via catalysis is achievable; however, balancing the requirements to do so and the associated life cycle impacts are critical to developing a hybrid system that is a more sustainable option compared to a conventional IX system. For example, Choe *et al* .[51] showed 87-95% nitrate reduction in a packed bed reactor, but the LCA results determined the packed-bed hybrid-IX design had higher environmental impacts than the conventional IX design. Catalytic reactor optimization and iterative Life Cycle Assessment will both be important in future work on the hybrid system.

2.5 Conclusions

A hybrid ion exchange-catalytic process for nitrate treatment leveraging brine reuse shows promise for reducing economic costs and environmental burdens associated with large salt inputs and waste brine disposal. Key conclusions include:

- Integrated models for hybrid IX/catalyst treatment systems can be used to examine critical factors influencing the cost, performance, and environmental impact.

- Model simulations indicate that non-target ions like sulfate and bicarbonate will buildup in waste brines over repeated cycles of reuse, but this buildup will not negatively impact IX performance or lead to permanent deactivation of the Pd metal catalyst.
- Adding makeup salt to treated waste brines is necessary to maintain long treatment cycle run times between regeneration.
- Salt costs and waste brine volumes can be decreased by up to 80% with the hybrid system.
- Achieving high catalyst activity and stability is critical for reducing the cost of the hybrid system.
- Reactor design plays an important role in the effectiveness of hydrogen mass transfer.
- Tradeoffs between regeneration length, treatment time, and salt warrant reevaluation in a hybrid system compared to a conventional system.

CHAPTER 3

CATALYTIC DENITRIFICATION IN A TRICKLE BED REACTOR: ION EXCHANGE WASTE BRINE TREATMENT

3.1 Abstract

Catalytic reduction of nitrate in ion exchange waste brine for reuse is a promising option for reducing ion exchange costs and environmental impacts. A recycling trickle bed reactor (TBR) was designed and optimized using 0.5wt%Pd-0.05wt%In catalysts supported on US Mesh size 12x14 or 12x30 activated carbon particles. Various liquid superficial velocities (U_L) and hydrogen gas superficial velocities ($U_{g\text{-}H2}$) were evaluated to assess performance in different flow regimes; catalyst activity increased with $U_{g\text{-}H2}$ at all U_L for both catalysts, and was greatest for the 12x30 catalyst at the lowest U_L (8.9 m/hr). The 12x30 catalyst demonstrated up to 100% higher catalytic activity and 280% higher mass transfer rate compared to the 12x14 catalyst. Optimal TBR performance was achieved with both catalysts in the trickle flow regime. The results indicate the TBR is a promising step forward, and continued improvements are possible to overcome remaining mass transfer limitations.

3.2 Introduction

Nitrate removal from drinking water using ion exchange (IX) is common and very effective. However, a brine is required for IX resin regeneration, and the cost of required salt can be up to 78% of the total ion exchange operations and maintenance budget [31]. Brine disposal can also be costly; depending on location and regulations, multiple options are available (i.e., deep well injection, evaporation pond, wastewater treatment plant) and can cost between

$0.60 and $4.44/1,000 gal of treated drinking water, approaching the cost of water treatment itself ($4.58/1,000 gal) [35]. Brine disposal also poses environmental risks for terrestrial and aquatic ecosystems [2, 112]. For these reasons, waste brine treatment to enable brine reuse has become an area of focus.

Treating waste brine to enable reuse has been shown to be technically feasible using both biological [37, 40, 43] and chemical means [51–53]; however, both methods have drawbacks. Biological treatment is sensitive to influent nitrate loading, has long start-up times and raises concerns over pathogens in drinking water. Among the chemical treatment methods, catalytic treatment using Pd-based metals shows the most promise. Catalytic treatment may suffer from high costs associated with the use of expensive precious metals. The latter technology is the focus of this effort because it is more robust to variable treatment conditions and remote operation, and a recent cost analysis suggests it can be a viable option if fixed-bed reactor activity can be improved [65].

During catalytic denitrification, hydrogen gas serves as the electron donor for nitrate reduction over a bimetallic catalyst. The proposed reaction pathway during nitrate reduction follows [64]:

$$NO_3^- + H_2 \rightarrow NO_2^- + H_2O \quad (1)$$

$$NO_2^- + 1.5H_2 \rightarrow 0.5N_2 + H_2O + OH^- \quad (2)$$

$$NO_2^- + 3H_2 \rightarrow NH_4^+ + 2OH^- \quad (3)$$

The most common catalysts combine Pd with a promoter metal, typically In or Cu, both supported on a porous solid [113]. In catalytic waste brine treatment, nitrate competes for reactive sites with other common ions found in waste brine, (i.e., chloride, bicarbonate and

sulfate), which can lower the overall activity of the catalyst [51]. While relatively high rates of nitrate reduction activity in waste brine have been obtained for experiments conducted in well mixed batch reactors where catalyst-to-water ratios are low, hydrogen mass transfer limitations in packed-bed reactors (where catalyst-to-water ratios are high) have limited nitrate reactivity to a small fraction of that observed in batch [51, 65]. Packed-bed reactors are the most likely configuration that would be deployed at water treatment facilities, due to ease of catalyst handling and low catalyst attrition rate. H_2 mass transfer from gas to water, and mass transfer through the bulk water phase to the catalyst surface, can both limit overall reactivity. Mass transfer limitations can translate into larger catalyst beds, and therefore greater reactor capital cost.

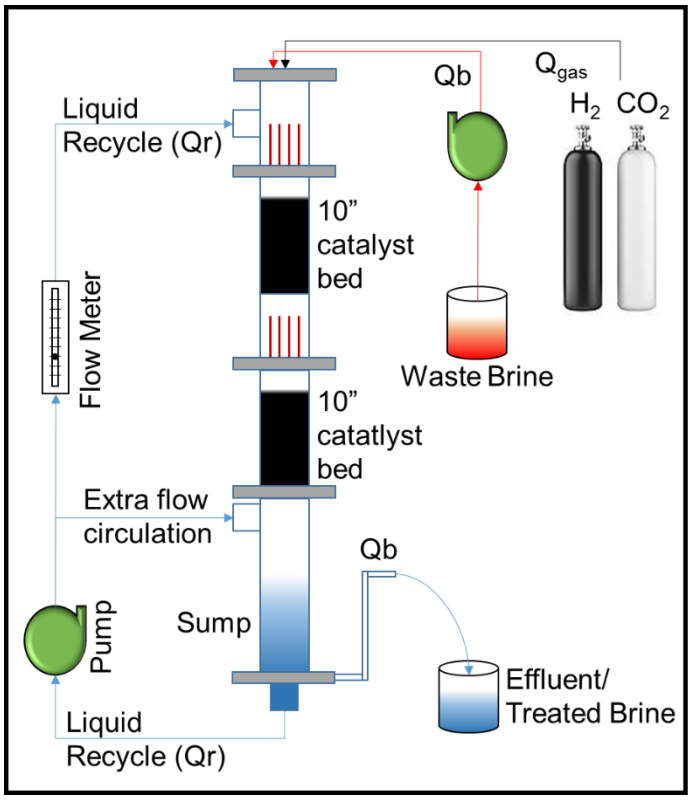

Figure 3.1: Diagram of the trickle bed reactor

Very little effort has been devoted to designing practical packed-bed reactors for catalytic nitrate reduction that minimize hydrogen mass transfer limitations. Among the most promising options are trickle bed reactors (TBR) (see Figure 3.1). TBRs are typically employed as co-current down-flow reactors, often with multiple beds of catalyst and liquid-gas redistribution between beds. They are often characterized by high gas to liquid mass transfer rates, and are used extensively in a variety of industrial applications, i.e., petroleum processing, oxidation reactions, and hydrogenation reactions [85, 114]. One form of a TBR, i.e., the trickling filter or biofilter, is common in wastewater treatment and used for biological nitrification [115], to remove organic matter [84] and, more recently, for biological denitrification [116]. The authors are unaware of any catalytic TBR used for drinking water purification in the U.S.

TBRs typically operate in one of four flow regimes (see Figure 3.2). The trickle flow regime is characterized by a continuous gas phase with relatively high gas superficial velocities, low liquid superficial velocities, and incomplete catalyst wetting. Higher gas superficial velocities and low liquid superficial velocities result in the spray flow regime, which has a continuous gas phase and highly dispersed liquid due to high shear forces. The pulse flow regime occurs with relatively high gas and liquid superficial velocities, with the bed having discontinuous gas and liquid flow. Lastly, the bubble flow regime occurs at relatively high liquid superficial velocities and low gas superficial velocities, and is characterized by a continuous liquid phase and complete catalyst wetting. Transitions between regimes vary with reactor size and operating conditions (e.g., temperature, pressure, superficial velocities), particle size/material, and gas/liquid properties (e.g., density, viscosity, surface tension) [85, 117].

The overall objective of this work is to develop a catalytic trickle bed reactor for nitrate removal from ion exchange waste brine with minimal overall hydrogen mass transfer limitations

to the catalyst surface. The specific objectives are to: 1) Design and build a lab-based pilot-scale TBR, 2) Evaluate TBR performance as a function of liquid and gas superficial velocities and activated carbon catalyst support size, 3) Develop a reactor model to estimate hydrogen mass transfer coefficients for the conditions tested, 4) Determine the effects of hydrogen mass transfer limitations on TBR performance, 5) Identify the TBR conditions that result in optimal performance, and 6) Identify the critical factors limiting nitrate reduction in the TBR.

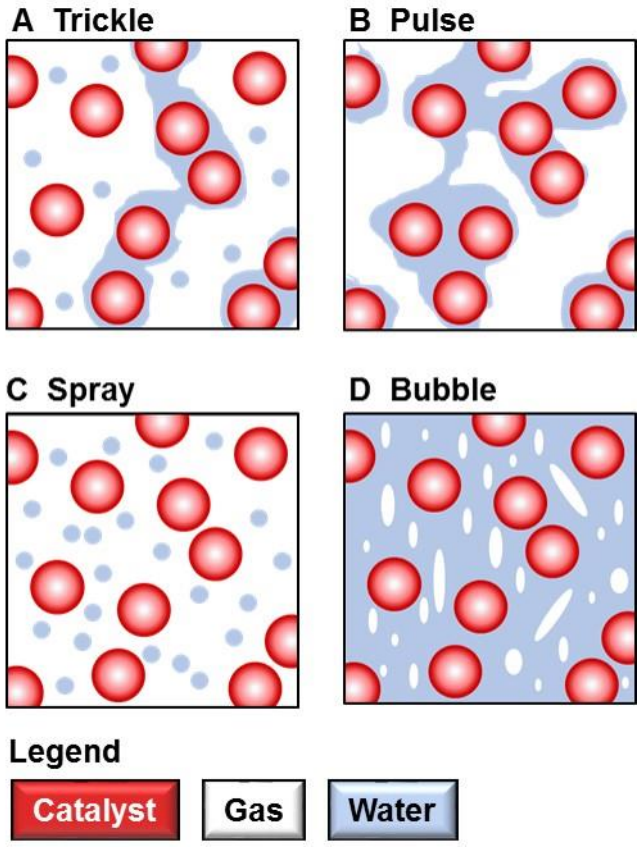

Figure 3.2: Diagram of the four primary flow regimes in TBRs, adapted from [81]

3.3 Methods

3.3.1 Chemical reagents and analytical methods.

Reagent-grade sodium salts (≥99% purity) of nitrate and chloride were obtained from Fisher. Tanks of H_2 (99.999%) and CO_2 (99.9%) were purchased from Praxair and Airgas, respectively. All synthetic brines were prepared with deionized (DI) water. Two 0.5wt%Pd-0.05wt%In/AC catalysts (U.S. mesh support sizes of 12x14 and 12x30) were provided by Johnson Matthey Inc. Previous work determined this metal ratio was the most active for nitrate reduction in waste brine [51]. Inert 12x14 carbon support was provided by Calgon Carbon. ICP analysis of fresh 12x14 catalyst confirmed metal loadings of 0.46 ± 0.06 wt% Pd and 0.05 ± 0.01 wt% In. ICP analysis of fresh 12x30 catalyst confirmed metal loadings of 0.51 ± 0.08 wt% Pd and 0.06 ± 0.01 wt% In. For simplicity, the metal loadings will be referred to by the nominal weight of 0.5wt%Pd and 0.05wt%In.

Aqueous chloride, nitrate and nitrite concentrations were quantified using ion chromatography with conductivity detection (Dionex ICS-2100, 4x250 mm IonPac AS-19). A superficial velocity of 1.0 mL/min, 32 mM KOH eluent concentration and 96 mA suppressor current were used. All samples and reference standards were diluted 50-fold prior to IC analysis. Ammonia concentrations were measured using the Hach High-Range test kit and a UV spectrophotometer (Nanodrop). External standards bracketing the concentration ranges of interest were used to calibrate all methods.

3.3.2 Batch Experiments

Batch experiments were performed as previously described [65] in a rapidly mixed and vigorously H_2-sparged round-bottom, five-neck flask. A synthetic waste brine containing 5,000

mg/L nitrate and 10 wt% NaCl was introduced to 150 mL DI water solution containing 1.0 g of catalyst. Solution pH was maintained at 5.0 using HCl via an automated titration manager (Radiometric Analytical TIM 840), and aqueous samples were periodically collected for analysis.

3.3.3 TBR Design

A continuous flow TBR was constructed from 5.08 cm (2") ID polyvinylchloride (PVC) (see Figure 3.1). Liquid phase recycle was used to accommodate space constraints in the laboratory and eliminate the need for mixing extremely high volumes of concentrated brine solution. The column was packed with two 25 cm (10") catalyst beds using 0.5wt%Pd-0.05wt%In on activated carbon support (Pd-In/AC). Catalysts with two different support sizes were tested, US mesh 12x14 and 12x30, both with the same metal loading. The ratio of reactor diameter to particle size (D/dp) exceeded 25, which is recommended to avoid wall effects and achieve plug flow [80].

Table 3.1: Materials and characteristics of the TBR

Catalyst Size (U.S. Mesh)	12 x 14	12 x 30
Particle Diameter, dp (mm)	1.68 - 1.41	1.68 - 0.595
Ave. Particle Diameter (mm)	1.545	1.137
D / dp (-)	33	44
Void Fraction (-)	0.43	0.43
Bulk Density (g/mL)	0.44	0.408
Mass of Catalyst Used (g)	479.9	499.44
Metal Loading (wt%)	0.5wt%Pd - 0.05wt%In	
Support Material	Activated Carbon	
Reactor Diameter, D (in (mm))	2 (50.8)	
Reactor Body Material	Harvel Clear PVC	

The total mass of catalyst used in the TBR was roughly 480 g (12x14) and 500 g (12x30). The porosities of catalyst beds packed with both support materials were measured to be 0.43 by pore volume displacement. Table 3.1 lists the TBR characteristics. Each bed was supported by 2.54 cm (1 in) of 6/0 crafting seed beads (3.77 mm diameter) and a 24 mesh wire cloth (c. 0.7 mm), both supported over a porous acrylic plate. Twenty-four 1.56 mm (1/16") diameter holes were drilled into each of two acrylic distributor plates to accommodate liquid superficial velocities between 8.9 – 28.12 m/hr (300 – 950 mL/min). Four 6.35 mm (1/4") stainless steel tubes were inserted in each acrylic plate to accommodate gas flow, with numerous 1.58 mm (1/16") perforations to facilitate gas flow.

3.3.4 TBR Experimental Protocol

A full list of experimental conditions is provided in Table 3.2. A synthetic brine (150 L) was prepared using deionized (DI) water with 10 wt% NaCl and 15,000 mg/L nitrate (1.5wt%). The brine was pumped (Masterflex peristaltic) at 2 to 4 mL/min to the top of the TBR via 1/4" Tygon tubing (L/S 16), where it mixed with the recycle flow (Danner AquaMag pump) that was measured via a rotameter (Omega). Liquid superficial velocities (U_L) varied between 8.9 – 28 m/hr, which corresponded with liquid recycle flow rates (Q_r) between 300 and 950 mL/min. These liquid superficial velocities fall within the range of typical commercial scale reactors [118]. Recycle superficial velocities were adjusted by closing or opening a diaphragm valve on the internal flow line, which increased or decreased, respectively, the recycle flow.

The synthetic brine superficial velocity (U_b) of 0.06 m/hr (Q_b = 2 mL/min) was evaluated for both catalysts. For the 12x30 catalyst, high nitrate removal efficiency at U_L = 8.9 m/hr necessitated testing U_b = 0.09, 0.10, and 0.12 m/hr (Q_b = 3.0, 3.5 and 4.0 mL/min) as well (see

Notes in Table 3.2). Influent waste brine samples were taken from the 150 L brine feed reservoir, and effluent samples were taken 2-3 times daily from the effluent line. Samples were stored at room temperature prior to analysis.

Hydrogen and carbon dioxide gases were delivered to the top of the reactor via two mass flow controllers (Alicat Scientific) and 1/8" stainless steel tubing. Hydrogen gas superficial velocity ($U_{g\text{-}H2}$) was added as the electron donor at superficial velocities of 0.59, 0.88, 1.18, 1.77, 2.37, 2.64 m/hr (20, 30, 40, 60 80, and 90 sccm), which correspond to $H_{(g)}/N_{(aq)}$ molar ratios of 1.8, 2.7, 3.7, 5.5, 7.4, and 8.3, respectively, at the column inlet. The minimum required stoichiometric molar ratio for nitrate reduction to dinitrogen gas is 2.5, and for nitrate reduction to ammonium is 4.0.

Carbon dioxide was added for pH control to maintain pH < 8.0, with the exception of some experimental conditions noted in Table 3.2 where the pH remained below 8.75. At these conditions, equipment limitations prevented higher CO_2 flow. All testing was done at atmospheric pressure and ambient temperature (27 ± 1 °C).

Table 3.2: Experimental Conditions Tested in the TBR

12 x 14 Catalyst				
Liquid Superficial Velocity (m/hr)	8.9	14.8†	19.8	28.12
Hydrogen Gas Superficial Velocity (m/hr)	0.59, 1.18, 1.77	0.59†$^{\varphi}$, 0.88, 1.18, 1.77†*	0.59, 0.88, 1.77	0.59, 1.18, 1.77
12 x 30 Catalyst				
Liquid Superficial Velocity (m/hr)	8.9	14.8	20.7	28.12
Hydrogen Gas Superficial Velocity (m/hr)	0.59, 1.18‡*, 1.77*, 2.37¥*, 2.64§*	0.59, 1.18$^{\varphi}$, 2.37*	0.59, 1.18, 2.37	0.59, 1.18, 2.37

Notes

Brine made from DI water
Brine Superficial Velocity = 0.06 m/hr unless noted below
† Conditions tested in 12 x 14 dilution experiment
‡ Brine Superficial Velocity = 0.06, 0.09 m/hr
¥ Brine Superficial Velocity = 0.06, 0.09, 0.10, 0.12 m/hr
§ Brine Superficial Velocity = 0.12 m/hr
φ Baseline Condition Tested
T = 27 °C and P = 1 atm
NaCl Concentration = 10 wt%
pH < 8.0 via CO_2 addition
**pH >8.0 and < 8.75*
Average Influent Nitrate Concentration = 15,000 mg/L as nitrate

3.3.5 TBR Model

A 1-D model of a recycle trickle bed reactor (TBR) was developed to determine the hydrogen mass transfer coefficients between the gas and liquid phases. Zero-order rate constants were measured for nitrate reduction in the batch reactor when the nitrate concentration was high and hydrogen was continually supplied in excess. Hydrogen concentration decreases along the reactor length, so a first order rate law for hydrogen consumption was assumed. Intrinsic first order rate constants were determined from zero-order rate constants using the following relationship:

$$r_p = \frac{k_1 C_{H_L} \eta}{\rho_{bed} \Psi} \tag{4}$$

Definitions of variables can be found at the end of the text. Mass balances were performed at steady state for nitrate in the liquid phase, and for hydrogen in the liquid and gas phases. The resulting mass balance equations are given as:

$$\frac{d(C_{NO_3^-})}{dz} = -\frac{\gamma r_p \rho_{bed} \Psi A}{(Q_r + Q_b)} = \frac{\gamma k_1 C_{H_L} \eta A}{(R+1)Q_b} \; where \; R = \frac{Q_r}{Q_b} \quad (5)$$

$$\frac{d(C_{H_L})}{dz} = \left[-k_1 C_{H_L} + \left(k_{GL}a \left(\frac{C_{H_G}}{H_{CC}} - C_{H_L}\right)\right)\right]\left(\frac{\eta A}{(Q_r + Q_b)}\right) \quad (6)$$

$$\frac{d(C_{H_G})}{dz} = -k_{GL}a \left(\frac{C_{H_G}}{H_{CC}} - C_{H_L}\right)\frac{\eta A}{Q_G} \quad (7)$$

Carbon dioxide flow was incorporated into the model through calculation of the hydrogen gas concentration at the reactor inlet and calculation of the gas superficial velocity.

3.3.6 Model Assumptions

Recycle ratio (R) was defined as the liquid recycle superficial velocity (Q_r) divided by the brine superficial velocity (Q_b). Based on experimental results, a fixed selectivity of 50% towards N_2 was assumed, which is important due to the stoichiometric variation in hydrogen consumed for the formation of different end products. It was assumed that N_2 was the only gas product formed during the reaction and that liquid intermediate products (i.e., nitrite) were present in small amounts and not modeled. The impact of a changing gas superficial velocity (Q_g) along the reactor length with H_2/CO_2 consumption, and N_2 production, was explored by adjusting Q_g based on reaction stoichiometry, but the differences in the resulting mass transfer rates were within 1%, so Q_g was maintained constant for simplicity. The catalyst bed was assumed to have constant catalytic activity and the reactor was assumed to be at steady state.

3.3.7 Model Application

An explicit finite difference method was used to solve equations 5 - 7. A small discretization of 0.0001 m was used to prevent instability in the model. Model input parameters included measured influent and effluent C_{NO3}-, hydrogen and carbon dioxide gas flow rates (Q_q-

$_{H2}$ and $Q_{g,CO2}$, respectively), Q_b, and Q_r. The gas-liquid mass transfer coefficient ($k_{GL}a$) was adjusted to fit the simulated effluent nitrate concentration to the experimental nitrate effluent concentration. Experimental data from the TBR were used to fit the mass transfer coefficients for 13 (12x14) and 18 (12x30) unique experimental conditions.

3.4 Results and Discussion

3.4.1 Batch Experimental Results

Batch experiments were performed with both the 12x14 and 12x30 catalysts in rapidly mixed aqueous suspensions to determine their activity in the absence of inter-particle mass transfer limitations. Nitrate reduction followed zero-order kinetics for both formulations, as expected based on the high initial nitrate concentration in brine. The Pd mass-normalized activities were found to be 165.0 ± 4.49 mg NO_3^- min^{-1} gPd^{-1} for the 12x14 catalyst and 210.4 ± 1.93 mg NO_3^- min^{-1} gPd^{-1} for the 12x30 catalyst (see Figure 3.10). Choe, *et al.* [51] demonstrated Pd-mass normalized batch rate constants between 11 and 24 mg NO_3^- min^{-1} gPd^{-1}, using a 2.5wt%Pd-0.25wt%In/AC catalyst in a 7wt% NaCl brine solution; and 47 mg NO_3^- min^{-1} gPd^{-1} using a 0.5wt%Pd-0.05wt%In/AC catalyst in a 7wt% NaCl brine solution.

Table 3.3: Activities, mass transfer coefficients, and selectivity results for all experimental conditions tested in the TBR

12 x 14 Catalyst

U-L (Qr) [m/hr]	Qg H_2 [sccm]	U-g H_2 [m/hr]	U-g total [m/hr]	Pd-Normalized Activity [mg/min-gPd]	$k_{GL}a$ [1/min]	Selectivity for N_2 [%]
8.9 (300 mL/min)	20	0.59	0.88	4.24	2.52	50 ± 6.6
	40	1.18	1.58	5.92	2.70	50 ± 0.6
	60	1.77	2.19	6.68	2.55	52 ± 6.3
14.8 (500 mL/min)	20	0.59	0.88	7.02, 6.68, 7.22	4.58, 4.29, 5.52	61 ± 2.2
	30	0.88	1.27	7.89	4.59	58 ± 2.5
	40	1.18	1.58	8.12	4.00	52 ± 3.7
	60	1.77	2.23	8.85	3.62	48 ± 5.0
19.8 (670 mL/min)	20	0.59	0.88	6.17	2.70	59 ± 5.0
	30	0.88	1.27	7.11	2.96	57 ± 7.0
	40	1.18	1.58	7.60	2.75	50 ± 2.2
28.1 (950 mL/min)	20	0.59	0.88	4.98	0.37	48 ± 6.7
	40	1.18	1.58	5.80	0.54	56 ± 2.5
	60	1.77	2.19	6.11	0.54	50 ± 6.7

12x14: Overall selectivity for N_2 = 53% ± 2.8

12 x 30 Catalyst

U-L (Qr) [m/hr]	Qg H_2 [sccm]	U-g H_2 [m/hr]	U-g total [m/hr]	Pd-Normalized Activity [mg/min-gPd]	$k_{GL}a$ [1/min]	Selectivity for N_2 [%]
8.9 (300 mL/min)	20	0.59	1	7.25	17.55	63 ± 3.5
	40	1.18	1.77	12.72, 11.57	21.12, 14.43	34 ± 9.4
	60	1.77	2.36	11.82	8.44	19 ± 13.4
	80	2.37	2.95	16.60, 15.94, 16.48	11.61, 12.95, 12.47	44 ± 5.3
	90	2.64	3.25	17.4	12.49	46 ± 7.1
14.8 (500 mL/min)	20	0.59	1	7.00	7.76	54 ± 4.4
	40	1.18	1.68	9.36, 9.46	6.26, 6.96	42 ± 8.5
	80	2.37	2.95	10.65	5.04	28 ± 7.6
20.7 (700 mL/min)	20	0.59	1	4.03	0.99	52 ± 1.6
	40	1.18	1.71	7.05	2.87	51 ± 1.1
	80	2.37	2.95	9.49	3.5	38 ± 9.5
28.1 (950 mL/min)	20	0.59	0.88	6.68	1.23	60 ± 5.2
	40	1.18	1.59	7.22	1.69	49 ± 4.8
	80	2.37	2.92	8.34	1.95	48 ± 5.3

12x30: Overall selectivity for N_2 = 41% ± 8.7

3.4.2 TBR Experimental Results

The results of nitrate reduction in the TBR for different U_L and $U_{g\text{-}H2}$ but the same U_b (0.06 m/hr) are shown in Figure 3.3. In both graphs, the effluent nitrate values for each liquid and gas superficial velocity condition plateau, indicating the reactor performance is stable during operation. The results of nitrate reduction in the TBR for different U_L and $U_{g\text{-}H2}$, with U_b from 0.06 to 0.12 m/hr, are shown in Figure 3.4 for the 12x30 catalyst. The effluent nitrate concentration returns to the same value at the beginning and end of the TBR experiment when the same U_L (14.8 m/hr), $U_{g\text{-}H2}$ (1.18 m/hr), and U_b (0.06 m/hr) conditions were evaluated. This indicates both reactor performance and the catalyst were stable over 90 days of operation.

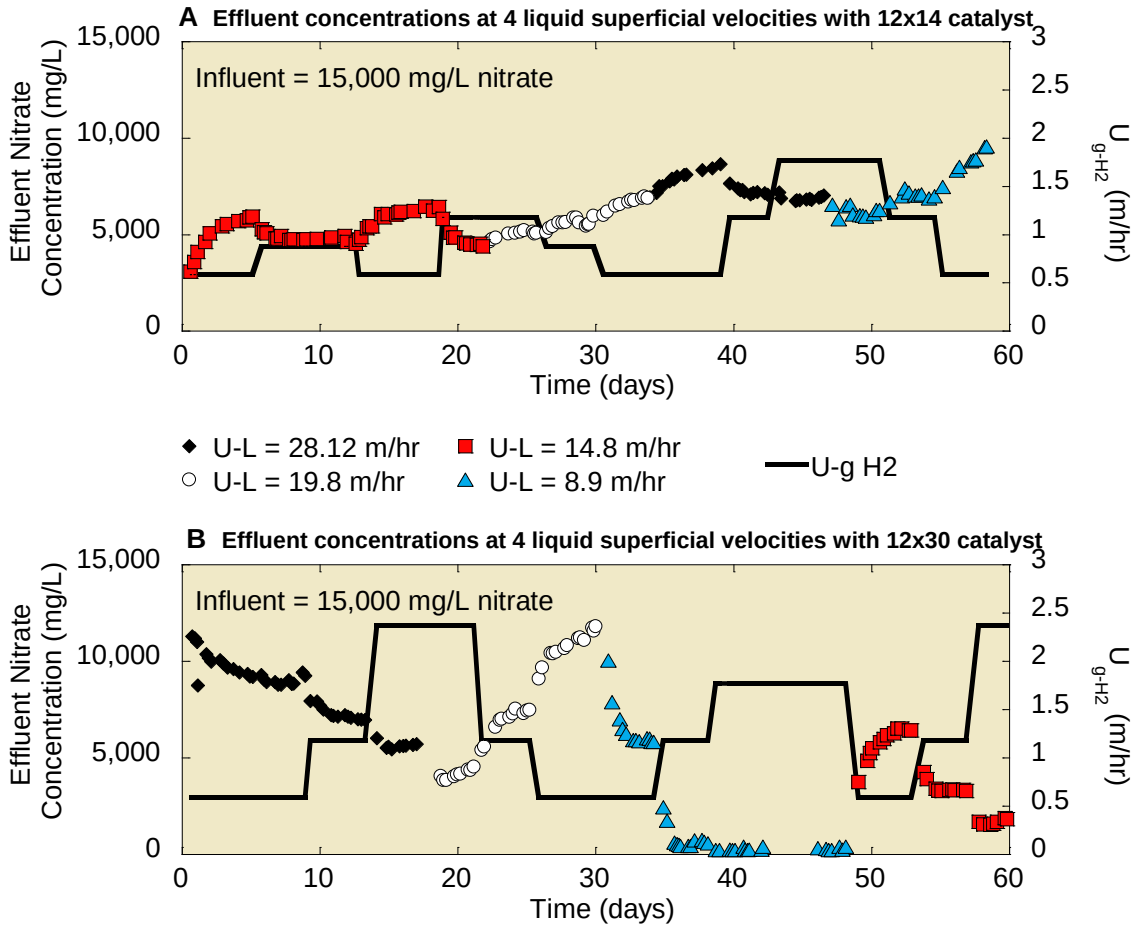

Figure 3.3: Nitrate removal in synthetic waste brine with one brine superficial velocity over 60 days

Pd-normalized activities were calculated from TBR influent and effluent nitrate concentrations. The Pd-normalized activities are shown in Figure 3.5, part A (12x14) and part B (12x30), and listed in Table 3.3 for all experiments as a function of U_L and $U_{g\text{-}H2}$. Greater activity was observed with increasing hydrogen gas superficial velocity for both catalysts. This trend is expected because higher gas superficial velocities correspond to greater H_2

concentrations in the gas phase along the column length, and a steeper concentration gradient driving H_2 into the liquid phase and onto the catalyst surface.

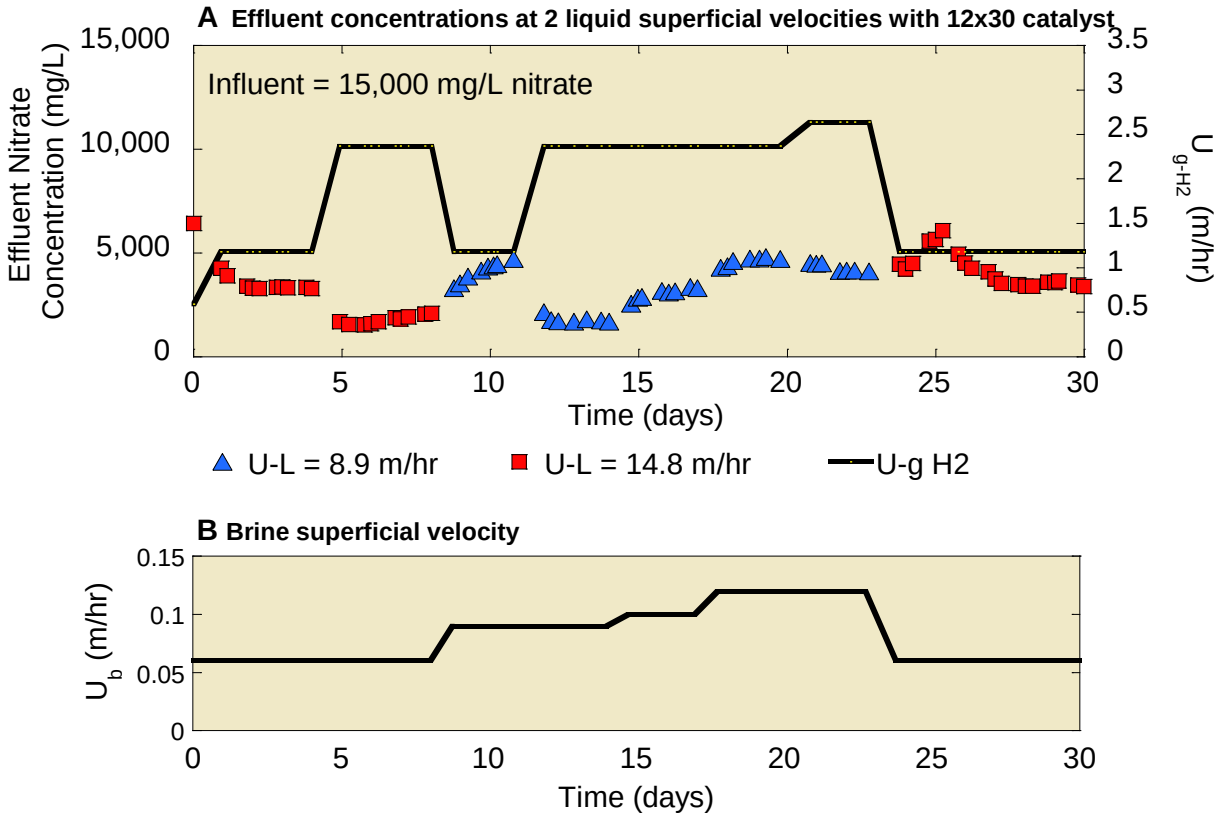

Figure 3.4: Nitrate removal in synthetic waste brine with varying brine superifical velocities over 30 days

The dependence of activity on liquid superficial velocity is not as straight forward. For the 12x14 catalyst, the activity increases with increasing U_L to a maximum at 14.8 m/hr, and then decreases at higher U_L. For the 12x30 catalyst, the greatest activity occurs at the lowest U_L of 8.9 m/hr, and then decreases with increasing U_L. Greater activity was observed for the 12x30 than the 12x14 catalyst. This result is expected because smaller catalyst supports promote more uniform liquid and gas flow, as well as thinner boundary layers around particles [119, 120]. The

highest Pd-normalized activity achieved is 17.4 ± 0.04 mg/min-gPd for the 12x30 catalyst at U_L = 8.9 m/hr and U_g-$_{H2}$ = 2.64 m/hr. This is 8.3 percent of the activity measured in the batch reactor experiments, and suggests hydrogen mass transfer limitations from the gas phase to the catalyst surface are limiting apparent catalyst activity in the TBR. A comparison to other rates in the literature is discussed below.

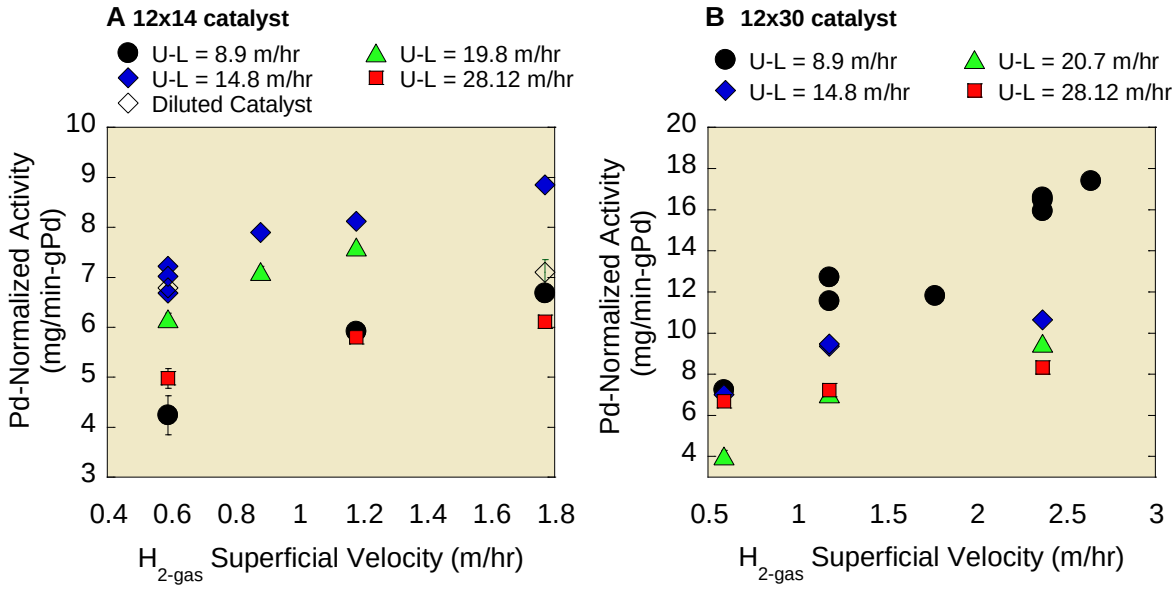

Figure 3.5: Catalyst activity for nitrate reduction measured in TBR at various gas and liquid superficial velocities

3.4.3 Selectivity

Measured TBR selectivities for N_2 are listed in Table 3.3. For the 12x14 catalyst, selectivities for N_2 are very close to an average value of 53 ± 2.8%, regardless of U_g-$_{H2}$ and U_L values. In contrast, for the 12x30 catalyst, selectivities decreased with increasing hydrogen gas superficial velocity at U_L, with an average of 41 ± 8.7%. Pintar and Batista [87] achieved 35% selectivity for N_2 in a TBR, while Bergquist *et al.* [65] achieved 70% selectivity for N_2 in an up-

flow, flooded bed reactor with the same pH, NaCl loading, and initial nitrate concentration used in the present study. However, the maximum activity for nitrate reduction in the latter study was only 12-25% of the activity observed in the current effort, indicating greater H_2 mass transfer limitations were present and limited NH_4^+ production (i.e., greater H_2 concentrations in water result in less selectivity for N_2 [121]).

3.4.4 TBR Flow Regimes

For the 12x14 catalyst, the highest catalyst activity was obtained at U_L = 14.8 m/hr. At this recycle rate, gas pockets were readily visible along the reactor wall and no fluid pulsing was observed. The same conditions were observed for U_L = 8.9 m/hr. At U_L = 19.8 m/hr, the bed appeared almost completely water saturated and pulsing was observed. At U_L = 28.12 m/hr, the bed appeared completely water saturated with no fluid pulsing. For the 12x30 catalyst, the highest activity was obtained at U_L = 8.9 m/hr. At this liquid superficial velocity, gas pockets were readily visible along the reactor wall and no fluid pulsing was observed. At U_L = 14.8 m/hr, the bed appeared almost completely saturated and fluid pulsing was observed. At U_L = 20.7 m/hr, the catalyst appeared completely saturated and fluid pulsing was observed. At U_L = 28.12 m/hr, the bed was completely water saturated and no fluid pulsing was visible.

The observed flow characteristics suggest the greatest Pd-normalized activity was obtained near the transition between the trickle and pulse flow regimes, and just prior to the transition to pulse flow. Many industrial TBRs are operated at the transition between trickle and pulse regimes [84, 122], and my results support operation near this transition for the brine treatment system.

In a companion study [123], a TBR reactor was developed and evaluated for reduction of NO_3^- in fresh water; the influent NO_3^- concentration was considerably lower (70 mg/L) than in this study (15,000 mg/L), an alumina rather than activated carbon support was used, and a single pass instead of recycle flow configuration was used. In contrast to results in this study, the greatest NO_3^- reduction activity for the TBR treating fresh water was obtained under pulse flow conditions. The transition between different flow regimes can be subtle, and it is possible that the pulse flow conditions were near the trickle flow regime. It is also possible that different wetting properties of alumina support particles can shift the flow regime where optimal activity is obtained.

A comparison of TBR liquid and gas superficial velocities reported in the literature and those in this study is shown in Figure 3.6; also shown are observed flow regimes. Liquid and gas superficial velocities are expressed as Reynolds numbers ($Re=ud_p\rho/\mu$) and include the effect of their respective velocity (u), viscosity (μ) and density (ρ), as well as support size (d_p). Liquid superficial velocities in this study were on the lower end of the range of those reported in the literature. Gas superficial velocities in this study were relatively low, based on stoichiometric needs; the lower gas Re values in this study were also affected by the low density of hydrogen and a relatively small catalyst support particle size. Typical catalytic applications in industry use orders of magnitude higher gas superficial velocities to meet or exceed stoichiometric needs, help control reactor temperature, and improve mass transfer rates [79, 84]. The low gas Re values in this study place the catalytic TBR for nitrate reduction outside the operating range of prior efforts. Nevertheless, optimal TBR performance in this study occurred near the trickle-pulse flow regime transition, in agreement with TBR studies performed at much higher gas Re values.

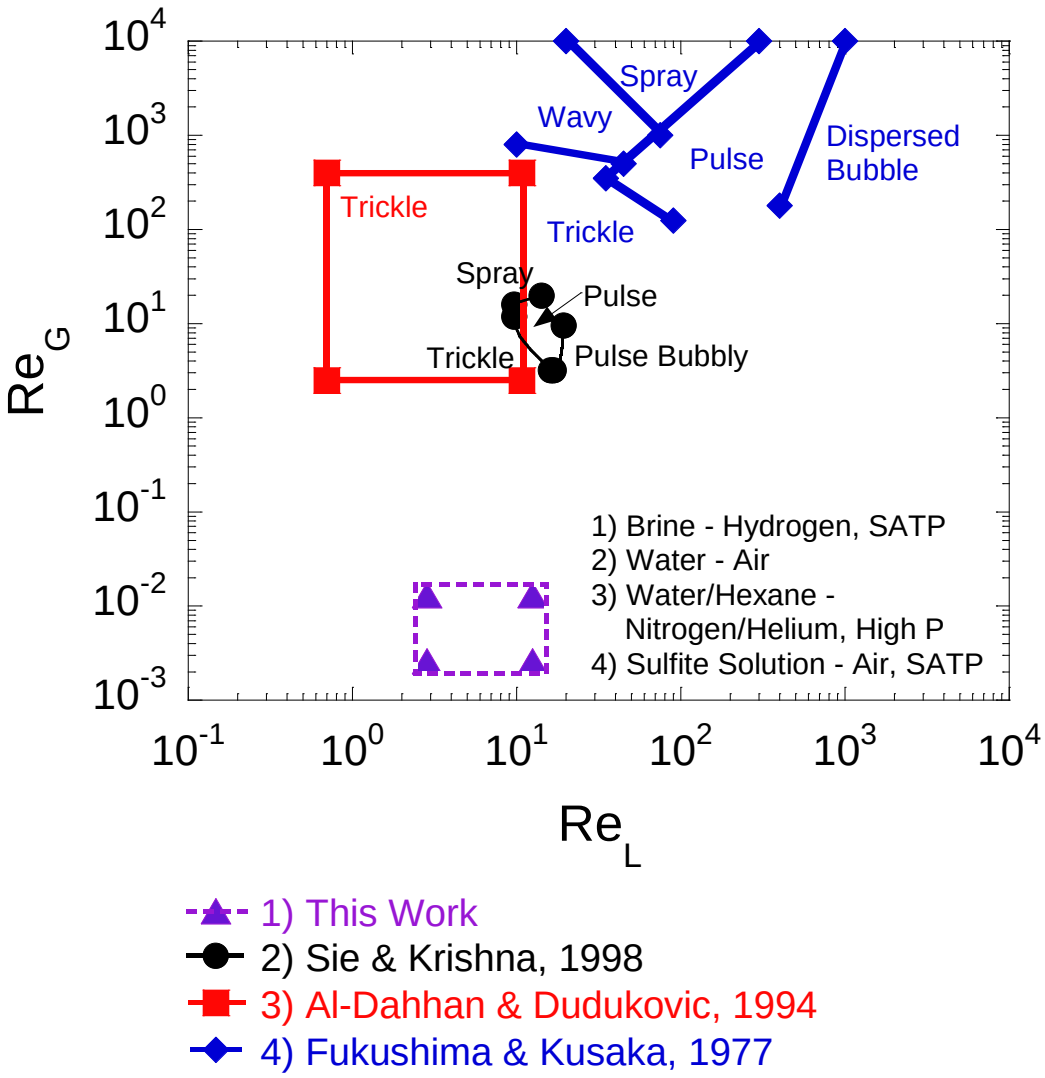

Figure 3.6: Previously observed TBR flow regimes and the flow region covered experimentally in this study

3.4.5 TBR Model Results

Mass transfer coefficients were determined from the TBR model, and results at all operating conditions are shown in Figure 3.7 and Table 3.3. Past work suggests mass transfer rates should increase with gas superficial velocity [96], which is only observed when the TBR was at the high end of pulse flow or in the bubble flow regime (12x14: U_L = 28.12 m/hr, 12x30:

U_L = 20.7 and 28.12 m/hr). However, both catalysts demonstrated a flat or downward trend in mass transfer rate in the trickle and early pulse regimes, in agreement with results from the aforementioned companion study [123].

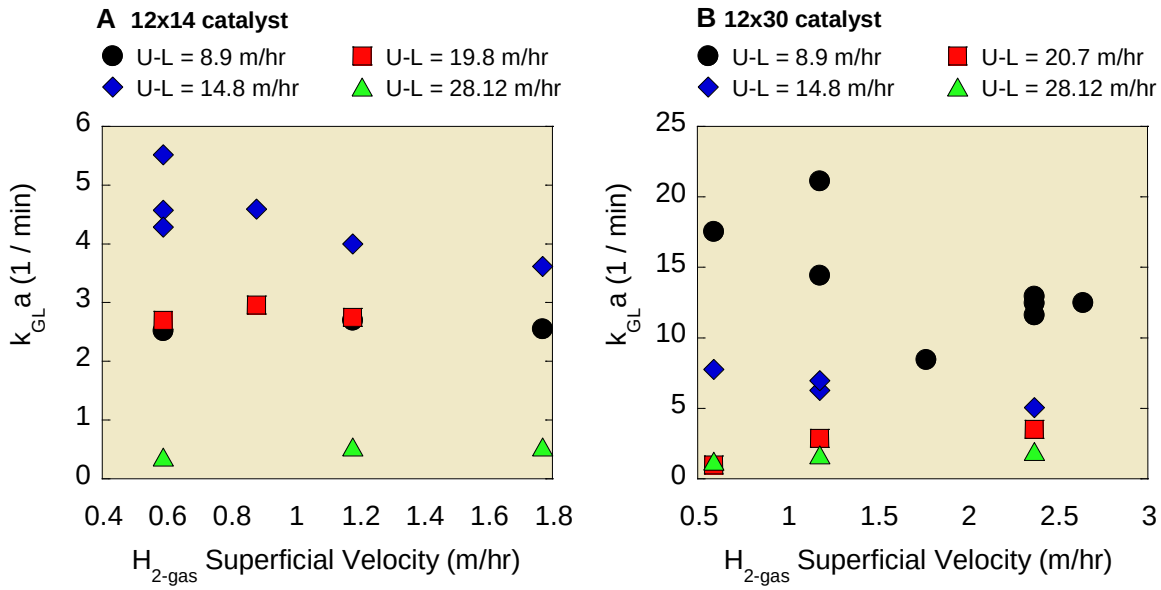

Figure 3.7: Estimated hydrogen mass transfer coefficients in TBR at different hydrogen gas and liquid superficial velocities

This unexpected result may be related to the very low $U_{g\text{-}H2}$ values tested. The mass transfer rates achieved in Bertoch *et al.* [123] are similar to those obtained in this study using the 12x14 catalyst; the highest mass transfer rate in Bertoch *et al.* (2016) is c. 40% of the highest mass transfer rate obtained using the 12x30 catalyst. In a prior study, the oxygen absorption rate into water was independent of O_2 gas superficial velocity between 1.77 – 7.1 m/hr [54], which is higher than the range tested here. Additional studies are needed to determine if the observed trend is general at low $U_{g\text{-}H2}$ values, or specific to the reactor configuration used in this study.

Mass transfer coefficients were plotted versus Pd-normalized activity in Figure 3.8; there is generally a positive correlation. This is expected for a mass transfer-limited reaction.

Comparing the mass transfer rates obtained with the 12x14 support with those of the 12x30 support, the best mass transfer rate with the 12x30 (21.12 1/min) was 280% of the best mass transfer rate with the 12x14 (5.52 1/min), as expected because smaller particle sizes result in more uniformly distributed liquid flow and a smaller liquid boundary layer. The enhanced mass transfer may also be due to the larger range of particle sizes for the 12x30 catalyst (see Table 3.1). Smaller particles can fill void spaces between larger particles, and increase liquid spreading [124].

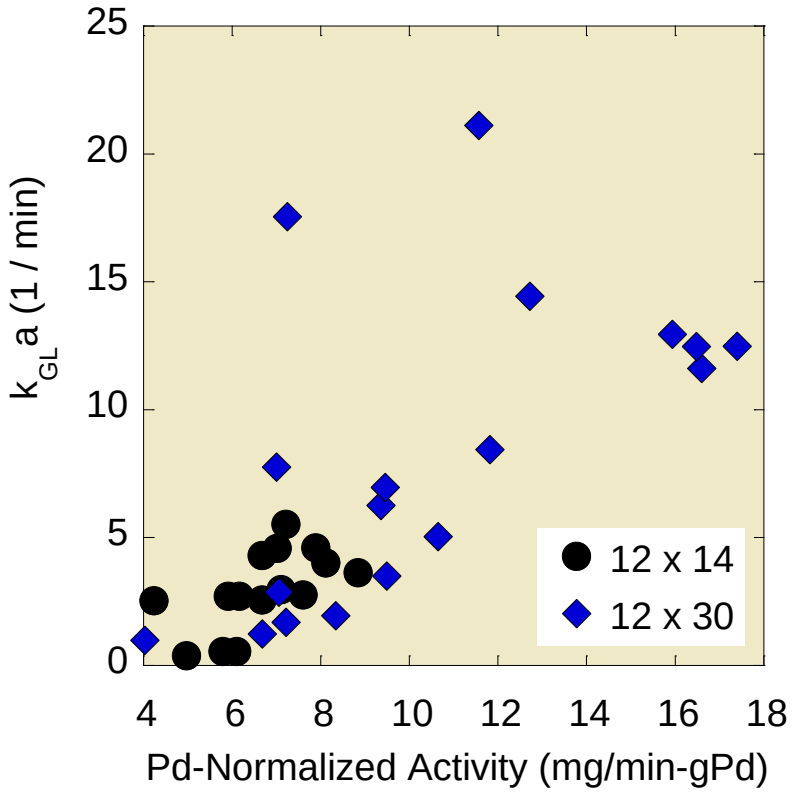

Figure 3.8: Measured Pd-normalized catalyst activity versus hydrogen mass transfer coefficient

For both the 12x14 (all U_L) and 12x30 (U_L = 14.8-28.12 m/hr) catalysts, with $U_{g\text{-}H2}$ = 0.59-1.18 m/hr, the mass transfer rates are similar to those reported (between 0.01-0.1 1/sec) for

liquid-phase benzene hydrogenation at the same superficial gas velocities using 2.38 mm Ni/Al_2O_3 tri-lobe catalyst in a single-pass TBR at high temperature and pressure (100-150 °C, 16 bar) [78]. These results demonstrate comparable performance for the authors' TBR in the absence of high pressure and temperature, which generally improves mass transfer rates.

All mass transfer rates using the 12x14 catalyst and those using the 12x30 catalyst where U_L = 14.8-28.12 m/hr are similar to those found in a single-pass TBR with a lower liquid superficial velocity using hydrogen gas superficial velocities from 0 – 47.4 m/hr to hydrogenate α-methyl styrene using 0.3-3 mm Pd/Al_2O_3 catalyst at high pressure (0.1-1.5 MPa) [125]. At superficial gas velocities 10-100x higher and liquid superficial velocities slightly higher than those tested in this study, Haase, *et al.* used 0.8 mm Pd-catalyzed particles in a fixed bed reactor with mini-channel packing to hydrogenate α-methyl styrene; a maximum mass transfer rate of 2.63 1/sec (157.8 1/min) was obtained [126]. These results suggest that re-designing the reactor in this study to accommodate higher gas superficial velocities might result in higher mass transfer rates.

These studies [125, 127] correlated an increase in mass transfer using gas Reynold's number (Re_g) and a power law between $Re_g^{0.3}$ and $Re_g^{0.9}$. When compared to the data in this work, the 12x30 data from the late pulse flow regime (Re_L = 7.99) and bubble flow regime (Re_L = 10.85), were largely consistent with the predictions. At Re_L = 7.99, the power law was $Re_g^{0.94}$ and at Re_L = 10.85, the power law was $Re_g^{0.34}$. The other 12x30 data showed a negative correlation between mass transfer and Re_g, which was addressed above. With the 12x14 catalyst, the data from the bubble flow regime (Re_L = 10.85) was also consistent with the correlations, showing a power law of $Re_g^{0.36}$.

3.4.6 Mass Transfer Mechanisms

A schematic of mass transfer processes and length scales in the TBR under different flow regimes is illustrated in Figure 3.9. In the trickle flow regime, catalyst particles are partially wet, meaning that liquid is flowing over only a portion of the catalyst surface [84]. Non-wetted portions of the catalyst surface are coated with only a very thin film of stagnant liquid and gas fills interstitial spaces, which was observed at low liquid superficial velocities. Because hydrogen mass transfer in the gas phase is fast compared to the liquid-phase, hydrogen mass transfer resistance on non-wetted surfaces resides only in the thin stagnant liquid film around catalyst particles [128].

In the pulse flow regime, catalyst particles range from partially to fully wetted, meaning interstitial pore bodies may be filled with liquid or gas. Gas is not a continuous phase and periodically flushes liquid from pores when capillary pressures are exceeded, creating the visual appearance of a pulse, which the authors observed at moderate U_L. There are at least two mass transfer resistances in liquid filled pores: mass transfer resistance in a mobile liquid film adjacent to the gas phase, and mass transfer resistance in the more stagnant liquid boundary layer surrounding each catalyst particle.

Many studies have demonstrated higher reaction rates for gas-limited reactions with partially wetted catalyst particles because the liquid-side mass transfer step is significantly faster through thin stagnant films on non-wetted surfaces [97, 124, 129, 130]. It follows that the greatest TBR activity and mass transfer rates were obtained in this study at the transition between trickle and pulse flow.

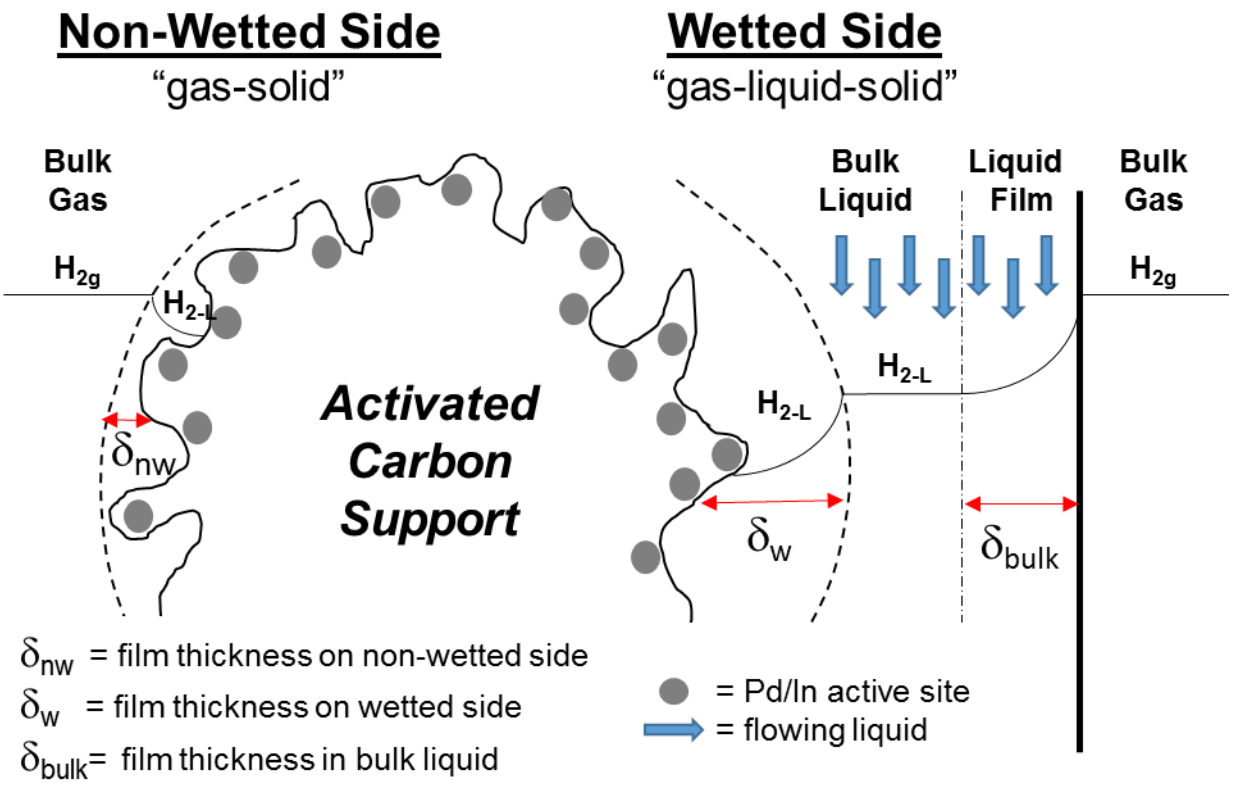

Figure 3.9: Diagram of different mass transfer schemes in a TBR

3.4.7 Comparison to Other Denitrification Reactors

When compared to past waste brine denitrification studies (see Figure 3.10), the TBR represents a 300% and 220% improvement in activity over up-flow, flooded bed reactors with the 05wt%Pd-0.05%In/AC 12x14 catalyst [65] and 2.5wt%Pd-0.25wt%In/AC 12x14 catalyst [51], respectively. The 12x30 catalyst was not tested in the up-flow flooded bed reactor, so a comparison is not possible. The nitrate reduction activity in studies of direct nitrate removal from fresh water using a TBR with alumina supported catalysts are also shown. The TBR activity with 12x30 catalysts is similar to that for the aforementioned companion study (Bertoch, et al, 2016), and 1200% better than a TBR with 1.7 mm 1wt%Pd-0.3wt%Cu/alumina catalyst [87].

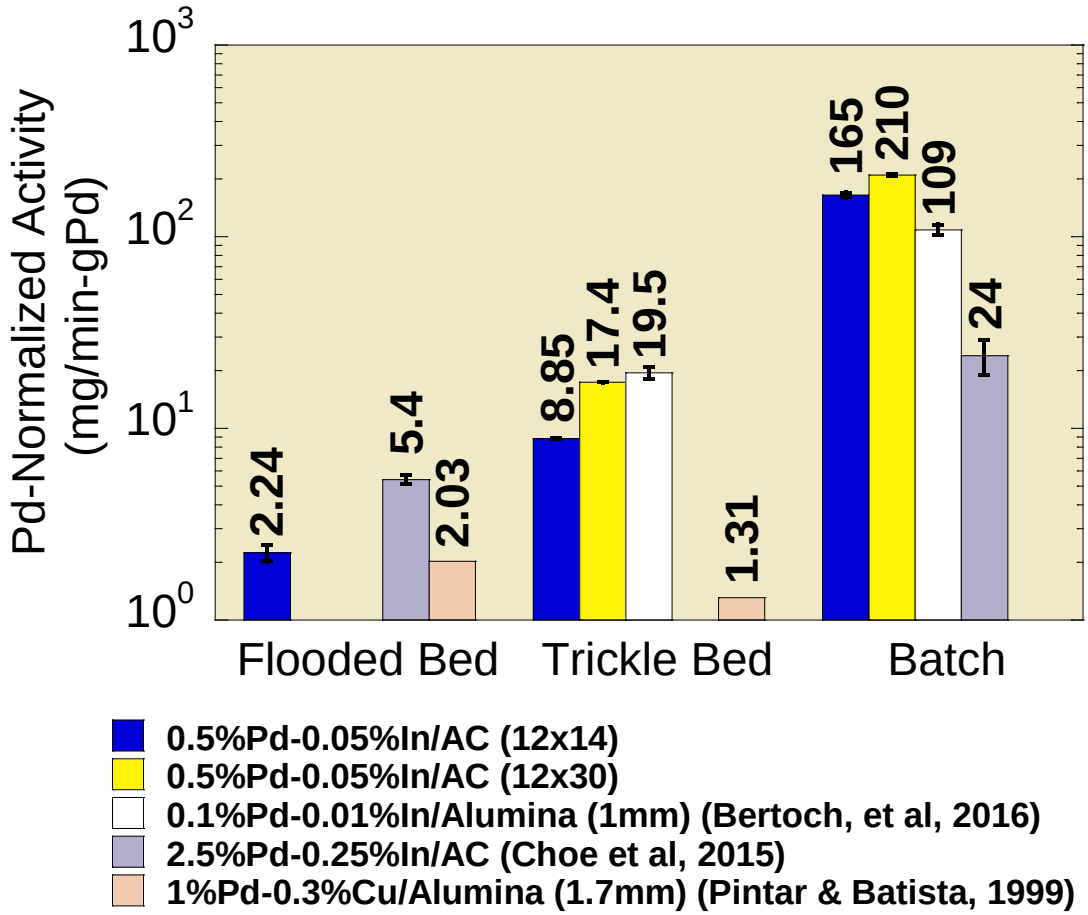

Figure 3.10: Nitrate hydrogenation activity in brine (activated carbon) and groundwater (alumina) using different reactors and catalysts

Comparing all TBR rates to those achieved in the batch reactor indicate there is significant room for improvement. In the batch reactor, hydrogen is provided in excess, which eliminates inter-particle mass transfer limitations. In the TBR, mass transfer of H_2 from the gas to the liquid phase appears to limit activity. Potential strategies to overcome mass transfer limitations include pressurizing the reactor or using formic acid in place of hydrogen. For example, pressurizing the reactor to 5 atm (0.5 MPa) at 50 °C would increase the solubility of hydrogen by 500% [131], which would increase the driving force for H_2 mass transfer. Formic

acid has a very high solubility in water, and could be delivered at stoichiometric levels to eliminate the need for a separate gas phase [121]. However, formic acid requires reduction over Pd to produce H_2 and CO_2, and while one study demonstrated higher nitrate reduction activity with formic acid in a batch reactor, there was an "induction period" that delayed the onset of nitrate reduction [60].

3.4.8 TBR Catalyst Deactivation

At the conclusion of the TBR experiments, the reactor was disassembled and catalysts were removed for re-assessment of the used catalyst's metal content and activity in batch experiments to compare with fresh catalysts. The Pd-normalized activity of the used 12x14 catalyst was 86.75 ± 26.4 mg NO_3^- min^{-1} gPd^{-1}, while the Pd-normalized activity for the used 12x30 catalyst was 129.13 ± 16.8 mg NO_3^- min^{-1} gPd^{-1}. These values represent a 48% and 39% decrease, respectively, in activity relative to the fresh catalysts. A possible reason for the decrease in activity is metal leaching from catalyst particles. Metals analysis indicate that the Pd and In mass loadings of the 12x14 catalyst decreased from 0.46 ± 0.06 wt% and 0.05 ± 0.01 wt% to 0.34 ± 0.09wt% and 0.034 ± 0.003wt%, respectively. The Pd and In mass loadings of the 12x30 catalyst decreased from 0.51 ± 0.08 wt% and 0.06 ± 0.01 wt% to 0.39 ± 0.07wt% and 0.049 ± 0.007wt%, respectively. Therefore, at least some of the apparent loss in activity can be attributed to loss of active metals from the catalyst supports.

Figure 3.11: Predicted 12x30 TBR reduction activity at various intrinsic catalyst activities assuming $k_{GL}a = 7.76\ min^{-1}$

The steady TBR performance, despite the drop in batch activity, can be attributed to the H_2 mass transfer limitations. This contrast is shown in Figure 3.11, which models the change in TBR activity over a wide range of intrinsic rates when the mass transfer rate is held constant using the 12x30 catalyst. The change in TBR activity between the batch rate measured with fresh catalyst (210 mg NO_3^- min^{-1} gPd^{-1}) versus the used catalyst (129 mg NO_3^- min^{-1} gPd^{-1}) would not be apparent in the packed bed reactor experiments where H_2 mass transfer is limiting. Alternately, modeling the higher mass transfer rate from literature cited above (157.8 min^{-1}) and the 12x30 fresh batch rate (210 mg NO_3^- min^{-1} gPd^{-1}), the effluent nitrate concentration would decrease by 23%, which further demonstrates the impact of current hydrogen mass transfer

limitations. It is likely that, with continued operation for many months, additional metals might be lost from the activated carbon support, eventually reducing the surface reactivity to an extent that would affect nitrate treatment in the TBR. Hence, designing a more resilient catalyst for use in a brine matrix is needed to ensure long-term operation of the TBR over many years in a practical water treatment system.

3.4.9 TBR Cost Implications

In a previous report [65], salt costs for ion exchange (IX) alone, and salt and Pd metal costs for a hybrid ion exchange – catalyst treatment system, were evaluated based on IX system information from a Vale, OR demonstration plant treating 0.5 MGD of influent water [31] containing 80 mg/L NO_3^-. Only salt and Pd costs were considered because the former dominates costs for IX alone, and both dominate costs for the hybrid system. Costs were calculated assuming 1 billion gallons of water treated, two bed volumes of brine for IX regeneration, and either single use brine treatment for IX alone versus 10x brine reuse for the hybrid system.

Salt costs for the IX system alone are $433K. Salt costs for IX in the hybrid system are $102K, independent of the catalytic system. Using 12x30 catalyst activity from a batch reactor (210 mg min^{-1} gPd^{-1}), the Pd cost would be approximately $15K; however, this reactor type is not realistic for commercial applications. A fixed bed reactor is more suitable. Using activity from a previously developed up-flow fixed bed reactor (Bergquist *et al.*, 2016), the Pd cost would be approximately $1.4M. Using the highest activity obtained for the TBR in this study (i.e., 12x30 catalyst, k=17.4 mg min^{-1} gPd^{-1}), the Pd cost decreases to approximately $182K. This cost reduction brings the catalyst cost within the range of NaCl savings, bringing it closer to a realistic economic option. Further improvements in catalyst activity, substitution of lower cost

metals, or reactor modifications that reduce H_2 mass transfer limitations can reduce these costs even further.

3.5 Conclusions

Waste brine denitrification using a TBR was evaluated for different liquid and H_2 superficial velocities for both 12x14 and 12x30 catalysts. The highest activity of 17.4 mg min^{-1} gPd^{-1} and the highest H_2 mass transfer coefficients of 21.12 min^{-1} were obtained with the 12x30 catalyst. The implications of these improved results are better understood when put into context of a scenario I previous developed to evaluate potential commercial costs. Key findings include:

- Smaller catalyst support size (12x30) demonstrated higher activity and mass transfer.
- TBR demonstrated c. 300% higher activity than an up-flow fixed bed reactor from previous work using the same 0.5wt%Pd-0.05wt%In/AC catalyst (12x14).
- Mass transfer was the highest in the trickle flow regime with partially wet catalyst.
- Hydrogen mass transfer limitations remain significant and prevent full realization of intrinsic catalyst activity.
- Metals loss from the catalyst indicates the need to develop a more robust catalyst for use in the brine matrix.
- TBR performance is a step forward to developing an economically-viable system.

3.6 Symbols used

$A=$	Area [m^2]	$r_p=$	Reaction rate [mol/hr/gPd]
$a=$	Interfacial area [m^2/m^3]	$U_L=$	Liquid superficial velocity [m/hr]
$C=$	Concentration [mol/m^3]	$U_b=$	Brine superficial velocity [m/hr]
$d_p=$	Particle diameter [m]	$U_{g\text{-}H2}=$	H_2 gas superficial velocity [m/hr]
$H_{cc}=$	Dimensionless Henry's constant [-]	$V_{pore}=$	Pore volume [mL]
$k_{GL}a=$	Gas-liquid mass transfer across and interfacial area [1/min]	$z=$	Reactor length [m]
$k_1=$	First order rate constant [1/min]	$\eta=$	Porosity [m^3_{water} / m^3_{bed}]
$k_0=$	Zero-order rate constant [mg/min/gPd]	$\gamma=$	Stoichiometric coefficient [mol-H_2 / mol-NO_3^-]
$Q_b=$	Brine superficial velocity [mL/min]	$\rho_{bed}=$	Density [g_{cat} / $m^3_{reactor}$]
$Q_r=$	Recycle superficial velocity [mL/min]	$\rho_{gas=}$	Density [kg/m^3]
$R=$	Recycle ratio (Q_r/Q_b) [-]	$\mu_{gas}=$	Viscosity [$N*sec/m^2$]
$Re=$	Reynolds Number ($u*d_p*\rho/\mu$)	$\Psi=$	Palladium content [g_{Pd}/g_{cat}]

CHAPTER 4

SELECTIVITY OF NITRATE REDUCTION WITH PALLADIUM-INDIUM ON ACTIVATED CARBON CATALYSTS IN DIFFERENT REACTOR SYSTEMS

4.1 Introduction

Nitrate is a widespread groundwater contaminant and is regulated by the EPA due to the harmful human health impacts [3, 20]. Recently, catalytic treatment of nitrate emerged as a promising technology [51, 53, 87]. The three main characteristics of a catalyst were the activity, stability and selectivity [132]. Activity refered to the intrinsic rate of reaction the catalyst was capable of producing, given optimal conditions (i.e., temperature and pressure), which varied according to the chemistry involved. Stability refered to the mechanical strength of the catalyst and its ability to perform optimally under a range of temperature, pressure, flow and matrix conditions. The stability was reflected in the length of time the catalyst could be employed for a certain application and what type of catalytic deactivation may occur. The selectivity of a catalyst related to the end products produced during the course of the reaction and was the focus of this work. During nitrate reduction, ammonia and dinitrogen were the two possible end products (see Figure 4.1), the latter of which was generally preferred due to its inert nature and lack of environmental impacts.

Catalytic nitrate reduction required a bimetallic catalyst (primary and promoter metals) and an electron donor. When hydrogen was used as the electron donor, H_2 sorbed to the surface of primary metal and dissociated into H• [60]. H• then spilled over (i.e., surface diffusion) to

neighboring promoter metal sites, where nitrate was reduced to nitrite [133, 134]. Afterwards, nitrite reduction to the final end product occured on reactive sites on the primary metal.

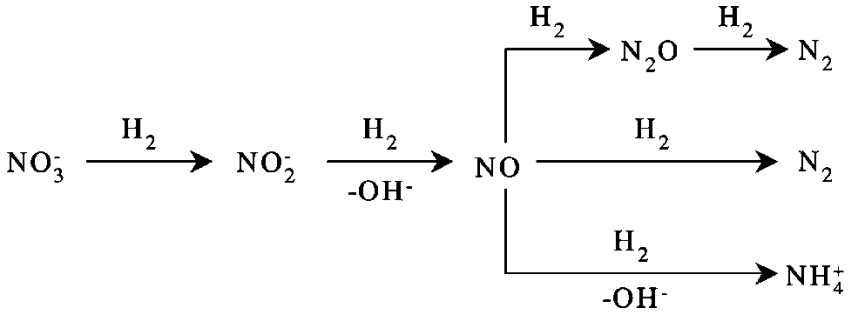

Figure 4.1: Catalytic reduction path of nitrate with hydrogen [135]

There were many factors that affected the selectivity of the catalyst. Below, a brief description of the prominent factors was described:

Solution pH and method of pH control. The pH of the solution impacted selectivity of the catalyst, with higher pH leading to more ammonium formation [133, 136–138]. Acidic conditions favored N_2 production, but the specific pH required for optimal selectivity may vary by support type [139]. Additionally, local pH at the reactive site was influenced by the OH^- produced during nitrate reduction. This OH^- in pores near reactive sites had to diffuse to the bulk liquid to be neutralized, so supports with smaller pores have been shown to reduce the challenge of local pH variation [137].

The two primary methods of pH control in nitrate reduction were hydrochloric acid (HCl) and carbon dioxide (CO_2). Compared to a reaction with no buffering, CO_2 addition led to an increase in selectivity for N_2 from 20% to 60% [55] and 10% to 50% [140]. When compared to HCl, a CO_2 buffer resulted in higher selectivity towards N_2, which might be due to CO_2 acting as a local buffer within the pores [137, 141, 142]. Acetate provided similar results as CO_2 for

selectivity in nitrate reduction, but was not a common method of pH control [141]. In this work, pH was controlled by HCl.

Temperature. Multiple studies have demonstrated an increase in selectivity for N_2 with decreasing temperature, but artificially cooling source water to improve selectivity was not practical for economic reasons [137, 138]. Temperature was not a focus of this work because a commercial scale denitrification reactor would be operated at ambient temperature.

Catalyst metals and support material. Metal amount and ratio were two important factors in the overall effectiveness of the reduction process [60, 143]. Adequate metal coverage of the support surface, as well as physical proximity of the two metals (primary and promotor) played a critical role in facilitating hydrogen spill-over [56, 133]. The structure of the microcrystals in the primary metal (i.e., prevalence of edge, corner and terrace sites) was found to impact selectivity because different types of sites had different hydrogenation abilities, leading to variation in preferential reduction pathways [144, 145].

The primary/noble metals were elements typically found in Group VII of the periodic table [138]. Reactive sites on the noble metal were where nitrite reduction occured until the reaction was complete. As such, experiments were frequently conducted with monometallic catalyst (noble metal only) and nitrite to facilitate de-coupling the effect of the noble metal from the promoter metal.

When Pd and Pt were tested in isolation for nitrite reduction, Pd was found to have a higher selectivity towards N_2 than Pt (61% vs 33%, respectively), which the authors suggested was due to Pd's less noble character or the difference in particle size [133]. Further work testing monometallic catalysts for nitrite reduction found Pd was more selectivity than Pt or Ir [61, 138].

The promoter metals were typically found in Group 1B of the periodic table [138]. Copper and indium have emerged as the most active and selective promoter metals, but there were no direct comparisons of their effect on selectivity for dinitrogen gas in a waste brine, and/or with an activated carbon support [59–61, 138]. Using Pd on different activated carbon supports, Cu was found to have much higher selectivity than Sn or In [55]. Using an alumina support with 5 wt% Pd, Chaplin *et al.* [62, 63] found that selectivity was similar using In or Cu, but that only In (not Cu) was stable during periodic oxidative catalyst regeneration to reverse sulfide fouling. Based on these results, a Pd-In metal combination was chosen for waste brine denitrification and used in this work.

A wide variety of support materials have been tested for nitrate reduction, including alumina (Al_2O_3), multiple types of activated carbon (i.e., granules, extrudates, cloths), graphite, ceria (CeO_2), titania (TiO_2), and tin oxide (SnO_2) [59, 61, 140, 146–149]. The focus of this work was activated carbon. Physical and chemicals properties of the support (i.e., point of zero charge, functional groups) influenced the pH on the surface, which impacted the selectivity of the reaction [150–152]. As noted above, lower pH led to higher selectivity for N_2. Al Bahri, *et al.* [55] proposed that the presence of stable surface phosphate groups on a grape-seed activated carbon caused a lower natural pH and higher selectivity when compared to a commercial activated carbon with no phosphate groups present. Recently, oxygen functional groups were shown to increase hydrogen spillover on Pd supported activated carbon, leading to greater hydrogen storage capacity of the Pd [153]. Increased H_2 storage could impact the N:H• ratio on the surface, which has a significant impact on selectivity of end products. When the ratio was higher and there were more intermediate N-species adsorbed to the surface, greater incidents of N-N pairing occured, which resulted in higher selectivity towards N_2 [138, 154]. Conversely, a

lower ratio led to great production of NH_4^+ because H• was in relative excess to N on the reactive sites [154].

Competing ions. An important distinction between nitrate reduction in groundwater and waste brine matrices was the concentration of chloride, which was low in groundwater (<200 mg/L) and very high in brine (40,000-70,000 mg/L). It was known that ions such as chloride, sulfate and bicarbonate competed for reactive sites and resulted in lower catalytic activity [51, 53, 155]. Therefore, it followed the presence of abundant chloride may alter the N/H• surface ratio and impact selectivity. Studies addressing this phenomenon were limited, but have shown sulfate and chloride impacted selectivity during nitrate and nitrite reduction [53, 64, 156].

The overall objective of this work was to evaluate selectivity in multiple reactor systems and determine the impact of diluting the catalyst with same-size inert support at a 1:2 ratio. The specific objectives were to: 1) Evaluate nitrate reduction and selectivity in a flow-through trickle bed reactor, 2) Evaluate nitrate and nitrite reduction and selectivity in a continuously stirred batch reactor, 3) Determine the impact of catalyst dilution on selectivity, 4) Assess the influence of chloride, hydrogen and nitrite concentration in determining selectivity, and 5) Develop a model to describe selectivity in brine conditions.

4.2 Methods

4.2.1 Materials

Reagent-grade sodium salts (≥99% purity) of nitrate and chloride were obtained from Fisher. Tanks of H_2 (99.999%) and CO_2 (99.9%) were purchased from Praxair and Airgas, respectively. A tank of 5% H_2 – 95% N_2 was obtained from Praxair. All synthetic brines were prepared with deionized (DI) water (18.2 MΩ-cm resistivity, Millipore system). The 0.5wt%Pd-

0.05wt%In/AC catalyst with US Mesh support size of 12x14 and an inert 12x14 carbon support were provided by Johnson Matthey Inc.

4.2.2 Trickle Bed Reactor (TBR) Experimental Set-up and Protocol

A continuous flow TBR was constructed from 5.08 cm (2") ID polyvinylchloride (PVC) and the column was packed with two 25 cm (10") catalyst beds using 0.5wt%Pd-0.05wt%In/AC. A US Mesh 12x14 catalyst support was used for all experiments. More details about the reactor set-up were provided in Chapter 3 and were shown in Figure 4.2.

Continuous flow experiments were run with two different catalyst loadings: 1) all catalyst (480 g) and 2) catalyst diluted with same-size inert support at a 1:2 ratio – 1 part catalyst (150 g), 2 parts support (300 g). See Figure 4.2 for a detailed diagram of the catalyst bed. The 1:2 diluted catalyst was first combined in a plastic wash-pan and gentle mixed by hand. Next, the mixted catalyst/inert support was poured slowly into a large glass jar, sealed and rolled slowly to increase mixing. A liquid recycle superficial velocity (U_L) of 14.8 m/hr was tested and a synthetic brine containing 10wt% NaCl and 16,000 mg/L nitrate was used. Two hydrogen superficial velocities were tested: 0.59 and 1.77 m/hr. Each condition was tested for 3 – 8 days and samples were taken 1 – 3 times per day. Reactor pH was maintained between 6.5 and 8.0 using CO_2. All experiments are listed in Table 4.1.

Table 4.1: Experimental conditions tested in the trickle bed reactor

Catalyst Loading	Hydrogen Superficial Velocity	Length	NaCl	$[NO_3^-]$	Avg. [NO3-] Out	Average pH	Avg. [NO2-] Remaining	Selectivity for N_2	Mass Normalized Zero-Order Rate Constant
	m/hr	days	wt%	mg/L	mg/L		%	%	mg/min-gPd
Non-Diluted	0.59	8	10	16,000	7,815	7.66	4.6% ± 0.4	56% ± 4	7.22 ± 0.08
Non-Diluted	1.77	5	10	16,000	5,652	8.02	3.7% ± 0.5	48% ± 5	8.85 ± 0.07
1:2 Diluted	0.59	5	10	16,000	13,448	7.39	9.1% ± 0.6	2% ± 5	6.79 ± 0.19
1:2 Diluted	1.77	5	10	16,000	13,317	7.35	11.5% ± 1.1	6% ± 6	7.10 ± 0.25

Notes: Liquid recycle superficial velocity = 14.8 m/hr, pH controlled with carbon dioxide

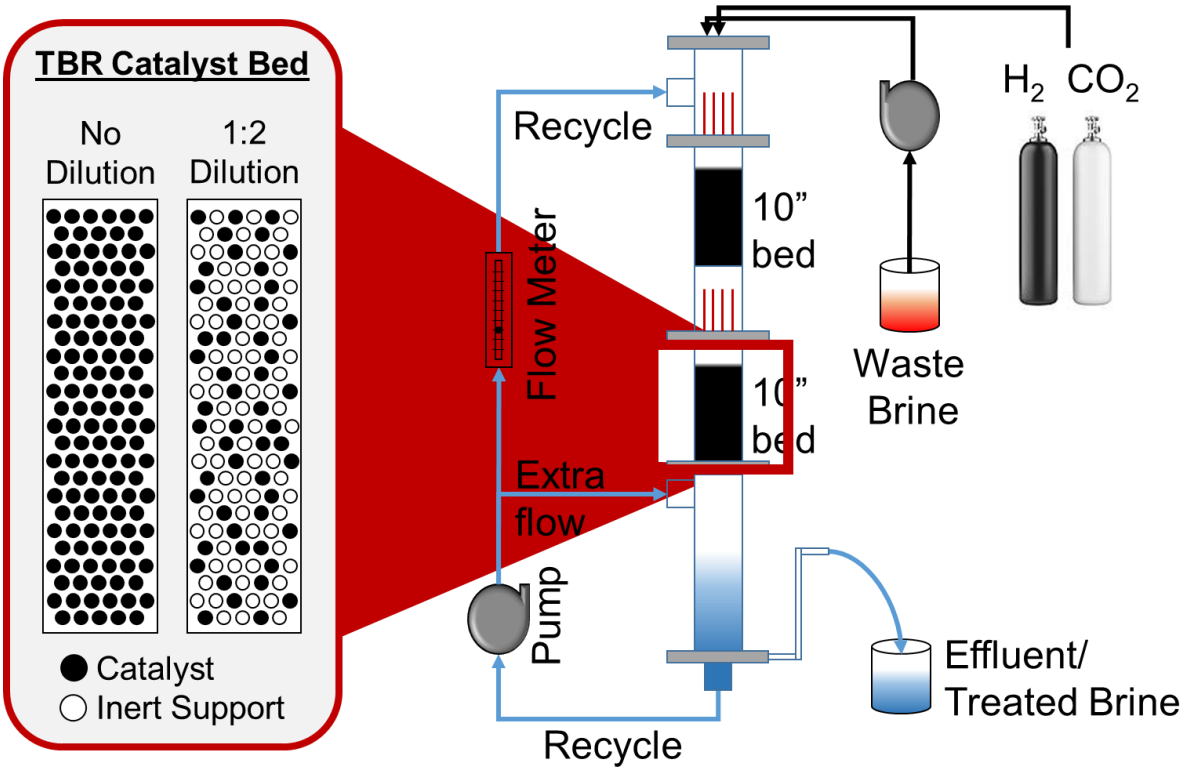

Figure 4.2: Diagram of the TBR reactor (right) with a blow-up of one catalyst bed (left) when filled with 1:2 diluted and non-diluted catalyst. Details of the TBR are discussed in Chap 3.

4.2.3 Batch Reactor Experimental Set-up and Protocol

A continuously-stirred (1,200 rpm) batch reactor was operator for 5-48 hours using a five-neck, round-bottom flask containing 2.20 or 6.67 g/L catalyst. Hydrogen or a hydrogen/nitrogen mixture was continuously supplied at 150 mL/min and solution pH was maintained at 5.0 using 0.1 M HCl via an automated titration manager (Radiometic TIM840). Synthetic brines containing 10 wt% NaCl and either 5,000 mg/L nitrate or 4,000 mg/L nitrite were tested. Two solutions with no NaCl were tested and had nitrite concentrations of 130 mg/L and 4,000 mg/L. Experiments were performed with non-diluted catalyst, 1:1 diluted catalyst (1 part catalyst : 1 part inert support), and 1:2 diluted catalyst (1 part catalyst : 2 parts inert support). All experiments were listed in Table 4.2.

4.2.4 Analytic Methods

Aqueous chloride, nitrate and nitrite concentrations were quantified using ion chromatography with conductivity detection (Dionex ICS-2100, 4×250 mm IonPac AS-19). A superficial velocity of 1.0 mL/min, 32 mM KOH eluent concentration and 96 mA suppressor current were used. All brine samples and reference standards were diluted 50-fold prior to IC analysis. Ammonium concentrations were measured with Hack kit vials and UV-Spectrophotometer (Nanodrop) at 655 nm wavelength. Dinitrogen concentrations were calculated via a mass balance, taking into account remaining aqueous species$\left([\mathrm{N_2}]_g = [\mathrm{NO_3^-}]_0 - [\mathrm{NO_3^-}]_\mathrm{i} - [\mathrm{NO_2^-}]_\mathrm{i} - [\mathrm{NH_4^+}]_\mathrm{i}\right)$. Selectivity was calculated as the distribution of end products from nitrite reduction, using the following formula: $\mathrm{Sel_{N_2}} = \frac{[\mathrm{N_2}]_{\mathrm{g,i}}}{[\mathrm{N_2}]_{\mathrm{g,i}} - [\mathrm{NH_4^+}]_\mathrm{i}}$. For batch experiments, the last 2-3 samples from each experiment were used to calculate the selectivity

from that experiment. For the TBR, selectivity for each condition was calculated using 8-12 samples from that condition.

4.3 Results and Discussion

4.3.1 Trickle Bed Reactor

Nitrate effluent concentrations during a 23 day experiment testing non-diluted catalyst and diluted catalyst were shown in Figure 4.3. The experimental conditions tested were listed in Table 4.1. Nitrate reduction remained consistent during each condition tested, as noted by the steady effluent data points. For the non-diluted catalyst (Fig 4.3a), the increase in hydrogen superficial velocity resulted in an increase in nitrate removal. This was expected because more hydrogen in the gas phase increased the concentration gradient between the gas and liquid phases, causing more hydrogen to transfer to the liquid phase. Because the reaction was hydrogen limited, this led to increased reactivity and a lower effluent nitrate concentration. In contrast, the 1:2 diluted catalyst (Fig 4.3b) did not result in a lower effluent nitrate concentration when hydrogen superficial velocity was increased. The pH of both experiments (Fig 4.3c) was relatively steady around 7.5 for all conditions except with non-diluted catalyst at H_2 = 60 sccm (yellow circles), when the pH increased to c. 8.0. Equipment limitations prevented further CO_2 addition to maintain pH at 7.5.

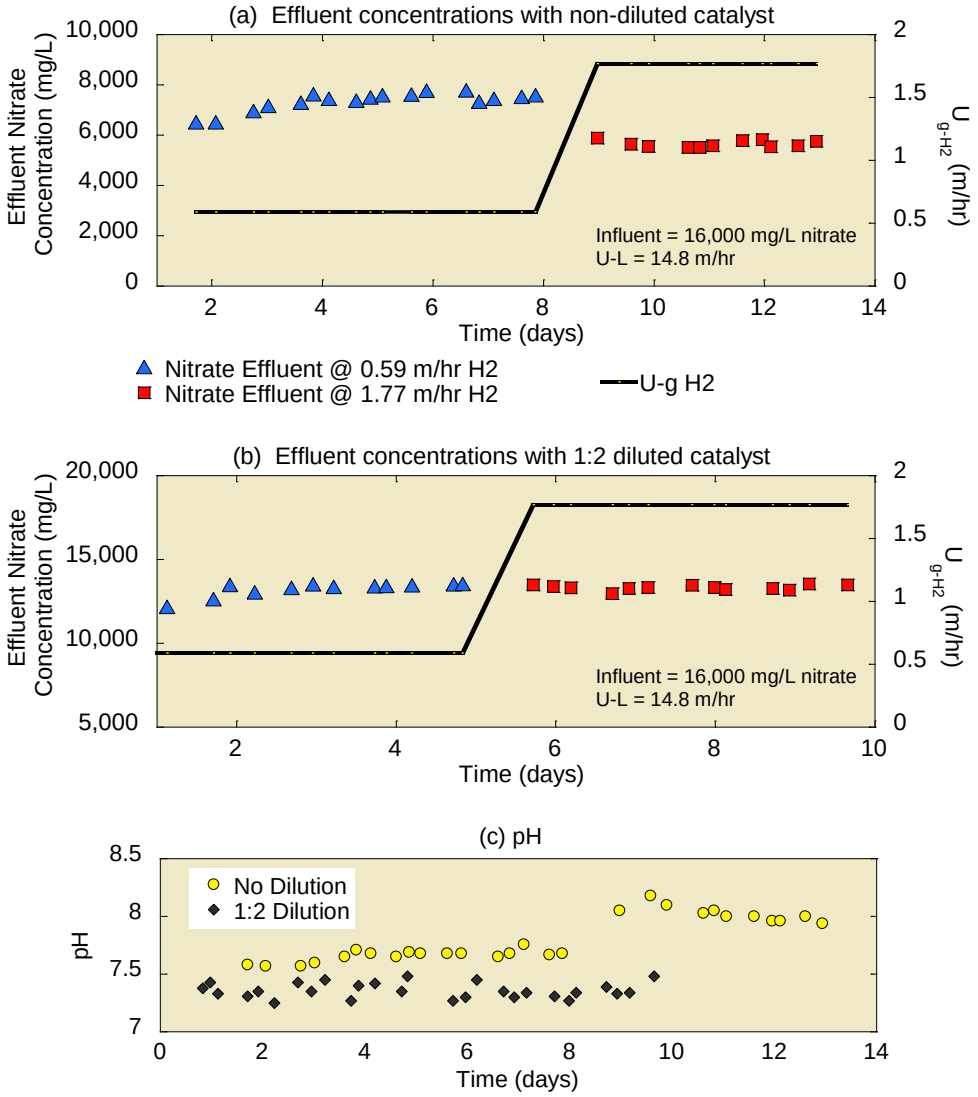

Figure 4.3: Nitrate effluent concentrations and hydrogen superficial velocities in a 23 d TBR experiment for a) non-diluted catalyst b) catalyst diluted 1:2 with same-size inert support, as well as c) pH from both experiments

The kinetics demonstrated among all the conditions tested were very similar and were shown in Figure 4.4a. As expected with the non-diluted catalyst (light yellow bars), the rate increased when the hydrogen superficial velocity was increased from 0.59 m/hr to 1.77 m/hr, due to a stronger driving force for mass transfer. With the 1:2 diluted catalyst (blue bars), the

increase in hydrogen superficial velocity did not result in a statistically significant change in activity. This result was not expected and was discussed below. Overall, all rates were very similar, when considered in the context of the TBR's performance under all conditions discussed in Chapter 3.

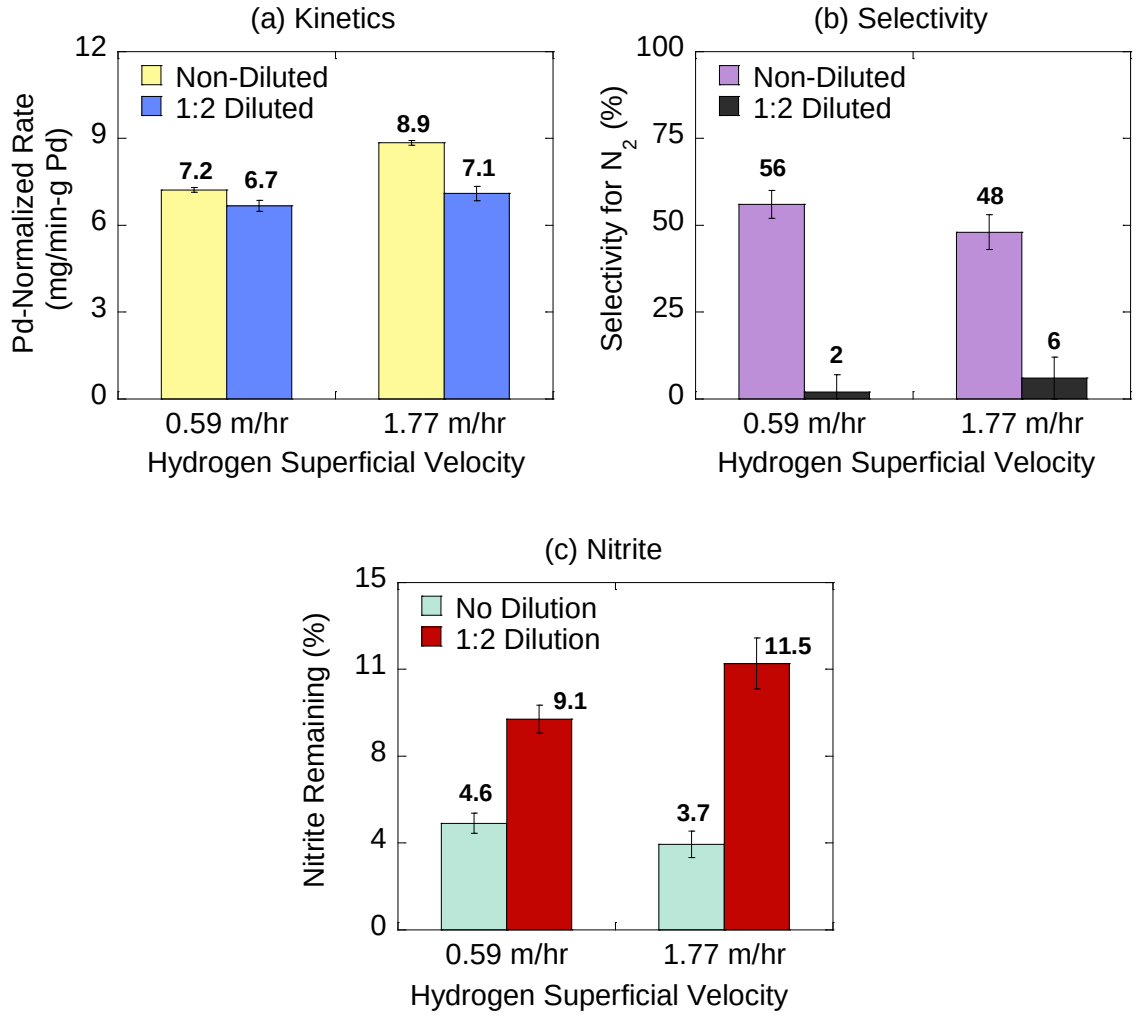

Figure 4.4: Nitrate reduction results for 23 d flow-through TBR experiment with non-diluted and 1:2 diluted catalyst showing a) activity, b) selectivity and c) nitrite production

Selectivity for dinitrogen during the experiments was shown in Figure 4.4b. When the TBR contained non-diluted catalyst (purple bars), the selectivity for N_2 remained very close to

the average of 53% ± 2.8, regardless of gas superficial velocity. When the catalyst was diluted (grey bars), the selectivity for N_2 dropped to nearly zero. As indicated by the error bars, there was some uncertainty contained with closing the mass balance during these experiments; however, it was clear the selectivity dropped significantly and approached zero.

Remaining nitrite concentration also varied between the non-diluted catalyst and the diluted catalyst and was shown in Fig 4.4c. With the non-diluted catalyst (blue bars), the residual nitrite was c. 4% regardless of the increase in hydrogen superficial velocity. When the catalyst was diluted (dark red bars), residual nitrite in solution increased by 100-200%. The explanation as to why nitrite concentrations increased was discussed below.

The selectivity results with the non-diluted catalyst were better than those achieved by Pintar and Batista [87], which was 35% selectivity towards N_2 with a TBR using Pd-Cu/alumina. Calvo *et al.* [135] achieved a maximum of 45% selectivity towards N_2 using Pd-Cu/AC in a TBR. However, the selectivity with the non-diluted catalyst was lower than results achieved in a previous study (c. 70%), using an up-flow fixed bed reactor with the same NaCl, pH, and initial nitrate concentration [65]. These results were discussed in detail in Chapter 3.

Though selectivity in the TBR was lower than desired, it was less of a concern for waste brine treatment compared to direct water treatment. Ammonium in waste brine would not impact water quality and accumulated NH_4^+ would increase the already-high cation concentration in brine (i.e., Na^+). One study found the impact of Na^+ and NH_4^+ on IX nitrate selectivity was similar for all water activities and resins tested [157]. A later study showed the type of co-ion present (i.e., Na^+ or K^+) present had a slight impact on resin regeneration efficiency, but the authors did not investigate NH_4^+ [158].

4.3.2 Batch Reactor Results

Results from the TBR led to a series of batch studies to determine if the same phenomenon could be replicated in the batch reactor and to probe the reduction pathway to evaluate the role of several system components, including hydrogen concentration, nitrite concentrations, chloride concentration, and inert support. Experimental conditions were listed in Table 4.2. Each "Case" was numbered and described an experiment performed with non-diluted and 1:2 diluted catalyst, which mimiced the TBR catalyst loading and the results of each condition were discussed together. Case 1 was also performed with 1:1 diluted catalyst; Case 2 was only performed with inert support.

Table 4.2: Experimental conditions tested in the batch reactor

		Mass Catalyst	Mass Inert Support	Exp Length	[NaCl]	Gas Tank Used		Selectivity for N2	Mass Normalized Zero-Order Rate Constant
		g	g	hr	wt%	no units		%	mg/min-gPd
Nitrate Reduction Experiments							Nitrate (mg/L)		
Case 1	No Dilution	0.33	0.00	48	10	100% H_2	5,000	81% ± 3.0	104.9 ± 4.5
Case 1	1:1 Dilution	0.33	0.33	48	10	100% H_2	5,000	75% ± 9.5	87.32
Case 1	1:2 Dilution	0.33	0.66	48	10	100% H_2	5,000	76% ± 1.6	117.45
Nitrite Reduction Experiments							Nitrite (mg/L)		
Case 2	Inert Support	0.00	0.66	10	10	100% H_2	2,500	n/a	no activity
Case 3	No Dilution	0.33	0.00	5	0	100% H_2	130	36% ± 2.1	98.88 ± 0.29
Case 3	1:2 Dilution	0.33	0.66	5	0	100% H_2	130	43% ± 4.2	114.54 ± 3.8
Case 4	No Dilution	0.33	0.00	8	0	100% H_2	4,000	100% ± 0.1	414.46 ± 28.1
Case 4	1:2 Dilution	0.33	0.66	8	0	100% H_2	4,000	98% ± 0.2	664.61 ± 1.19
Case 5	No Dilution	0.33	0.00	24	10	100% H_2	4,000	94% ± 4.2	201.96 ± 13.7
Case 5	1:2 Dilution	0.33	0.66	24	10	100% H_2	4,000	93% ± 0.7	196.93 ± 0.88
Case 6	No Dilution	0.33	0.00	24	10	5% H_2, 95% N_2	4,000	100% ± 0	23.6 ± 0.30
Case 6	1:2 Dilution	0.33	0.66	24	10	5% H_2, 95% N_2	4,000	100% ± 0	27.6 ± 0.007
All Experiments: Solution volume = 150 mL, pH maintained @ 5.0 with HCl, Stir rate = 1200 rpm, Gas Flow Rate = 150 sccm									

Nitrate Reduction in Brine. Three experiments were performed in brine conditions with high hydrogen concentrations to test nitrate reduction at three different catalyst-support ratios: 1) no dilution, 2) 1:1 dilution and 3) 1:2 dilution (Case 1). The kinetics and selectivity results were shown in Figure 4.5. The kinetics of all three catalyst ratios were similar (Fig 4.5a), which was in agreement with the results achieved with the TBR using two different catalyst ratios. In contrast, the selectivity of the three batch experiments were also very similar (Fig 4.5b) and all above 70% towards N_2, which was not in agreement with TBR results. The batch results from Case 1 match past work, which achieved >70% selectivity towards N_2 using a Pt-Cu/alumina catalyst in a batch reactor with a starting nitrate concentration of 62 mg/L [143].

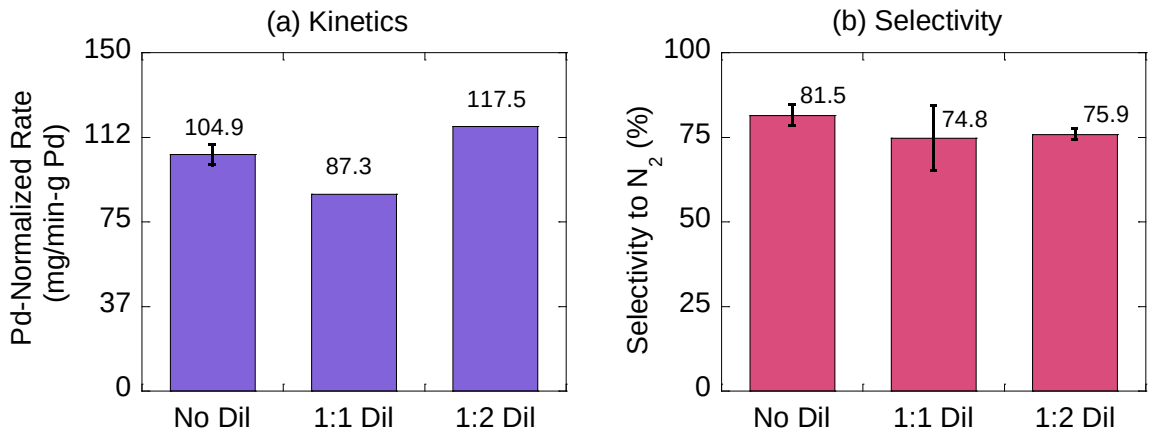

Figure 4.5: Batch results showing a) kinetics and b) selectivity for nitrate reduction in brine conditions with high hydrogen concentrations (Case 1)

The results of the batch experiments for Case 1 indicated the TBR conditions were not replicated in the batch reactor and further experiments were required to examine different components of the system. Evaluating nitrite reduction removed the nitrate-to-nitrite reduction step and provided a more clear perspective on the mechanisms influencing selectivity. Experiments were performed to test the influence of high and low nitrite concentrations, high and low hydrogen concentrations and the presence or absence of NaCl. All conditions were tested with non-diluted catalyst and 1:2 diluted catalyst; the pair of experiments were discussed together.

Nitrite Reduction in DI Water. The impact of nitrite concentration was tested in Case 3 (low = 130 mg/L) and Case 4 (high = 4,000 mg/L) in the absence of NaCl and with high hydrogen concentrations. The experimental results from nitrite reduction and the production of ammonium and dinitrogen in Case 3 were shown in Figure 4.6. Both reactions followed a similar progression, which indicated the presence of inert support had no impact on activity or selectivity.

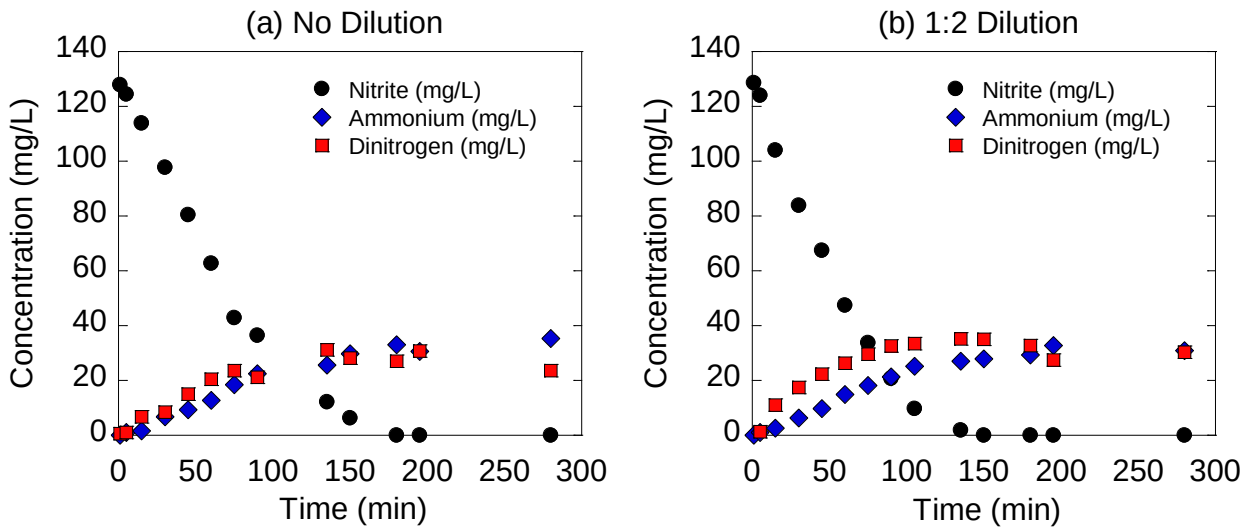

Figure 4.6: Nitrite reduction in DI water with no brine for a) non-diluted catalyst and b) 1:2 diluted catalyst (Case 3)

Activity and selectivity results from Case 3 and Case 4 were shown in Figure 4.7 and there were significant differences between both Cases. When the initial concentration of nitrite was low (Case 3), the activity was similar between the non-diluted and diluted catalyst (Fig 4.7a). When the initial concentration of nitrite was high (Case 4), the activity of the 1:2 diluted catalyst was 160% of the activity of the non-diluted catalyst. This was unexpected and did not occur in any other condition tested. When the experimental data was examined, reduction started within the first 15 m and followed a zero-order profile for the duration of the experiment with an $R^2 > 0.97$. Steady reduction with the 1:2 diluted catalyst ruled out the hypothesis that the increased particle concentration in the reactor (6.67 g/L diluted vs 2.20 g/L non-diluted) led to greater collisions between particles and created more powder-like catalyst fines, which are known to have higher activity. If this was the case, a change in kinetics would have been observed in the experimental data during the course of the experiment. No change was observed.

The explanation for the higher activity with 1:2 diluted catalyst remained unclear and warranted additional experiments.

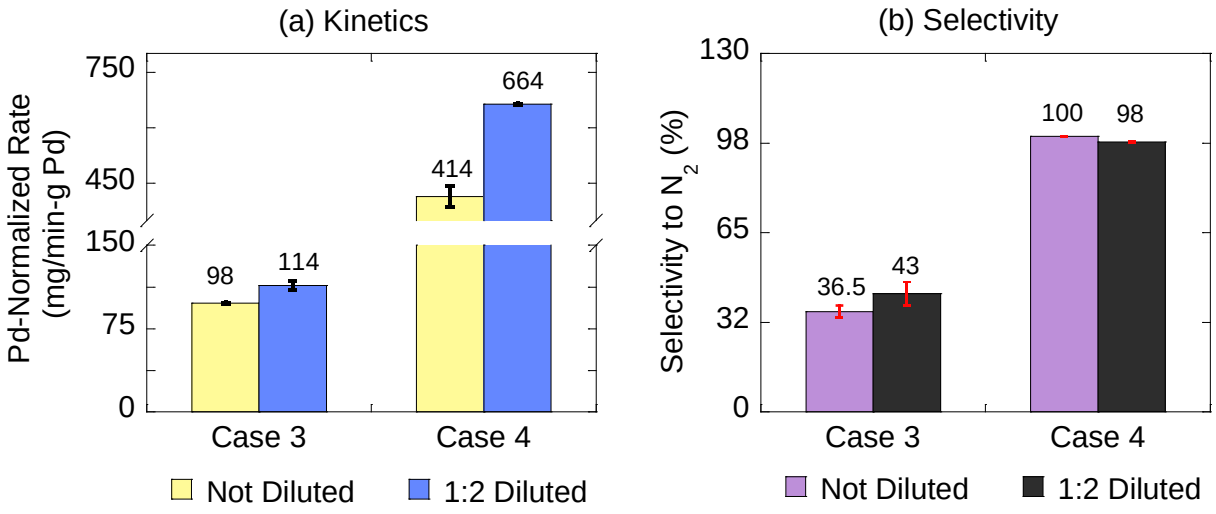

Figure 4.7: Batch results showing a) kinetics and b) selectivity for low (Case 3) and high (Case 4) initial nitrite concentrations, no brine, and high hydrogen concentrations

As shown in Figure 4.6b, there was a significant difference in selectivity between Case 3 and Case 4. In both Cases, the presence of inert support had no impact on the selectivity. When the initial concentration of nitrite was low (Case 3), the selectivity towards N_2 was c. 40%. When the initial concentration of nitrite was high (Case 4), selectivity increased to c. 99%.

Nitrite Reduction in Brine. The impact of hydrogen concentration was tested in Case 5 (high = 100%) and Case 6 (low = 5%) in brine conditions with high initial nitrite concentrations. In both Cases, the inert support did not have an impact on the results. As shown in Figure 4.8, high hydrogen concentrations led to significantly faster reduction rates (c. 200 vs 25 mg/min-gPd), which was expected due to the steeper concentration gradient and stronger driving force for hydrogen mass transfer into the liquid phase. The hydrogen supplied in Case 6 was 5% of the hydrogen supplied in Case 5, resulting in a Case 6 activity 12% of the Case 5 activity.

Differences in hydrogen concentration also had a direct impact on selectivity, as can be seen in Fig 4.8b. Low hydrogen concentrations (Case 6), led to nearly 100% selectivity toward N_2, while high hydrogen concentrations (Case 5) reduced the selectivity to c. 93%.

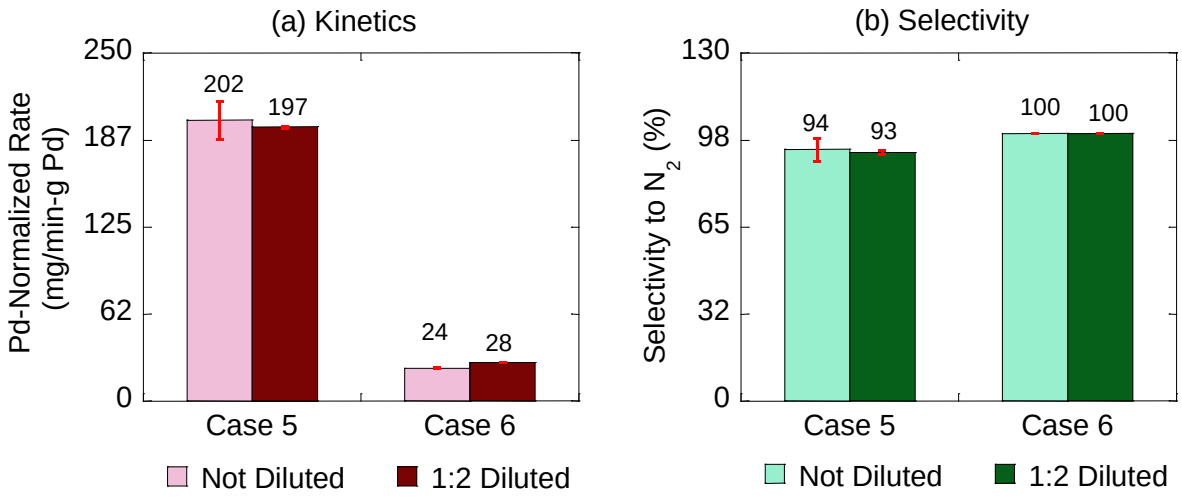

Figure 4.8: Batch results showing a) kinetics and b) selectivity for low (Case 6) and high (Case 5) hydrogen concentrations with the same high initial nitrite concentration and brine conditions

The impact of chloride can be seen by comparing the results from Case 4 (no brine) and Case 5 (brine) with high initial nitrite concentrations and high hydrogen concentrations (see Figure 4.9). As shown in Figure 4.9a, reduction activity was higher in the absence of NaCl. The difference in kinetics between Case 4 and Case 5 was expected due to past work demonstrating chloride competition for reactive sites and its presence lowered activity [51, 53, 155]. As seen in Figure 4.9b, the presence of chloride also impacted selectivity. In the absence of chloride (Case 4), selectivity was nearly 100%, but when chloride was present (Case 5), the selectivity dropped to c. 94%. Though the difference in values was small, a higher concentration of NH_4^+ was clearly present during sample analysis.

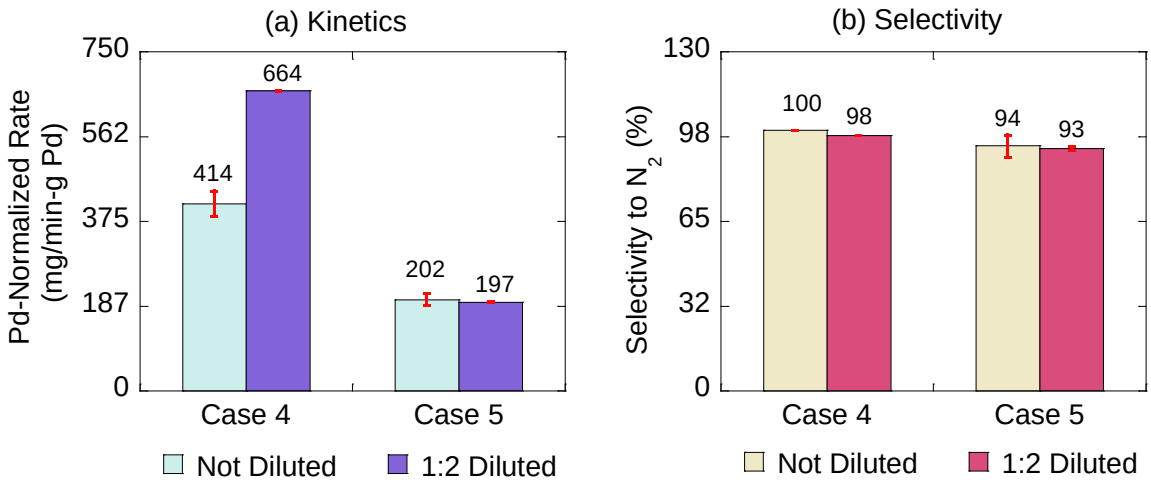

Figure 4.9: Batch results showing a) kinetics and b) selectivity for no brine (Case 4) and brine (Case 5), hydrogen concentrations with the same high initial nitrite concentration

Nitrite Reduction with Inert Support. An experiment was run to determine if the inert activated carbon support had any intrinsic capacity for nitrite reduction (Case 2). Using an initial nitrite concentration of 2,500 mg/L, 10wt% NaCl, and a high hydrogen concentration, no reduction was observed over a 10 hour period. These results suggested the inert support in the 1:2 diluted system did not play a role in nitrite reduction in the batch or flow-through TBR reactors.

4.3.3 Proposed Model for TBR Selectivity

A proposed model for selectivity in a non-diluted and diluted TBR was shown in Figure 4.10 and depicted the palladium metal surface with chloride, atomic hydrogen and NO sorbed to the surface. NO was depicted because it was the most prevalent and active reduction intermediate [154]. In the non-diluted TBR, every particle in the reactor was a catalyst particle with active sites (see Fig 4.2 above). In a flow-through system, that meant there was less time

available for hydrogen mass transfer from the gas to the liquid phase, resulting in fewer H• per active site and a high N:H ratio. As discussed above, hydrogen-limited conditions favored N-N pairing and higher selectivity for N_2. Conversely, in the TBR with diluted catalyst, the active sites were more geographically dispersed throughout the reactor, allowing more time for hydrogen mass transfer to each site. This resulted in higher H• per active site, decreased the N:H ratio, decreased N-N pairing opportunities and shifted selectivity towards NH_4^+. In both cases, chloride competed for active sites with nitrate, nitrite, hydrogen and NO. [138].

The model also served to explain the TBR results depicted in Figure 4.4c. Though the model above depicted NO on the surface of the catalyst, NO_2^- was also reduced on the palladium surface. NO_2^- has been shown to be least competitive for active sites when compared to NO or H• [159]. In the non-diluted TBR, there was less competition by H• for active sites on the palladium surface, which allowed more NO_2^- to access the sites and be reduced to NO, leaving a lower concentration of residual nitrite in the TBR effluent. However, in the diluted TBR, there was greater competition by H• for active sites on the palladium surface, limiting the amount of N_2O reduced and increasing its concentration in the TBR effluent.

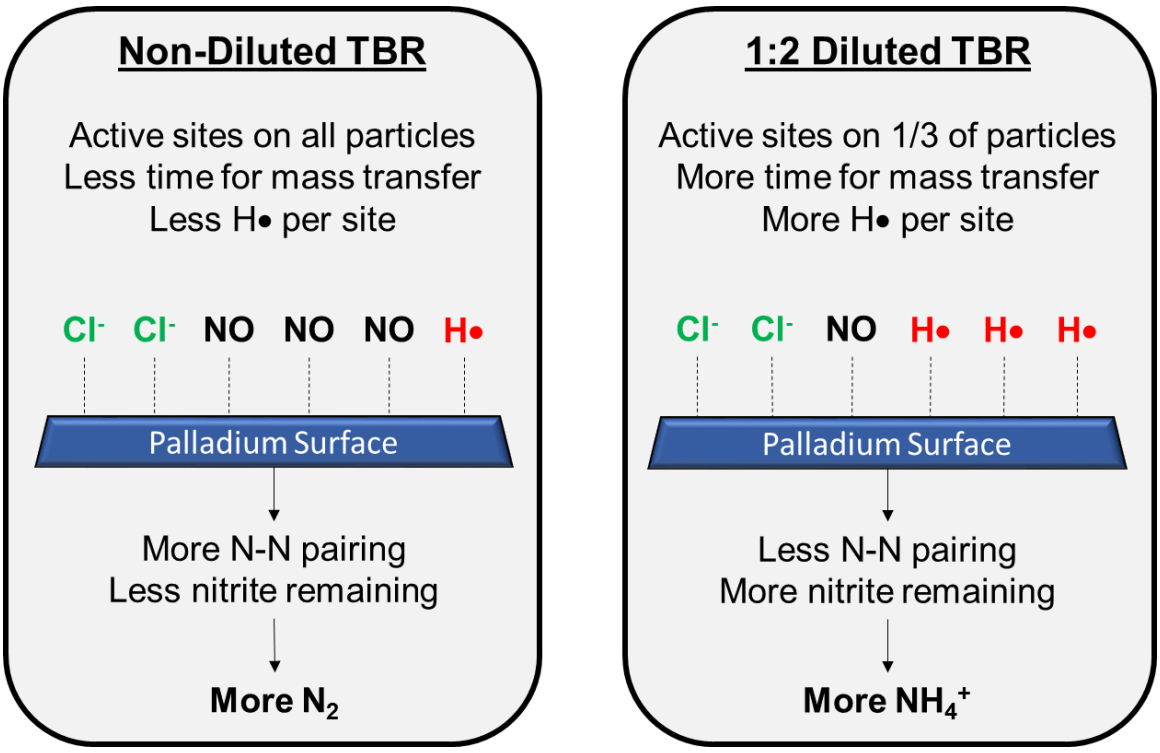

Figure 4.10: Proposed model for selectivity nitrate hydrogenation in a non-diluted and diluted TBR

Direct comparison of these results with those in literature was difficult. Industrial TBRs use catalyst dilution for two main purposes: 1) controlling the temperature profile along the reactor in highly exothermic reactions [73, 160], and 2) improving catalyst wetting efficiency [161–163]. Both purposes were inter-related and impacted overall reactor performance in the form of yield and selectivity. Catalyst wetting influenced activity, which increased temperature and yield. Temperature influenced side reactions, which impacted yield and selectivity. For example, in the case of ethylene oxidation, selectivity decreased with increasing temperature, so 10-30% bed dilution was used to maintain a reactor temperature near 228 °C, which achieved the desired optimal trade-off between yield and selectivity of 53% and 70%, respectively [76].

These results and their underlying insights were difficult to directly apply to this work because my reactor was operated at ambient temperature, nitrate reduction was not highly exothermic and was not encumbered by side reactions. One aspect that may be applicable was the "improved" hydrogen mass transfer with diluted catalyst, evidenced in the selectivity results by higher selectivity towards NH_4^+. However, the "improved" mass transfer was more likely due to time and distance available between reactive sites in the diluted bed (as discussed above) rather than the rate of mass transfer. In industrial TBRs, bed dilution for improved mass transfer was pursued via addition of fines (smaller-sized) and not same-sized inert supports because fines decreased voidage and increased liquid distribution [161]. Dilution with same-size inert support neither effect, leading to the reasonable conclusion that hydrogen mass transfer likely occurred at the same rate in my TBR regardless of catalyst dilution or not.

Results of the nitrite reduction experiments in the batch reactor were in agreement with the proposed model. The differences between the selectivity results of Case 3 and Case 4 were explained by the nitrite concentrations and the ratio of N:H on the catalyst surface. When the ratio was higher (Case 4), there were more intermediate N-species adsorbed to the surface and greater incidents of N-N pairing occurred, which resulted in c. 98% towards N_2. Conversely, a lower nitrite concentration (Case 3) led to greater production of NH_4^+ because H• was in relative excess to N on the reactive site and decreased selectivity to c. 40%. Similarly, the 100% selectivity with low concentrations of hydrogen (Case 6) was attributed to high N:H ratio on the surface and high N-N pairing, while high hydrogen concentrations (Case 5) resulted in a lower N:H ratio and c. 93% selectivity for N_2. Lastly, the presence of chloride (Case 4) lowered the number of available reactive sites and decreased N-N pairing, which resulted in a lower selectivity (94%) compared to when chloride was absent (99%).

Other recent reports in literature supported the results obtained in this study regarding competitive sorption of reactive surface sites. In NO_3^- reduction experiments with Pd-Cu/Al_2O_3 catalyst in simulated groundwater, Chaplin *et al.* [64] demonstrated a decrease in N_2 selectivity with increasing Cl^- concentration; 50 mg/L Cl^- resulted in 76% N_2 and 1,000 mg/L Cl^- resulted in 59% N_2. In contrast, chloride was demonstrated to have no impact on selectivity during photo catalytic nitrate reduction with TiO_2 in synthetic ion exchange waste brines with up to 10 wt% NaCl [53]. This may be due to the differences in a photo catalytic system when compared to a traditional bimetallic/granular support catalyst, namely high surface area of TiO_2 nanoparticles and the stabilizing effect of higher ionic strength, which also led to a slight increase in nitrate removal. Testing a real waste brine, the authors found sulfate had a stronger negative impact than chloride [53].

In addition to high chloride levels found in waste brine, another anion expected was sulfate, which has been shown to compete more strongly (vs Cl^-) for reactive sites even at low concentrations. In an electrochemical reactor with a Pt-Cu electrode, the presence of 0.01 M NaCl decreased nitrate-to-nitrite conversion by 24% and reduced selectivity by 2.8%, whereas sulfate (0.01 M) decreased conversion by 35% and selectivity by 4.3%. The authors used electrochemical impedance spectroscopy (EIS) to verify the greater surface coverage by sulfate (vs chloride) on Pt-Cu, cyclic voltammetry to show sulfate inhibited NO_2^- reduction to a greater degree than chloride, and X-ray photoelectron spectroscopy (XPS) to verify stronger binding energies of both sulfate and chloride, which indicated they would out-compete H• ions for reactive sites [156].

4.3.4 Practical Implications for IX Waste Brine Treatment

Denitrification of IX waste brine to enable its reuse encompassed the assumption that chloride was a critical component of the brine, as it was required for IX resin regeneration. As such, nothing can be done to eliminate competitive sorption of chloride at active sites. On the other hand, sulfate was not required for IX resin regeneration, but was shown above to be more competitive than chloride for reactive sites. Additionally, sulfur species were shown to poison catalysts and deactivated their reducing capability [62, 63]. Removing sulfate from waste brine has been effectively demonstrated with sulfur-reducing bacteria [41] or precipitation as $BaSO_4$ [164]. Both methods could be options for addressing competitive sulfate adsoption to the catalyst surface during IX waste brine regeneration.

4.4 Conclusions

A three-phase trickle bed reactor was evaluated for nitrate reduction and selectivity in synthetic ion exchange waste brine with non-diluted and diluted beds of Pd-In/AC catalyst. It was found that multiple factors contributed to selectivity in the TBR, including concentration of N-species, concentration of hydrogen, presence of competing ions and the concentration of active sites in the reactor. The purpose of adding the inert support was to geographically separate active catalyst sites to allow more time for hydrogen mass transfer from the gas to liquid phase. Specific findings included:

- Diluting the TBR with same-size inert support did not improve the activity for nitrate reduction.
- Catalyst dilution in the TBR significantly decreased selectivity for N_2 and increased nitrite concentration in the reactor effluent.

- The N:H ratio on the catalyst surface in TBR and batch experiments played a significant role in the resulting selectivity of end-products.
- Inert carbon support demonstrated no activity for nitrite reduction.
- Catalyst dilution had no impact on selectivity in the batch reactor experiments.
- Chloride in brine competed for surface sites, decreased reduction activity and selectivity in the batch reactor.
- The proposed model of competitive sorption on the palladium surface elucidated selectivity mechanisms with different solution components.

CHAPTER 5

SUMMARY AND CONCLUSIONS

5.1 Summary and Conclusions

This dissertation examined a novel hybrid ion exchange-catalyst system in order to achieve the following objectives: (1) Using an experimental and modeling approach, determine whether the accumulation of bicarbonate and sulfate in reused waste brine will negatively impact the hybrid system performance and model key IX system variables using a case-study approach; (2) Evaluate reactor performance in continuously stirred batch reactors and fixed bed reactors; and optimize a fixed bed reactor to reduce hydrogen mass transfer limitations to the catalyst surface; and (3) Evaluate selectivity of Pd-In/AC catalyst using different reactor types and matrix conditions. Findings from these efforts were as follows:

5.1.1 Objective 1

- Experimental results and model simulations indicated that concentrations of non-target ions like sulfate and bicarbonate would accumulate in waste brines over repeated cycles of reuse, but this buildup would not negatively impact IX performance or lead to permanent deactivation of the Pd metal catalyst.
- Adding makeup salt to treated waste brines was necessary to maintain long treatment cycle run times between regeneration.
- Salt costs and waste brine volumes could be decreased by up to 80% with the hybrid system.

- Tradeoffs between regeneration length, treatment time, and salt warranted reevaluation of operations in a hybrid system compared to a conventional system:
    - By switching from 2 BV regeneration without brine reuse to 10 BV regeneration with brine reuse, the plant operator would realize a 53% reduction in total NaCl required and 50% increase in treatment length each cycle.
    - Brine reuse resulted in a 300% - 600% increase in NaCl efficiency, which was defined as the ratio of bed volumes of water treated per kilogram of NaCl used.
    - Using catalytic activity rates from the SBR, a 2 BV regeneration led to nitrate concentrations around 9,000 mg/L in the IX waste brine and an anticipated reactor palladium cost of $55.5K; whereas 10 BV regeneration led to nitrate concentrations around 4,100 mg/L in the waste brine and a palladium cost of about $63.2K.
- Achieving high catalyst activity and stability was critical for reducing the cost of the hybrid system. The catalyst reactor cost was roughly estimated by considering the cost of palladium only. The cost of palladium for fixed bed reactor with 2 BV regeneration would be around $1.4M, while the higher catalyst activity in the SBR resulted in a Pd cost of only $55.5K. These costs were off-set by lower expenses for NaCl purchase but $1.4M was significantly more expensive. Improving catalyst activity in the fixed bed reactor was critical for lowering the costs and moving the hybrid system closer to commercial viability.
- Reactor design played an important role in the effectiveness of hydrogen mass transfer.

5.1.2 Objective 2

Results from Objective 1 led to efforts designing a new reactor that would improve hydrogen mass transfer and overall catalytic activity, which was critical for reducing system costs and approaching economic viability of the hybrid system. Key findings included:

- Waste brine denitrification using a TBR was evaluated for different liquid and H_2 loading rates for both 12x14 and 12x30 Pd-In/AC catalysts.
- The highest activity of 17.4 mg min^{-1} gPd^{-1} and the highest H_2 mass transfer coefficients of 21.12 min^{-1} were obtained with the 12x30 catalyst.
- The TBR demonstrated c. 300% higher activity than an up-flow fixed bed reactor from previous work using the same 0.5wt%Pd-0.05wt%In/AC catalyst (12x14).
- Smaller catalyst support size (12x30) demonstrated higher activity and mass transfer.
- Mass transfer was the highest in the trickle flow regime with partially wet catalyst.
- Hydrogen mass transfer limitations remained significant and prevented full realization of intrinsic catalyst activity.
- Metals loss from the catalyst indicated the need to develop a more robust catalyst for use in the brine matrix.
- TBR performance was a step forward to developing an economically-viable system.

5.1.3 Objective 3

A three-phase trickle bed reactor was evaluated for nitrate reduction and selectivity in synthetic IX waste brine with non-diluted and diluted beds of Pd-In/AC catalyst. It was found that multiple factors contributed to selectivity in the TBR, including concentration of N-species,

concentration of hydrogen, presence of competing ions and the concentration of active sites in the reactor. The purpose of adding the inert support was to geographically separate active catalyst sites to allow more time for hydrogen mass transfer from the gas to liquid phase. Specific findings include:

- Diluting the TBR with same-size inert support did not improve the activity for nitrate reduction.
- Catalyst dilution in the TBR significantly decreased selectivity for N_2 and increased nitrite concentration in the reactor effluent.
- The N:H ratio on the catalyst surface in TBR and batch experiments played a significant role in the resulting selectivity of end-products.
- Inert carbon support demonstrated no activity for nitrite reduction.
- Catalyst dilution had no impact on selectivity in the batch reactor experiments.
- Chloride in brine competed for surface sites, decreased reduction activity and selectivity in the batch reactor.
- The proposed model of competitive sorption on the palladium surface elucidated selectivity mechanisms with different solution components.

5.2 Implications for Future Research

Based on the work conducted in this dissertation, four future research directions are described below:

5.2.1 Reactor Design

While results in Chapter 3 represented a step forward in demonstrating the efficacy of the hybrid system, further studies are needed to determine the best reactor design. Improving the current TBR holds promise for overall improvement of the system, but other reactor types should be considered.

Structured reactors represent an alternative reactor type and are those in which the catalyst is deliberately organized and fixed inside the reactor casing, rather than dumped via the conventional random packing method [165]. Structured reactors have been shown to reduce mass transfer limitations and support process intensification, and can be applied to fluidized beds or slurry bubble columns [165, 166]. A variety of materials have been demonstrated as successful supports for catalysts in these reactors, such as nickel foam, carbon foam, ceramic foam, wire gauze, cloth, and fibers [167–173]. Some of these supports are synthesized with carbon nano-materials and are discussed below.

Using a structured reactor for nitrate hydrogenation would improve mass transfer by increasing reactive surface area and reducing diffusion lengths. The structured aspect would also increase repeatability and reliability of results by eliminating the variation in packing inherent with the conventional packing method. Lastly, the hydrodynamics would be more consistent and more readily measurable, which would help during performance analysis and facilitate tracer studies and residence time distribution (RTD) analysis.

One type of structured reactor that has been used for many years is a ceramic monolithic reactor, also called a honeycomb. First used with automobile exhaust treatment, monolithic reactors are advantageous over pellet catalysts due to lower pressure drop and the ability to withstand higher superficial velocities [174]. A monolithic reactor holds promise for denitrification and has been shown to scale reliably. Alternately, micro-structured reactors have recently become a focus of research and present numerous options for reactor configuration depending on the desired chemistry (see Figure 5.1) [175]. The primary drawback to a micro-structured reactor relates to scale-up options and the reliability of data gained from bench-scale micro-structure reactor experiments.

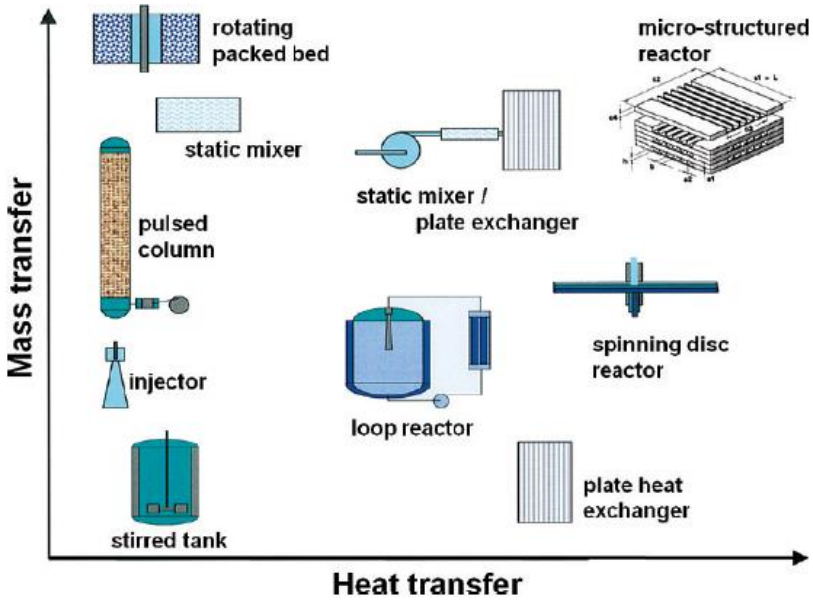

Figure 5.1: Relative advantages of different micro-reactor configurations [175]

A fluidized bed reactor and slurry reactor are two different names for a co-current, up-flow reactor in which the gas or liquid superficial velocity is high enough to maintain suspension of the catalyst particles, increasing mixing and mass transfer rates [71]. Typically, "fluidized

bed" indicates when high gas superficial velocities cause catalyst suspension, while "slurry reactor" indicates when high liquid superficial velocities cause catalyst suspension. In both cases, catalyst particles experience increased collisions, potentially causing physical destruction of the particles.

Liu and Ji [66] found a fluidized bed reactor with Ni-W/TiO_2-SiO_2 performing syngas methanation demonstrated higher conversion, higher selectivity and better bed temperature control as compared to the same reaction conducted with a fixed bed reactor. Patel, *et al.* [48] used a recycling slurry reactor with activated carbon inoculated with high-salt tolerant bacteria for nitrate and perchlorate reduction from IX waste brine. They reported no destruction of the carbon supports, but did report AC with nitrogen bubbles attached were continuously carried out of the system; they prevented this by adding a baffle and also modified the liquid superficial velocity [48]. Slurry reactors have been studied extensively for some industrial applications (i.e., Fischer-Tropsch synthesis and hydrocarbon production), so there is extensive literature from which to draw [176].

The work in this dissertation focused on an activated carbon catalyst support, which is brittle and suffers from physical destruction in reactors other than fixed beds. Therefore, if an alternate reactor configuration were chosen, that would necessitate an evaluation of different catalysts which would be amenable to the conditions present in the reactor.

5.2.2 Catalysts: Finding or Developing an Alternative

As noted above, activated carbon was identified as a more active and selective support for nitrate reduction in a brine matrix. However, given the hydrogen mass transfer limitations

reported and discussed in this work, a compromise between activity, selectivity and stability may lead to choosing a novel catalyst that improves the overall performance of waste brine denitrification. The selectivity of the catalyst is less important for this application because the production of ammonium during waste brine denitrifaction does not directly impact drinking water quality. Research and development of a wide range of nano-materials and new catalyst formulations provide many avenues to pursue.

Improvement of catalyst stability is critical for the viability of the hybrid system. Catalysts used in fix bed reactors in this work suffered from metal loss over time, which decreased the intrinsic activity of the catalyst. The cause of metal loss is not known, but could be related to the brine matrix or hydraulic loading over time in a high flow environment. The use of precious metals (i.e., Pd) for bimetallic catalysts constitutes the greatest portion of the cost of the catalyst system. If the catalysts are known to leach metals during short periods of operation, the ability to recover the metals will be significantly reduced, which decreases the cost effectiveness of catalysts. Cost will always be an important consideration for adoption of new technology and a more robust catalyst will improve the economics of the hybrid system.

Catalyst stability is also referred to as mechanical strength in the literature. In a review of mechanical strength of solid catalysts, Wu *et al.* [177] discussed the various scales of mechanics relating to catalysts: micro scale, pellet scale, pellet-packing scale and reactor scale. Brittle fracture is one of the key attributes describing a catalyst's mechanical strength and catalyst analysis should incorporate all steps from manufacturing to industrial application [177].

Carbon nano-fibers (3-100 nm diameter and 0.1-100 μm length) and nano-tubes have attracted recent attention for their high activity, mechanical strength and versatility [178–180]. Synthesis of carbon nanofibers and nanotubes have been investigated on ceramic and nickel

foams for general catalytic applications [181, 182]. Espinosa and Lefferts [183] demonstrated fast nitrite reduction and high ammonia selectivity with carbon nano-fibers supported by nickel foam nanoparticles in the absence of Pd. An activated carbon cloth (ACC) and glass fiber cloth (GFC) supporting Pd-Cu catalysts were used for nitrate hydrogenation in water and the ACC demonstrated higher activity and selectivity than the GFC [168].

Hydrocarbon processing is one field where a catalyst's ability to remain highly active, withstand fluctuations in temperature and pressure, withstand high gas and liquid superficial velocities, and maintain mechanical strength are significantly valued. For atmospheric applications, the additional of a binding agent, such as silicon dioxide, has been used to increase the mechanical strength of the catalyst [184]. Titanium-silicalite microsphere catalysts made from silica and titanium have been proposed for high mechanical strength due to Si-O-Si bridges and applied to hydrocarbon conversion [185].

In the field of fuel cells, electrochemical processes are used in conjunction with catalysts, providing a body of literature from which to explore alternate support materials. Tungsten oxide has been investigated as an alternate support for carbon because it does not oxidize and can withstand acidic conditions when used in membrane fuel cells [186, 187]. Alternately, functionalized graphene sheets supporting Pt catalyst have demonstrated high surface area and improved stability when compared to commercial catalysts for membrane fuel cells [188]. Multiple conducting polymers show promise as catalyst supports for direct methanol fuel cell anodes, including poly(3,4-ethylenedioxythiophene) (a.k.a. PEDOT), which demonstrated high activity and long-term stability as a Pt catalyst support [189].

Given the range of options regarding reactor design and catalysts discussed above, developing a new approach would need to be accomplished in a thoughtful and methodical

manner. My approach would be to consider new carbon supports used within a structured reactor. The properties and performance demonstrated by novel nano-carbon supports are impressive and show great promise for nitrate reduction, but my concern would be scale-up. Incorporating nano-carbon supports into structured reactors would leverage the benefits of the nano-catalyst, while also potentially supporting scale-up. Some types of structured reactors are not "scaled-up", but rather they are "scaled-out," which is the type I would pursue. Scale-out means the dimensions of the reactor are not altered, but the process is intensified by using multiple copies of the small reactor. A major benefit to scale-out is that lab-based performance is replicated in the field because the same reactor is used, which eliminates the complicated process of scale-up predictions and testing. Scale-out is a technique that may present a viable option for leveraging new nano-materials on the large scale required for IX waste brine regeneration.

5.2.3 Hydrogen Delivery

Despite the improvements in hydrogen mass transfer demonstrated with the trickle bed reactor, hydrogen mass transfer limitations remain the single biggest factor limiting the performance of the catalyst reactor and overall improvement of the hybrid system. Below, three avenues of future research that could improve electron donor availability are described:

Increased Reactor Pressure. Pressurizing the reactor is one potential strategy to overcome mass transfer limitations. For example, pressurizing the reactor to 5 atm (0.5 MPa) at 50 °C would increase the solubility of hydrogen by 600% [131], which would increase the driving force for H_2 mass transfer. While pressurized reactors are used regularly in industrial applications, their use at water treatment plants would require a thorough analysis. Pressurized

reactors require using different components (i.e., steel), which are more expensive than the plastics or PVC used to construct non-pressurized reactors. Space limitations and safety considerations would also need to be evaluated, as adding a pressurized reactor using hydrogen gas may present challenges.

Formic Acid Reduction for H_2 Production. When considering alternate hydrogen sources, formic acid has a very high solubility in water, and could be delivered at stoichiometric levels to eliminate the need for a separate gas phase [121]. However, formic acid requires reduction over Pd to produce H_2 and CO_2, and while one study demonstrated higher nitrate reduction activity with formic acid in a batch reactor, there was an "induction period" that delayed the onset of nitrate reduction [60]. The same study found nitrate activity in a continuous flow hollow fiber reactor was 7x slower using formic acid, when compared to hydrogen, which was attributed to the much slower diffusion rate of formic acid (0.96×10^{-5} vs 4.34×10^{-5} cm^2 sec^{-1} for H_2) and small pores (<10 nm) of the hollow fiber reactor.

Electrochemical H_2 Production. Electrochemical production of hydrogen is one method that shows potential for increasing the supply of hydrogen in water at the stoichiometric levels required. Electrolysis of water to generate hydrogen is clean and can be controlled by the current applied [190]. Advantages of electrochemical systems include ambient operating conditions, rapid start up, minimal sludge generation, and high efficiency [191]. Bio-electrochemical processes, which combine electrochemical hydrogen production and biological denitrification, also show promise as an improvement over conventional biological denitrification [190, 192]. Examples of some reactions involved in electrochemical nitrate reduction are shown in Figure 5.2.

Oxygen generation by anode reaction:

$$5H_2O \rightarrow 2.5O_2(g) + 10\,H^+ + 10e^-$$

Generation of electron donor by cathode reaction:

$$10H_2O + 10e^- \rightarrow 5H_2(g) + 10\,OH^-$$

Sequential reactions of nitrate reduction to nitrogen gas:

$$NO_3^- + H_2(g) \rightarrow NO_2^- + H_2O$$
$$NO_2^- + 0.5H_2 + H^+ \rightarrow NO(g) + H_2O$$
$$2NO(g) + H_2 \rightarrow N_2O(g) + H_2O$$
$$N_2O(g) + H_2 \rightarrow N_2(g) + H_2O$$

Net reaction

$$2NO_3^- + 6H_2O + 10e^- \rightarrow N_2(g) + 12OH^-$$

Overall reaction

$$2NO_3^- + 2.5C + H_2O \rightarrow N_2(g) + 2.5CO_2(g) + 2OH^-$$

Figure 5.2: Sequential reactions of bio-electrochemical denitrification by autohydrogentropic bacteria [190]

Electrochemical systems are complex and effort would be required to determine the appropriate materials and configuration for each component. Ghafari *et al.* [193] provides an excellent review of different materials and numbers of cathodes in various shapes and configuration in bio-electrochemical reactors, as well as denitrification studies in water and wastewater.

A biofilm-electrode reactor (BER) can use autotrophic denitrifying microorganisms immobilized on the cathodic surface and hydrogen produced by electrolysis of water on a carbon anode to denitrify surface and groundwater sources [193, 194]. In one study, 100 mg/L nitrate was completely removed with 100% selectivity towards N_2; the stoichiometric amount of electric current required was 5 mA [194]. In a waste brine system with 15,000 mg/L nitrate, the comparable stoichiometric current would be roughly 750 mA, which is equivalent to 0.75 W or

0.75 amps. Additional calculations are required to assess the true power requirement and potential cost of this process at a commercial scale.

In a different BER study, wastewater with roughly 2,200 mg/L nitrate was denitrified by 98% using autotrophic microorganisms immobilized on the cathode and an applied current of 200 mA. The high level of reduction in this study was notable because it indicated hydrogen was not the limiting factor in the reaction and demonstrated the microorganisms were capable of taking the electron directly from the cathode in the absence of organic substances [195]. Though these initial nitrate levels are not as high as those in IX waste brine, these results show promise regarding the scalability of BERs and ability to maintain an inorganic system.

I am not aware of any studies testing BERs with high salt concentrations, although some species of salt-tolerant bacteria have already been shown to be successful with denitrifying IX waste brine, as noted in the introduction of Chapter 2. The presence of high chloride concentration in waste brine may present challenges in an electrochemical system if chlorine gas production became one of the predominant reactions ($2Cl^- = Cl_2 + 2e^-$). Chlorine gas is toxic, which would present a significant health and safety hazard. Its production would also reduce the chloride concentration in the waste brine, which is undesirable because chloride concentrations need to remain high for multiple cycles of reuse in IX resin regeneration.

5.2.4 Techo-Economic Analysis of the Hybrid System

A thorough technology economic analysis (TEA) of the hybrid system and barriers to commercial adoption would support and inform additional future research efforts. Most research efforts occur at the bench-scale and understanding their scalability and limitations would provide

important insights into their potential economic viability within the hybrid system. In practice, the hybrid ion exchange-catalyst system would be sold as one multi-part unit or a catalytic waste brine denitrifaction system would be sold individually and retro-fitted into an existing ion exchange system. With these configurations in mind, a techno-economic analysis of the most efficient and cost-effect methods of joining the two systems would provide valuable insight into different parts of the hybrid system.

As noted in Chapter 2, modeling results indicate when the conventional IX system is altered to include waste brine denitrification, re-evaluating IX operations may result in lower overall costs and longer run-times. A TEA may also provide insight into considerations for the catalytic reactor configuration and operation during the research phase at the bench scale. For example, existing resources at the water treatment plant may provide alternate sources of pH control for the catalytic reactor. Using an existing HCl source rather than adding a CO_2 source may be more cost effective, but the impact of switching to HCl pH control in the fixed bed reactor would need to be thoroughly evaluated at the bench scale. Activated carbon supports, for instance, could be destroyed at low pH levels, so careful tuning of pH control with HCl would be required if activated carbon were used in the catalytic reactor. The TEA would likely lead to new insights regarding a commercial-sized hybrid system that would be difficult to discover otherwise.

Pending the results, a TEA may also be an important communication tool for discussing adoption of the hybrid system with potential clients. Its holistic analysis may provide compelling justification and rationale for a utility to consider adopting the technology. It could also be used as a tool to help educate the public and try to gain their support for new technology

adoption. Public support may or may not be required financially, but positive public opinion is powerful and helpful to maintain.

REFERENCES

1. Erisman, J.W., Galloway, J., Seitzinger, S., Bleeker, A., Butterbach-Bahl, K.: Reactive nitrogen in the environment and its effect on climate change. Curr. Opin. Environ. Sustain. 3, 281–290 (2011).
2. Galloway, J.N., Townsend, A.R., Erisman, J.W., Bekunda, M., Cai, Z., Freney, J.R., Martinelli, L.A., Seitzinger, S.P., Sutton, M.A.: Transformation of the Nitrogen Cycle: Recent Trends, Questions, and Potential Solutions. Science. 320, 889–892 (2008).
3. Jenkinson, D.S.: The impact of humans on the nitrogen cycle, with focus on temperate arable agriculture. Plant Soil. 228, 3–15 (2001).
4. Kawashima, H., Bazin, M.J., Lynch, J.M.: Global N2O balance and nitrogen fertilizer. Ecol. Model. 87, 51–57 (1996).
5. Robertson, G.P.: Nitrogen Use Efficiency in Row-Crop Agriculture: Crop Nitrogen Use and Soil Nitrogen Loss. In: Ecology in Agriculture. Academic Press (1997).
6. Crews, T.., Peoples, M..: Legume versus fertilizer sources of nitrogen: ecological tradeoffs and human needs. Agric. Ecosyst. Environ. 102, 279–297 (2004).
7. Tilman, D.: Forecasting Agriculturally Driven Global Environmental Change. Science. 292, 281–284 (2001).
8. Xuejun, L., Fusuo, Z.: Nitrogen fertilizer induced greenhouse gas emissions in China. Curr. Opin. Environ. Sustain. 3, 407–413 (2011).
9. NAE: Manage the Nitrogen Cycle: NAE Grand Challenges for Engineering, http://www.engineeringchallenges.org/9132.aspx, (2016).
10. Dobermann, A., Cassman, K.G.: Cereal area and nitrogen use efficiency are drivers of future nitrogen fertilizer consumption. Sci. China C Life Sci. 48, 745–758 (2005).
11. WHO: Nitrate and nitrite in drinking-water: Background document for development of WHO guidelines for drinking-water quality, http://www.who.int/water_sanitation_health/dwq/chemicals/nitratenitrite2ndadd.pdf, (2011).
12. Jury, W.A., Vaux, H.J.: The Emerging Global Water Crisis: Managing Scarcity and Conflict Between Water Users. In: Advances in Agronomy. pp. 1–76. Elsevier (2007).
13. Galloway, J.N., Aber, J.D., Erisman, J.W., Seitzinger, S.P., Howarth, R.W., Cowling, E.B., Cosby, B.J.: The Nitrogen Cascade. BioScience. 53, 341 (2003).
14. Carle, S., Tompson, A.F.B., McNab, W.W., Esser, B.K., Hudson, G.B., Moran, J.E., Beller, H.R., Kane, S.R.: Simulation of nitrate biogeochemistry and reactive transport in a California groundwater basin. In: Cass T. Miller, M.W.F., William G. Gray and George F. Pinder (ed.) Developments in Water Science. pp. 903–914. Elsevier (2004).
15. Cantor, K.P.: Drinking water and cancer. Cancer Causes Control. 8, 292–308 (1997).
16. DeSimone, L.., Hamilton, P.A., Gilliom, R.J.: The Quality of Our Nation's Waters Quality of Water from Domestic Wells in Principal Aquifers of the United States: 1991-2004 Overview of Major Findings. (2009).
17. McCasland, M., Trautmann, N.M., Wagenet, R.J.: Nitrate: Health Effects in Drinking Water. (1985).
18. NGWA: Ground Water Use in the USA, http://www.ngwa.org/Fundamentals/Documents/usa-groundwater-use-fact-sheet.pdf, (2016).

19. Spalding, R.F., Exner, M.E.: Occurrence of Nitrate in Groundwater—A Review. J. Environ. Qual. 22, 392 (1993).
20. US EPA, O.: Drinking Water Contaminants – Standards and Regulations, http://www.epa.gov/dwstandardsregulations.
21. Eurpean Union: REPORT FROM THE COMMISSION Implementation of Council Directive 91/676/EEC concerning the protection of waters against pollution caused by nitrates from agricultural sources, (2000).
22. Fewtrell, L.: Drinking-Water Nitrate, Methemoglobinemia, and Global Burden of Disease: A Discussion. Environ. Health Perspect. 112, 1371–1374 (2004).
23. Lee, D.H.K.: Nitrates, nitrites, and methemoglobinemia. Environ. Res. 3, 484–511 (1970).
24. Sadeq, M., Moe, C.L., Attarassi, B., Cherkaoui, I., ElAouad, R., Idrissi, L.: Drinking water nitrate and prevalence of methemoglobinemia among infants and children aged 1–7 years in Moroccan areas. Int. J. Hyg. Environ. Health. 211, 546–554 (2008).
25. Walter, G.: Survey of Literature Relating to Infant Methemoglobinemia Due to Nitrate-Contaminated 'Water. American Journal of Public Health. (1951).
26. Ward, M.H., Brender, J.D.: Drinking Water Nitrate and Health, (2011).
27. Snyder, C.S., Bruulsema, T.W., Jensen, T.L., Fixen, P.E.: Review of greenhouse gas emissions from crop production systems and fertilizer management effects. Agric. Ecosyst. Environ. 133, 247–266 (2009).
28. WA DOH: Guidance Document: Nitrate Treatment. Alternatives for Small Water Systems, http://www.doh.wa.gov/portals/1/Documents/pubs/331-309.pdf, (2005).
29. Kapoor, A., Viraraghavan, T.: Nitrate Removal From Drinking Water—Review. J. Environ. Eng. 123, 371–380 (1997).
30. Camargo, J.A., Alonso, Á.: Ecological and toxicological effects of inorganic nitrogen pollution in aquatic ecosystems: A global assessment. Environ. Int. 32, 831–849 (2006).
31. Wang, L., Chen, A.S., Wang, A., Condit, W.E., Battelle, C., Sorg, T.J.: Arsenic and Nitrate Removal from Drinking Water by Ion Exchange US EPA Demonstration Project at Vale, OR Final Performance Evaluation Report. (2011).
32. Barranco, C.R., Brenes Balbuena, M., García García, P., Garrido Fernández, A.: Management of spent brines or osmotic solutions. J. Food Eng. 49, 237–246 (2001).
33. Karleskint, J., Schmidt, D., Anderson, R., Page, J.: Ion Exchange and Disposal Issues Associated with the Brine Waste Stream, http://www.hazenandsawyer.com/publications/ion-exchange-and-disposal-issues-associated-with-the-brine-waste-stream/, (2013).
34. SCVSD: Information Sheet: Deep well injection site for brine disposal; Santa Clarita Valley Sanitation District, http://www.lacsd.org/civicax/filebank/blobdload.aspx?blobid=9556, (2015).
35. Jensen, V., Darby, J.: Brine Disposal Options for Small Systems in California's Central Valley. J. Am. Water Works Assoc. 108, E276–E289 (2016).
36. Poulson, T.: Central Arizona Salinity Study: Strategic alternatives for brine management in the Valley of the Sun, http://www.usbr.gov/lc/phoenix/programs/cass/pdf/SABD.pdf, (2010).
37. Clifford, D., Liu, X.: Biological denitrification of spent regenerant brine using a sequencing batch reactor. Water Res. 27, 1477–1484 (1993).
38. Pintar, A., Batista, J., Levec, J.: Integrated ion exchange/catalytic process for efficient removal of nitrates from drinking water. Chem. Eng. Sci. 56, 1551–1559 (2001).

39. van der Hoek, J.P., van der Ven, P.J.M., Klapwijk, A.: Combined ion exchange/biological denitrification for nitrate removal from ground water under different process conditions. Water Res. 22, 679–684 (1988).
40. van der Hoek, J.P., Klapwijk, A.: Reduction of regeneration salt requirement and waste disposal in an ion exchange process for nitrate removal from ground water. Waste Manag. 9, 203–210 (1989).
41. Bae, B.-U., Jung, Y.-H., Han, W.-W., Shin, H.-S.: Improved brine recycling during nitrate removal using ion exchange. Water Res. 36, 3330–3340 (2002).
42. Vaudevire, E.: Further treatment of ion exchange brine with dynamic vapour recompression. Water Pract. Technol. 7, 1–14 (2012).
43. Lehman, S.G., Badruzzaman, M., Adham, S., Roberts, D.J., Clifford, D.A.: Perchlorate and nitrate treatment by ion exchange integrated with biological brine treatment. Water Res. 42, 969–976 (2008).
44. Clifford, D., Liu, X.: Ion Exchange for Nitrate Removal. J. Am. Water Works Assoc. 85, 135–143 (1993).
45. Hiremath, T., Roberts, D.J., Lin, X., Clifford, D.A., Gillogly, T.E.T., Lehman, S.G.: Biological Treatment of Perchlorate in Spent ISEP Ion-Exchange Brine. Environ. Eng. Sci. 23, 1009–1016 (2006).
46. Okeke, B.C., Giblin, T., Frankenberger, W.T.: Reduction of perchlorate and nitrate by salt tolerant bacteria. Environ. Pollut. 118, 357–363 (2002).
47. Lin, X., Roberts, D. j., Hiremath, T., Clifford, D. a., Gillogly, T., Lehman, S.G.: Divalent Cation Addition (Ca2+ or Mg2+) Stabilizes Biological Treatment of Perchlorate and Nitrate In Ion-Exchange Spent Brine. Environ. Eng. Sci. 24, 725–735 (2007).
48. Patel, A., Zuo, G., Lehman, S.G., Badruzzaman, M., Clifford, D.A., Roberts, D.J.: Fluidized bed reactor for the biological treatment of ion-exchange brine containing perchlorate and nitrate. Water Res. 42, 4291–4298 (2008).
49. Van Ginkel, S.W., Tang, Y., Rittmann, B.E.: Impact of precipitation on the treatment of real ion-exchange brine using the H_2 -based membrane biofilm reactor. Water Sci. Technol. 63, 1453 (2011).
50. Ebrahimi, S., Roberts, D.J.: Sustainable nitrate-contaminated water treatment using multi cycle ion-exchange/bioregeneration of nitrate selective resin. J. Hazard. Mater. 262, 539–544 (2013).
51. Choe, J.K., Bergquist, A.M., Jeong, S., Guest, J.S., Werth, C.J., Strathmann, T.J.: Performance and life cycle environmental benefits of recycling spent ion exchange brines by catalytic treatment of nitrate. Water Res. 80, 267–280 (2015).
52. Pintar, A., Batista, J.: Improvement of an integrated ion-exchange/catalytic process for nitrate removal by introducing a two-stage denitrification step. Appl. Catal. B Environ. 63, 150–159 (2006).
53. Yang, T., Doudrick, K., Westerhoff, P.: Photocatalytic reduction of nitrate using titanium dioxide for regeneration of ion exchange brine. Water Res. 47, 1299–1307 (2013).
54. Goto, S., Smith, J.M.: Trickle-bed reactor performance. Part I. Holdup and mass transfer effects. AIChE J. 21, 706–713 (1975).
55. Al Bahri, M., Calvo, L., Gilarranz, M.A., Rodriguez, J.J., Epron, F.: Activated carbon supported metal catalysts for reduction of nitrate in water with high selectivity towards N2. Appl. Catal. B Environ. 138–139, 141–148 (2013).

56. Barrabés, N., Sá, J.: Catalytic nitrate removal from water, past, present and future perspectives. Appl. Catal. B Environ. 104, 1–5 (2011).
57. Marchesini, F.A., Irusta, S., Querini, C., Miró, E.: Spectroscopic and catalytic characterization of Pd–In and Pt–In supported on Al2O3 and SiO2, active catalysts for nitrate hydrogenation. Appl. Catal. Gen. 348, 60–70 (2008).
58. Soares, O.S.G.P., Órfão, J.J.M., Ruiz-Martínez, J., Silvestre-Albero, J., Sepúlveda-Escribano, A., Pereira, M.F.R.: Pd–Cu/AC and Pt–Cu/AC catalysts for nitrate reduction with hydrogen: Influence of calcination and reduction temperatures. Chem. Eng. J. 165, 78–88 (2010).
59. Palomares, A.E., Franch, C., Corma, A.: A study of different supports for the catalytic reduction of nitrates from natural water with a continuous reactor. Catal. Today. 172, 90–94 (2011).
60. Prüsse, U., Hähnlein, M., Daum, J., Vorlop, K.-D.: Improving the catalytic nitrate reduction. Catal. Today. 55, 79–90 (2000).
61. Soares, O.S.G.P., Órfão, J.J.M., Pereira, M.F.R.: Activated Carbon Supported Metal Catalysts for Nitrate and Nitrite Reduction in Water. Catal. Lett. 126, 253–260 (2008).
62. Chaplin, B.P., Shapley, J.R., Werth, C.J.: Oxidative Regeneration of Sulfide-fouled Catalysts for Water Treatment. Catal. Lett. 132, 174–181 (2009).
63. Chaplin, B.P., Shapley, J.R., Werth, C.J.: Regeneration of Sulfur-Fouled Bimetallic Pd-Based Catalysts. Environ. Sci. Technol. 41, 5491–5497 (2007).
64. Chaplin, B.P., Roundy, E., Guy, K.A., Shapley, J.R., Werth, C.J.: Effects of Natural Water Ions and Humic Acid on Catalytic Nitrate Reduction Kinetics Using an Alumina Supported Pd−Cu Catalyst. Environ. Sci. Technol. 40, 3075–3081 (2006).
65. Bergquist, A.M., Choe, J.K., Strathmann, T.J., Werth, C.J.: Evaluation of a hybrid ion exchange-catalyst treatment technology for nitrate removal from drinking water. Water Res. 96, 177–187 (2016).
66. Liu, B., Ji, S.: Comparative study of fluidized-bed and fixed-bed reactor for syngas methanation over Ni-W/TiO2-SiO2 catalyst. J. Energy Chem. 22, 740–746 (2013).
67. Torres, D., de Llobet, S., Pinilla, J.L., Lázaro, M.J., Suelves, I., Moliner, R.: Hydrogen production by catalytic decomposition of methane using a Fe-based catalyst in a fluidized bed reactor. J. Nat. Gas Chem. 21, 367–373 (2012).
68. NASA: Field pilot testing of a dynamic suspended bred reactor for removal of perchlorate in groundwater at JPL – Appendix H: Life cycle cost estimates for DSBR, CSTR, FBR, IE, and NF systems. (2003).
69. NASA, US Filter, Envirogen: GAC-Fluidized Bed Reactor Perchlorate Treatment Pilot Study. (2001).
70. Thon, A., Püttmann, A., Hartge, E.-U., Heinrich, S., Werther, J., Patience, G.S., Bockrath, R.E.: Simulation of catalyst loss from an industrial fluidized bed reactor on the basis of labscale attrition tests. Powder Technol. 214, 21–30 (2011).
71. Sanfilippo, D.: Dehydrogenations in fluidized bed: Catalysis and reactor engineering. Catal. Today. 178, 142–150 (2011).
72. Bazer-Bachi, F., Haroun, Y., Augier, F., Boyer, C.: Experimental Evaluation of Distributor Technologies for Trickle-Bed Reactors. Ind. Eng. Chem. Res. 52, 11189–11197 (2013).
73. Carruthers, J.D., DiCamillo, D.J.: Pilot plant testing of hydrotreating catalysts: Influence of Catalyst Condition, Bed Loading and Dilution. Appl. Catal. 43, 253–276 (1988).

74. Dudukovic, M.P.: Relevance of Multiphase Reaction Engineering to Modern Technological Challenges. Ind. Eng. Chem. Res. 46, 8674–8686 (2007).
75. Huang, T.-C., Kang, B.-C.: Naphthalene Hydrogenation over Pt/Al2O3 Catalyst in a Trickle Bed Reactor. Ind. Eng. Chem. Res. 34, 2349–2357 (1995).
76. Hwang, S., Smith, R.: Heterogeneous catalytic reactor design with optimum temperature profile I: application of catalyst dilution and side-stream distribution. Chem. Eng. Sci. 59, 4229–4243 (2004).
77. Maiti, R.N., Nigam, K.D.P.: Gas−Liquid Distributors for Trickle-Bed Reactors: A Review. Ind. Eng. Chem. Res. 46, 6164–6182 (2007).
78. Metaxas, K., Papayannakos, N.: Gas-Liquid Mass Transfer in a Bench-Scale Trickle Bed Reactor used for Benzene Hydrogenation. Chem. Eng. Technol. 31, 1410–1417 (2008).
79. Mills, P.L., Chaudhari, R.V.: Multiphase catalytic reactor engineering and design for pharmaceuticals and fine chemicals. Catal. Today. 37, 367–404 (1997).
80. Mederos, F.S., Ancheyta, J., Chen, J.: Review on criteria to ensure ideal behaviors in trickle-bed reactors. Appl. Catal. Gen. 355, 1–19 (2009).
81. Gunjal, P.R., Kashid, M.N., Ranade, V.V., Chaudhari, R.V.: Hydrodynamics of Trickle-Bed Reactors: Experiments and CFD Modeling. Ind. Eng. Chem. Res. 44, 6278–6294 (2005).
82. Saroha, A.K., Nigam, K.D.P., Saxena, A.K., Dixit, L.: RTD studies in trickle bed reactors packed with porous particles. Can. J. Chem. Eng. 76, 738–743 (1998).
83. Aydin, B., Larachi, F.: Trickle bed hydrodynamics and flow regime transition at elevated temperature for a Newtonian and a non-Newtonian liquid. Chem. Eng. Sci. 60, 6687–6701 (2005).
84. Satterfield, C.N.: Trickle-bed reactors. AIChE J. 21, 209–228 (1975).
85. Ranade, V.V., Chaudhari, R.V., Gunjal, P.R.: Chapter 2 - Hydrodynamics and Flow Regimes. In: Trickle Bed Reactors. pp. 25–75. Elsevier, Amsterdam (2011).
86. Sato, Y., Hirose, T., Takahashi, F., Toda, M.: Pressure Loss and Liquid Holdup in Packed Bed Reactor with Cocurrent Gas-Liquid down Flow. J. Chem. Eng. Jpn. 6, 147–152 (1973).
87. Pintar, A., Batista, J.: Catalytic hydrogenation of aqueous nitrate solutions in fixed-bed reactors. Catal. Today. 53, 35–50 (1999).
88. Hekmatzadeh, A.A., Karimi-Jashani, A., Talebbeydokhti, N., Kløve, B.: Modeling of nitrate removal for ion exchange resin in batch and fixed bed experiments. Desalination. 284, 22–31 (2012).
89. Boari, G., Liberti, L., Merli, C., Passino, R.: Exchange equilibria on anion resins. Desalination. 15, 145–166 (1974).
90. Helfferich, F.: Ion Exchange. McGraw Hill Book Co, New York (1962).
91. Valverde, J.L., Lucas, A. de, González, M., Rodríguez, J.F.: Ion-Exchange Equilibria of Cu2+, Cd2+, Zn2+, and Na+ Ions on the Cationic Exchanger Amberlite IR-120. J. Chem. Eng. Data. 46, 1404–1409 (2001).
92. Kim, J., Benjamin, M.M.: Modeling a novel ion exchange process for arsenic and nitrate removal. Water Res. 38, 2053–2062 (2004).
93. Flodman, H.R., Dvorak, B.I.: Brine Reuse in Ion-Exchange Softening: Salt Discharge, Hardness Leakage, and Capacity Tradeoffs. Water Environ. Res. 84, 535–543 (2012).

94. Brunner, K.M., Duncan, J.C., Harrison, L.D., Pratt, K.E., Peguin, R.P.S., Bartholomew, C.H., Hecker, W.C.: A Trickle Fixed-Bed Recycle Reactor Model for the Fischer-Tropsch Synthesis. Int. J. Chem. React. Eng. 10, (2012).
95. Kilpiö, T., Mäki-Arvela, P., Rönnholm, M., Sifontes, V., Wärnå, J., Salmi, T.: Modeling of a Three-Phase Continuously Operating Isothermal Packed-Bed Reactor: Kinetics, Mass-Transfer, and Dispersion Effects in the Hydrogenation of Citral. Ind. Eng. Chem. Res. 51, 8858–8866 (2012).
96. Metaxas, K.C., Papayannakos, N.G.: Kinetics and Mass Transfer of Benzene Hydrogenation in a Trickle-Bed Reactor. Ind. Eng. Chem. Res. 45, 7110–7119 (2006).
97. Rajashekharam, M.V., Jaganathan, R., Chaudhari, R.V.: A trickle-bed reactor model for hydrogenation of 2,4 dinitrotoluene: experimental verification. Chem. Eng. Sci. 53, 787–805 (1998).
98. Roininen, J., Alopaeus, V., Toppinen, S., Aittamaa, J.: Modeling and simulation of an industrial trickle-bed reactor for benzene hydrogenation: model validation against plant data. Ind. Eng. Chem. Res. 48, 1866–1872 (2009).
99. Coelhoso, I., Boaventura, R., Rodrigues, A.: Biofilm reactors: An experimental and modeling study of wastewater denitrification in fluidized-bed reactors of activated carbon particles. Biotechnol. Bioeng. 40, 625–633 (1992).
100. Koenig, A., Liu, L.H.: Kinetic model of autotrophic denitrification in sulphur packed-bed reactors. Water Res. 35, 1969–1978 (2001).
101. Sakakibara, Y., Flora, J.R.V., Suidan, M.T., Kurodo, M.: Modeling of electrochemically-activated denitrifying biofilms. Water Res. 28, 1077–1086 (1994).
102. Guter, G.: Nitrate Removal from Contaminated Groundwater by Anion Exchange. In: Sengupta, A. (ed.) Ion Exchange Technology: Advances in Pollution Control. pp. 61–113 (1995).
103. Pintar, A., Batista, J., Levec, J.: Catalytic denitrification: direct and indirect removal of nitrates from potable water. Catal. Today. 66, 503–510 (2001).
104. Chiavola, A., Baciocchi, R., D'Amato, E.: Application of a Two-Site Ideal Model for the Prediction of As–SO4–Cl Ion Exchange Equilibria. Water. Air. Soil Pollut. 225, (2014).
105. Gregor, H.P., Belle, J., Marcus, R.A.: Studies on ion-exchange resins. XIII. Selectivity coefficients of quaternary base anion-exchange resins toward univalent anions. J. Am. Chem. Soc. 77, 2713–2719 (1955).
106. Morgan, J.D., Napper, D.H., Warr, G.G.: Thermodynamics of Ion Exchange Selectivity at Interfaces. J. Phys. Chem. 99, 9458–9465 (1995).
107. Calgon Corporation: Strong Base Anion Resin Regeneration Efficiency with Catalytically Treated Recycled Spent Brine: Laboratory Test Procedure, Revision B, (2014).
108. Boari, G., Liberti, L., Merli, C., Passino, R.: Study of the SO42−/Cl− exchange on a weak anion resin. Desalination. 145–166 (1974).
109. Fernandez, A., Rendueles, M., Rodrigues, A., Diaz, M.: Co-ion behavior at high concentration cationic ion exchange. Ind. Eng. Chem. Res. 33, 2789–2794 (1994).
110. Kitco Metals: 24 Hours spot chart of palladium prices, 1 year price chart. (2015).
111. USGS: USGS Mineral Commodity Summary, January 2015, http://minerals.usgs.gov/minerals/pubs/commodity/indium/mcs-2015-indiu.pdf, (2014).
112. Erisman, J.W., Bleeker, A., Galloway, J., Sutton, M.S.: Reduced nitrogen in ecology and the environment. Environ. Pollut. 150, 140–149 (2007).

113. Chaplin, B.P., Reinhard, M., Schneider, W.F., Schüth, C., Shapley, J.R., Strathmann, T.J., Werth, C.J.: Critical Review of Pd-Based Catalytic Treatment of Priority Contaminants in Water. Environ. Sci. Technol. 46, 3655–3670 (2012).
114. Al-Dahhan, M.H., Larachi, F., Dudukovic, M.P., Laurent, A.: High-Pressure Trickle-Bed Reactors: A Review. Ind. Eng. Chem. Res. 36, 3292–3314 (1997).
115. Parker, D.S., Richards, T.: Nitrification in Trickling Filters. J. Water Pollut. Control Fed. 58, 896–902 (1986).
116. Biesterfeld, S., Farmer, G., Figueroa, L., Parker, D., Russell, P.: Quantification of denitrification potential in carbonaceous trickling filters. Water Res. 37, 4011–4017 (2003).
117. Sato, Y., Hirose, T., Takahashi, F., Toda, M., Hashiguchi, Y.: Flow Pattern and Pulsation Properties of Cocurrent Gas-Liquid Downflow in Packed Beds. J. Chem. Eng. Jpn. 6, 315–319 (1973).
118. Ranade, V.V., Chaudhari, R.V., Gunjal, P.R.: Chapter 5 - Reactor Performance and Scale-Up. In: Trickle Bed Reactors. pp. 171–210. Elsevier, Amsterdam (2011).
119. Clark, M.: Transport Modeling for Environmental Engineers and Scientists. John Wiley & Sons, Inc. (2009).
120. Weber, W., DiGiano, F.A.: Process Dynamics in Environmental Systems. John Wiley & Sons, Inc. (1996).
121. Prüsse, U., Vorlop, K.-D.: Supported bimetallic palladium catalysts for water-phase nitrate reduction. J. Mol. Catal. Chem. 173, 313–328 (2001).
122. Attou, A., Ferschneider, G.: A two-fluid hydrodynamic model for the transition between trickle and pulse flow in a cocurrent gas–liquid packed-bed reactor. Chem. Eng. Sci. 55, 491–511 (2000).
123. Bertoch, M., Bergquist, A., Gildert, G., Strathmann, T., Werth, C.: Catalytic Nitrate Removal in a Trickle Bed Reactor: Direct Drinking Water Treatmen. J. Am. Water Works Assoc. In Review, (2016).
124. Wu, Y., Khadilkar, M.R., Al-Dahhan, M.H., Duduković, M.P.: Comparison of Upflow and Downflow Two-Phase Flow Packed-Bed Reactors with and without Fines: Experimental Observations. Ind. Eng. Chem. Res. 35, 397–405 (1996).
125. Turek, F., Lange, R.: Mass transfer in trickle-bed reactors at low reynolds number. Chem. Eng. Sci. 36, 569–579 (1981).
126. Haase, S., Weiss, M., Langsch, R., Bauer, T., Lange, R.: Hydrodynamics and mass transfer in three-phase composite minichannel fixed-bed reactors. Chem. Eng. Sci. 94, 224–236 (2013).
127. Haase, S., Weiss, M., Langsch, R., Bauer, T., Lange, R.: Hydrodynamics and mass transfer in three-phase composite minichannel fixed-bed reactors. Chem. Eng. Sci. 94, 224–236 (2013).
128. Mata, A.R., Smith, J.M.: Oxidation of sulfur dioxide in a trickle-bed reactor. Chem. Eng. J. 22, 229–235 (1981).
129. Beaudry, E.G., Duduković, M.P., Mills, P.L.: Trickle-bed reactors: Liquid diffusional effects in a gas-limited reaction. AIChE J. 33, 1435–1447 (1987).
130. Herskowitz, M., Carbonell, R.G., Smith, J.M.: Effectiveness factors and mass transfer in trickle-bed reactors. AIChE J. 25, 272–283 (1979).
131. Baranenko, V.I., Kirov, V.S.: Solubility of hydrogen in water in a broad temperature and pressure range. Sov. At. Energy. 66, 30–34 (1989).

132. Pintar, A.: Catalytic processes for the purification of drinking water and industrial effluents. Catal. Today. 77, 451–465 (2003).
133. Gauthard, F.: Palladium and platinum-based catalysts in the catalytic reduction of nitrate in water: effect of copper, silver, or gold addition. J. Catal. 220, 182–191 (2003).
134. Pintar, A., Batista, J., Levec, J., Kajiuchi, T.: Kinetics of the catalytic liquid-phase hydrogenation of aqueous nitrate solutions. Appl. Catal. B Environ. 11, 81–98 (1996).
135. Calvo, L., Gilarranz, M.A., Casas, J.A., Mohedano, A.F., Rodriguez, J.J.: Denitrification of Water with Activated Carbon-Supported Metallic Catalysts. Ind. Eng. Chem. Res. 49, 5603–5609 (2010).
136. Devadas, A., Vasudevan, S., Epron, F.: Nitrate reduction in water: Influence of the addition of a second metal on the performances of the Pd/CeO2 catalyst. J. Hazard. Mater. 185, 1412–1417 (2011).
137. Gavagnin, R., Biasetto, L., Pinna, F., Strukul, G.: Nitrate removal in drinking waters: the effect of tin oxides in the catalytic hydrogenation of nitrate by Pd/SnO 2 catalysts. Appl. Catal. B Environ. 38, 91–99 (2002).
138. Hörold, S., Tacke, T., Vorlop, K.-D.: Catalytical removal of nitrate and nitrite from drinking water: 1. Screening for hydrogenation catalysts and influence of reaction conditions on activity and selectivity. Environ. Technol. 14, 931–939 (1993).
139. Doudrick, K., Yang, T., Hristovski, K., Westerhoff, P.: Photocatalytic nitrate reduction in water: Managing the hole scavenger and reaction by-product selectivity. Appl. Catal. B Environ. 136–137, 40–47 (2013).
140. Soares, O.S.G.P., Pereira, M.F.R., Órfão, J.J.M., Faria, J.L., Silva, C.G.: Photocatalytic nitrate reduction over Pd–Cu/TiO2. Chem. Eng. J. 251, 123–130 (2014).
141. D'Arino, M., Pinna, F., Strukul, G.: Nitrate and nitrite hydrogenation with Pd and Pt/SnO2 catalysts: the effect of the support porosity and the role of carbon dioxide in the control of selectivity. Appl. Catal. B Environ. 53, 161–168 (2004).
142. Rocha, E.P.A., Passos, F.B., Peixoto, F.C.: Modeling of Hydrogenation of Nitrate in Water on Pd–Sn/Al2O3 Catalyst: Estimation of Microkinetic Parameters and Transport Phenomena Properties. Ind. Eng. Chem. Res. 53, 8726–8734 (2014).
143. Epron, F., Gauthard, F., Pinéda, C., Barbier, J.: Catalytic Reduction of Nitrate and Nitrite on Pt–Cu/Al2O3 Catalysts in Aqueous Solution: Role of the Interaction between Copper and Platinum in the Reaction. J. Catal. 198, 309–318 (2001).
144. Duca, M., Koper, M.T.M.: Powering denitrification: the perspectives of electrocatalytic nitrate reduction. Energy Environ. Sci. 5, 9726 (2012).
145. Yoshinaga, Y., Akita, T., Mikami, I., Okuhara, T.: Hydrogenation of Nitrate in Water to Nitrogen over Pd–Cu Supported on Active Carbon. J. Catal. 207, 37–45 (2002).
146. Bae, S., Jung, J., Lee, W.: The effect of pH and zwitterionic buffers on catalytic nitrate reduction by TiO2-supported bimetallic catalyst. Chem. Eng. J. 232, 327–337 (2013).
147. Kim, M.S., Lee, K.Y.: Ceria modified titania supported Pd-Cu catalysts for nitrate reduction in water. In: AIChE (2014).
148. Say, Z., Vovk, E.I., Bukhtiyarov, V.I., Ozensoy, E.: Influence of ceria on the NOx reduction performance of NOx storage reduction catalysts. Appl. Catal. B Environ. 142–143, 89–100 (2013).
149. Wada, K., Hirata, T., Hosokawa, S., Iwamoto, S., Inoue, M.: Effect of supports on Pd–Cu bimetallic catalysts for nitrate and nitrite reduction in water. Catal. Today. 185, 81–87 (2012).

150. Babić, B.M., Milonjić, S.K., Polovina, M.J., Kaludierović, B.V.: Point of zero charge and intrinsic equilibrium constants of activated carbon cloth. Carbon. 37, 477–481 (1999).
151. Bhatnagar, A., Hogland, W., Marques, M., Sillanpää, M.: An overview of the modification methods of activated carbon for its water treatment applications. Chem. Eng. J. 219, 499–511 (2013).
152. Menendez, J.A., Illán-Gómez, M.J., y Leon, C.L., Radovic, L.R.: On the difference between the isoelectric point and the point of zero charge of carbons. (1995).
153. Chung, T.-Y., Tsao, C.-S., Tseng, H.-P., Chen, C.-H., Yu, M.-S.: Effects of oxygen functional groups on the enhancement of the hydrogen spillover of Pd-doped activated carbon. J. Colloid Interface Sci. 441, 98–105 (2015).
154. Zhang, R., Shuai, D., Guy, K.A., Shapley, J.R., Strathmann, T.J., Werth, C.J.: Elucidation of Nitrate Reduction Mechanisms on a Pd-In Bimetallic Catalyst using Isotope Labeled Nitrogen Species. ChemCatChem. 5, 313–321 (2013).
155. Zhang, F., Jin, R., Chen, J., Shao, C., Gao, W., Li, L., Guan, N.: High photocatalytic activity and selectivity for nitrogen in nitrate reduction on Ag/TiO2 catalyst with fine silver clusters. J. Catal. 232, 424–431 (2005).
156. Hasnat, M.A., Safwan, J.A., Rashed, M.A., Rahman, Z., Rahman, M.M., Nagao, Y., Asiri, A.M.: Inverse effects of supporting electrolytes on the electrocatalytic nitrate reduction activities in a Pt|Nafion|Pt–Cu-type reactor assembly. RSC Adv. 6, 11609–11617 (2016).
157. Marina, M.L., Esteban, F.J., Poitrenaud, C.: Study of the influence of the co-ion nature on the nitrate-chloride ion exchange in diluted and concentrated solutions. React. Funct. Polym. 31, 31–37 (1996).
158. Maul, G.A., Kim, Y., Amini, A., Zhang, Q., Boyer, T.H.: Efficiency and life cycle environmental impacts of ion-exchange regeneration using sodium, potassium, chloride, and bicarbonate salts. Chem. Eng. J. 254, 198–209 (2014).
159. Shuai, D., McCalman, D.C., Choe, J.K., Shapley, J.R., Schneider, W.F., Werth, C.J.: Structure Sensitivity Study of Waterborne Contaminant Hydrogenation Using Shape- and Size-Controlled Pd Nanoparticles. ACS Catal. 3, 453–463 (2013).
160. Luyben, W.L.: Catalyst dilution to improve dynamic controllability of cooled tubular reactors. Comput. Chem. Eng. 37, 184–190 (2012).
161. Al-Dahhan, M.H., Duduković, M.P.: Catalyst bed dilution for improving catalyst wetting in laboratory trickle-bed reactors. AIChE J. 42, 2594–2606 (1996).
162. Berger, R.J., Pérez-Ramírez, J., Kapteijn, F., Moulijn, J.A.: Catalyst performance testing: Radial and axial dispersion related to dilution in fixed-bed laboratory reactors. Appl. Catal. Gen. 227, 321–333 (2002).
163. van Klinken, J., van Dongen, R.H.: Catalyst dilution for improved performance of laboratory trickle-flow reactors. Chem. Eng. Sci. 35, 59–66 (1980).
164. Bae, B.U., Kim, C.H., Kim, Y.I.: Treatment of spent brine from a nitrate exchange process using combined biological denitrification and sulfate precipitation. Water Sci. Technol. 49, 413–419 (2004).
165. Bauer, T., Haase, S.: Comparison of structured trickle-bed and monolithic reactors in Pd-catalyzed hydrogenation of alpha-methylstyrene. Chem. Eng. J. 169, 263–269 (2011).
166. Gascon, J., Ommen, J.R. van, Moulijn, J.A., Kapteijn, F.: Structuring catalyst and reactor – an inviting avenue to process intensification. Catal. Sci. Technol. 5, 807–817 (2015).
167. Carty, W.M., Lednor, P.W.: Monolithic ceramics and heterogeneous catalysts: honeycombs and foams. Curr. Opin. Solid State Mater. Sci. 1, 88–95 (1996).

168. Matatov-Meytal, U., Sheintuch, M.: Activated carbon cloth-supported Pd–Cu catalyst: Application for continuous water denitrification. Catal. Today. 102–103, 121–127 (2005).
169. Niranjan, K., Pangarkar, V.G.: Hydrodynamic and mass transfer characteristics of polypropylene multifilament wire gauze packings. Chem. Eng. J. 27, 49–57 (1983).
170. Richardson, J.T., Remue, D., Hung, J.-K.: Properties of ceramic foam catalyst supports: mass and heat transfer. Appl. Catal. Gen. 250, 319–329 (2003).
171. Richardson, J.T., Peng, Y., Remue, D.: Properties of ceramic foam catalyst supports: pressure drop. Appl. Catal. Gen. 204, 19–32 (2000).
172. Twigg, M.V., Richardson, J.T.: Fundamentals and Applications of Structured Ceramic Foam Catalysts. Ind. Eng. Chem. Res. 46, 4166–4177 (2007).
173. Wenmakers, P.W.A.M., Schaaf, J. van der, Kuster, B.F.M., Schouten, J.C.: "Hairy Foam": carbon nanofibers grown on solid carbon foam. A fully accessible, high surface area, graphitic catalyst support. J. Mater. Chem. 18, 2426–2436 (2008).
174. Avila, P., Montes, M., Miró, E.E.: Monolithic reactors for environmental applications: A review on preparation technologies. Chem. Eng. J. 109, 11–36 (2005).
175. Kashid, M., Kiwi-Minsker, L.: Microstructured Reactors for Multiphase Reactions: State of the Art. Ind. Eng. Chem. Res. 48, 6465–6485 (2009).
176. Krishna, R., Sie, S.T.: Design and scale-up of the Fischer–Tropsch bubble column slurry reactor. Fuel Process. Technol. 64, 73–105 (2000).
177. Wu, D., Zhou, J., Li, Y.: Mechanical strength of solid catalysts: Recent developments and future prospects. AIChE J. 53, 2618–2629 (2007).
178. Jong, K.P.D., Geus, J.W.: Carbon Nanofibers: Catalytic Synthesis and Applications. Catal. Rev. 42, 481–510 (2000).
179. Ledoux, M.-J., Pham-Huu, C.: Carbon nanostructures with macroscopic shaping for catalytic applications. Catal. Today. 102–103, 2–14 (2005).
180. Nardelli, M.B., Yakobson, B.I., Bernholc, J.: Brittle and Ductile Behavior in Carbon Nanotubes. Phys. Rev. Lett. 81, 4656–4659 (1998).
181. Cordier, A., Flahaut, E., Viazzi, C., Laurent, C., Peigney, A.: In situ CCVD synthesis of carbon nanotubes within a commercial ceramic foam. J. Mater. Chem. 15, 4041–4050 (2005).
182. Jarrah, N.A., van Ommen, J.G., Lefferts, L.: Mechanistic aspects of the formation of carbon-nanofibers on the surface of Ni foam: A new microstructured catalyst support. J. Catal. 239, 460–469 (2006).
183. Brunet Espinosa, R., Lefferts, L.: Ni in CNFs: Highly Active for Nitrite Hydrogenation. ACS Catal. 5432–5440 (2016).
184. Kazakov, E.V., Balitsky, I.F., Sobolevsky, V.S., Semenov, V.P., Kashirina, G.N., Kruglikova, N.A., Yagodkin, V.I., Shpolyansky, M.A., Ruzinsky, S.I., Gorbachevich, I.D., Gergert, I.E.: Catalyst for conversion of hydrocarbons and method of preparing same, http://www.google.com/patents/US3931053, (1976).
185. Bellussi, G., Buonomo, F., Esposito, A., Clerici, M., Romano, U., Notari, B.: Catalyst of silicon and titanium having high mechanical strength and a process for its preparation., http://www.google.com/patents/US4701428, (1987).
186. Chhina, H., Campbell, S., Kesler, O.: Ex situ Evaluation of Tungsten Oxide as a Catalyst Support for PEMFCs. J. Electrochem. Soc. 154, B533–B539 (2007).

187. Huang, S.-Y., Ganesan, P., Park, S., Popov, B.N.: Development of a Titanium Dioxide-Supported Platinum Catalyst with Ultrahigh Stability for Polymer Electrolyte Membrane Fuel Cell Applications. J. Am. Chem. Soc. 131, 13898–13899 (2009).
188. Kou, R., Shao, Y., Wang, D., Engelhard, M.H., Kwak, J.H., Wang, J., Viswanathan, V.V., Wang, C., Lin, Y., Wang, Y., Aksay, I.A., Liu, J.: Enhanced activity and stability of Pt catalysts on functionalized graphene sheets for electrocatalytic oxygen reduction. Electrochem. Commun. 11, 954–957 (2009).
189. Drillet, J.-F., Dittmeyer, R., Jüttner, K.: Activity and long-term stability of PEDOT as Pt catalyst support for the DMFC anode. J. Appl. Electrochem. 37, 1219–1226 (2007).
190. Mousavi, S., Ibrahim, S., Aroua, M.K., Ghafari, S.: Development of nitrate elimination by autohydrogenotrophic bacteria in bio-electrochemical reactors – A review. Biochem. Eng. J. 67, 251–264 (2012).
191. Mook, W.T., Chakrabarti, M.H., Aroua, M.K., Khan, G.M.A., Ali, B.S., Islam, M.S., Abu Hassan, M.A.: Removal of total ammonia nitrogen (TAN), nitrate and total organic carbon (TOC) from aquaculture wastewater using electrochemical technology: A review. Desalination. 285, 1–13 (2012).
192. Mook, W.T., Aroua, M.K.T., Chakrabarti, M.H., Noor, I.M., Irfan, M.F., Low, C.T.J.: A review on the effect of bio-electrodes on denitrification and organic matter removal processes in bio-electrochemical systems. J. Ind. Eng. Chem. 19, 1–13 (2013).
193. Ghafari, S., Hasan, M., Aroua, M.K.: Bio-electrochemical removal of nitrate from water and wastewater—A review. Bioresour. Technol. 99, 3965–3974 (2008).
194. Feleke, Z., Araki, K., Sakakibara, Y., Watanabe, T., Kuroda, M.: Selective reduction of nitrate to nitrogen gas in a biofilm-electrode reactor. Water Res. 32, 2728–2734 (1998).
195. Park, H.I., Kim, D. kun, Choi, Y.-J., Pak, D.: Nitrate reduction using an electrode as direct electron donor in a biofilm-electrode reactor. Process Biochem. 40, 3383–3388 (2005).

APPENDIX A

ADDITIONAL INFORMATION FOR CHAPTER 2

A.1 Ion Exchange Experimental Setup

Ion exchange (IX) columns (see Fig A.1) were constructed from 101.6 cm (40”) long sections of 1.9 cm (0.75”) OD, 1.27 cm (0.5”) ID UV-stabilized acrylic tubing (US Plastic Corp #44026), equipped with stainless steel Swagelok fittings and L/S16 Tygon E-lab Masterflex tubing. Each end of the IX column had one exit tube that branched into two tubes: one for exit waste and the other for influent solution. Thus, either end of each column could be operated as influent or effluent depending on whether treatment or resin regeneration was occurring. Hand-operated valves were used to control the flow direction. A Masterflex peristaltic pump with three pump-heads was used for all solutions, and up to three IX columns were run simultaneously in parallel. The three pump heads were calibrated to ensure equivalent flow. The IX column was filled with IX resin to a depth of 91.4 cm (36”), corresponding to an empty bed volume (BV) of 116 mL.

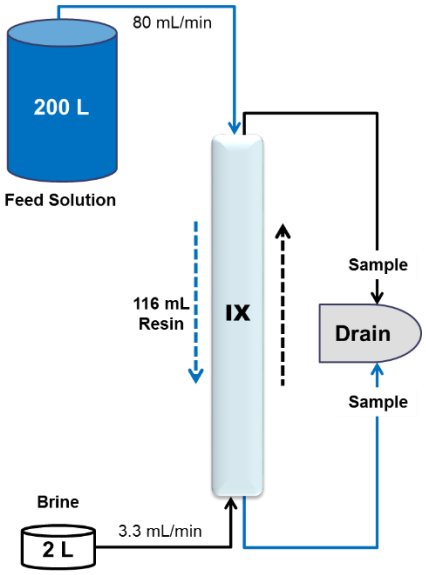

Figure A.1: Simple diagram of the IX experimental set-up. Three IX columns were run in parallel simultaneously. The treatment cycle (blue) travelled down-flow, while regeneration (black) was an up-flow process. The cycles alternate and the flow path is manually adjusted with valves.

A.2 Catalyst Experimental Setup

The catalyst column (see Fig A.2) was constructed from a 45.7 cm (18") length of 2.54 cm (1") OD, 1.9 cm (0.75") ID UV-stabilized acrylic tubing (US Plastic Corp #44029). It was equipped with stainless steel Swagelok fittings and PTFE tubing. The Swagelok fitting at the inlet was a tee, which allowed the simultaneous delivery of the feed brine and a gas mixture of H_2 (electron donor) and CO_2 (pH buffer). The brine flow was controlled by a reciprocating syringe pump (PhD Ultra, Harvard Apparatus) containing two 30 mL gas tight syringes and two dual check valves. A glass reservoir held the brine and was covered by aluminum foil. The gas flow was controlled by two Alicat Scientific adjustable, digital mass flow controllers. A plastic frit dispersed gas in the Swagelok tee at the column inlet. The column was filled with 80.7 g of

the Pd-In/AC catalyst, corresponding to an empty bed volume of 144 mL and a fluid pore space of 62 mL (0.43 void fraction).

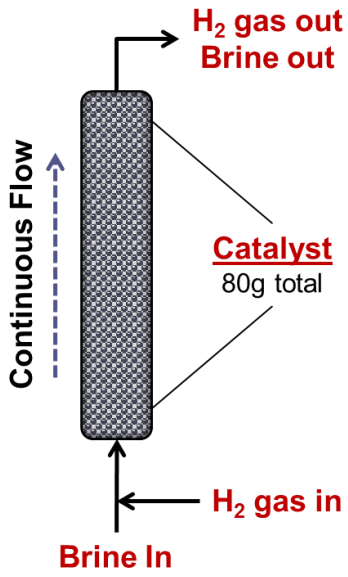

Figure A.2: Simple diagram of experimental continuous-flow fixed-bed catalytic reactor.

A.3 IX Experimental Protocol

Three sets of experiments were performed: one set designed to test different regeneration strategies (labeled 2-Cycle experiments 1 – 6 in Table 2.1), one set designed to calibrate the IX model under low ionic strength treatment conditions (labeled Model Treatment Exp. 1 – 4), and one set designed to calibrate the IX model under high ionic strength brine conditions used to regenerate the resins between treatment cycles (labeled Model Brine Exp. 1 – 4). The IX columns for the 2-Cycle experiments (Figure A.3) were sequentially flushed with (1) 10 wt% NaCl brine for 30 BV (17 h) to condition the column and ensure a uniform initial condition where the resin was fully loaded with ~100% chloride ions, (2) with a synthetic groundwater (Table 1) for 300 BV (7 h), (3) with regenerant brines of variable composition for varying BV (2-10 BV), and (4) the synthetic groundwater for a second treatment cycle for 300 BV (7 h) (i.e.,

two cycles of treatment). The synthetic groundwater was DI water spiked with chloride, nitrate, bicarbonate, and sulfate at levels representative of nitrate-contaminated groundwater source used by a water treatment plant in California, hereafter referred to as California groundwater. Effluent samples were collected every 0.3 BV (11 min) during regeneration, and every 21 – 42 BV (30 min – 1 h) during treatment.

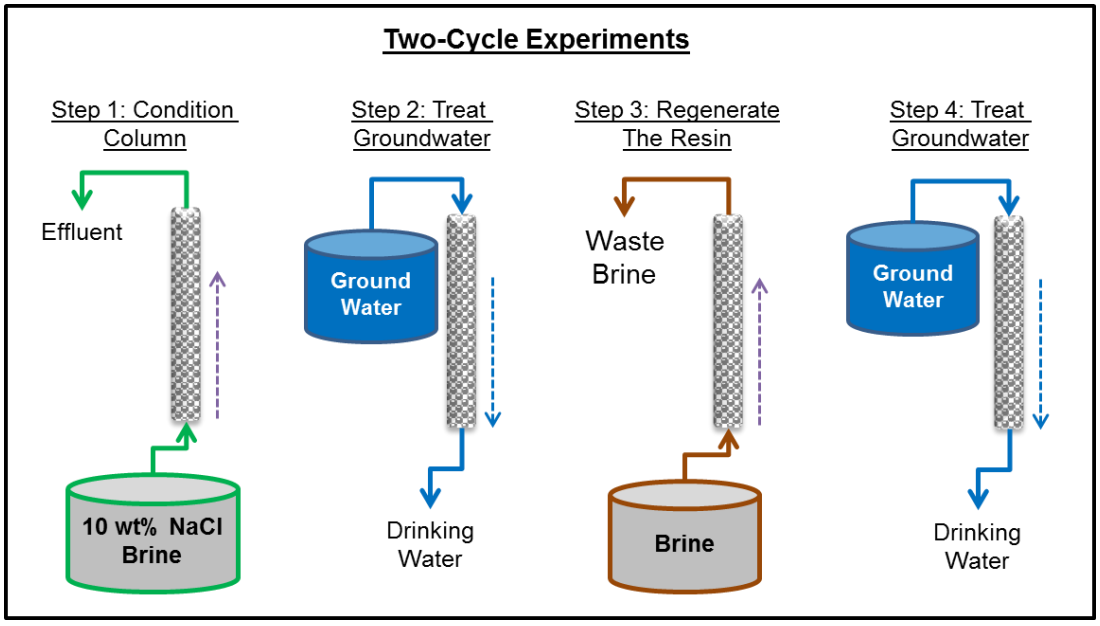

Figure A.3: Diagram of the steps involved in the 2-Cycle Experiments.

The IX columns for Model Treatment experiments (Figure A.4a) were also initially flushed with 10 wt% NaCl brine for 30 BV (17 h) to chloride load the resins. Columns were then flushed with DI water spiked with 200 mg/L of different anion combinations (i.e., nitrate, bicarbonate, and/or sulfate) to test exchange of each anion individually and in a mixed solution with chloride adsorbed on the resin (see Table 1).

The IX columns for Model Brine treatment experiments (Figure A.4b) were initially flushed with DI water containing only 200 mg/L nitrate in the down-flow mode for 600-815 BV

(14-19 h) to ensure uniform resin saturation with nitrate. The nitrate-saturated IX columns were then regenerated using one of four synthetic brine mixtures mimicking conditions expected following catalytic nitrate treatment of waste brines. All brines contained 10 wt% NaCl (i.e.,, 100,000 mg/L), and different combinations of 1,500 mg/L nitrate, 30,000 mg/L bicarbonate, and/or 30,000 mg/L sulfate. The non-zero nitrate concentration was selected as an expected value that would be present following 90% removal of nitrate from waste brines with an expected concentration of 15,000 mg/L following resin regeneration. The bicarbonate and sulfate concentrations were selected to mimic the expected buildup on these non-target anions in waste brines following repeated treatment/reuse cycles. IX column effluent samples were collected every 0.15 BV (5 min) during regeneration for the first 1.5 BV (50 min), and then at increasingly larger intervals (0.3 BV-1.7 BV) until steady state composition was reached.

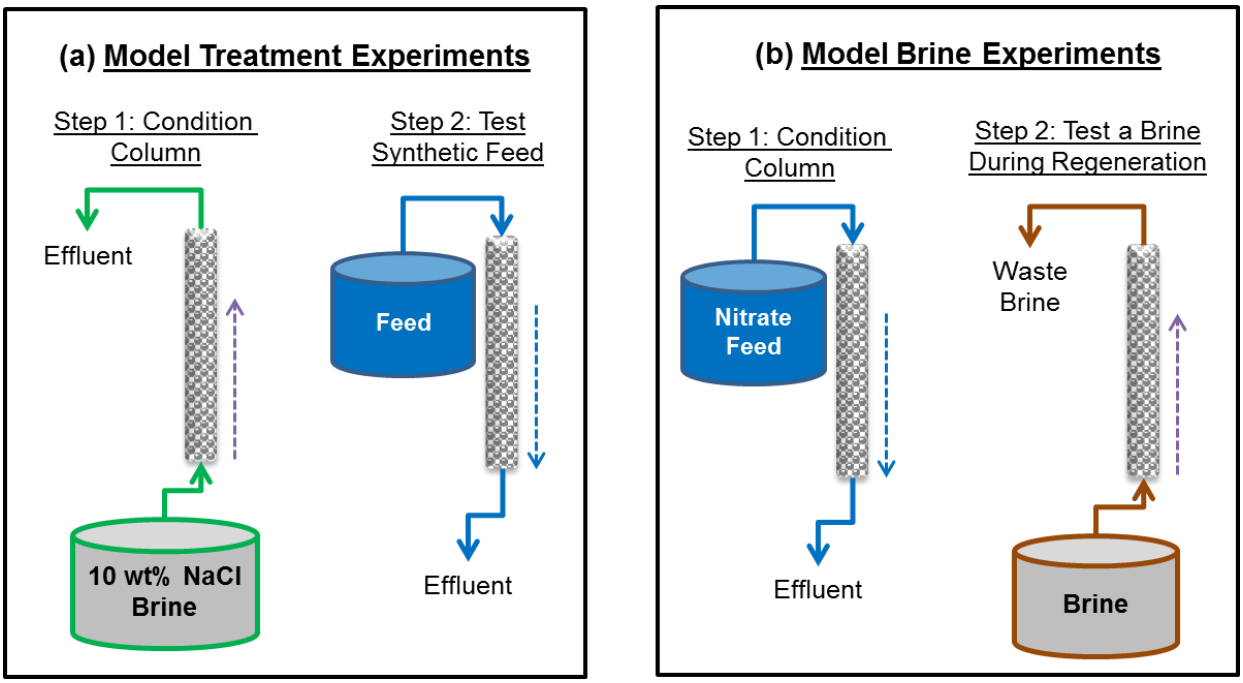

Figure A4: Diagrams of experimental steps for (a) model treatment experiments and (b) model brine experiments.

A.4 Catalyst Experimental Protocol

Details of packed bed experiments are listed in Table A.1. Influent samples (from the waste brine reservoir) were collected approximately every three days to verify stability of the brine feed, and effluent samples were collected daily to monitor catalyst reactor treatment performance. Liquid flow rate and pH were measured daily.

For the synthetic brine experiment, an initial brine containing 5 wt% NaCl and 10,000 mg/L nitrate was run continuously for 6 d to establish a baseline level of treatment. The feed brine was then altered to include the highest level of bicarbonate expected in waste brines (30,000 mg/L), and this condition was maintained for the next 6 d before switching back to the bicarbonate-free waste brine and monitoring for three additional days. Next, the waste brine was modified to include sulfate, which was increased by 5,000 mg/L every 3 d until a level of 30,000 mg/L was reached, and treatment of the brine amended with 30,000 mg/L sulfate was continued for 15 d. The synthetic brine compositions (5 wt% NaCl and 10,000 mg/L nitrate) were based on previously observed concentrations in a real California waste brine collected in 2011, plus maximum bicarbonate and sulfate levels expected based on IX modeling results for 10 cycles of brine treatment and reuse.

Real waste IX brine from a participating California utility (after a single cycle of use with no brine recycling) contained 11 wt% NaCl, 6,500 mg/L nitrate, 1,820 mg/L bicarbonate, 1,180 mg/L sulfate, 11.1 mg/L calcium, 3.14 mg/L magnesium, 2.94 mg/L phosphorous, 0.09 mg/L iron, and 0.014 mg/L manganese. Chloride, nitrate, bicarbonate and sulfate levels were replicated; the other ions were not.

Table A.1: Packed-bed catalyst experiments with real and synthetic waste brines.

Name of Brine	Length (days)	Brine Composition				Avg. [NO3-] Out	Avg. [NO3-] Reduction	Selectivity for N_2 (single point)	pH
		NaCl	$[NO_3^-]$	$[HCO_3^-]$	$[SO_4^{2-}]$				
		wt%	mg/L	mg/L	mg/L	mg/L			
Synthetic Brines									
Chloride, nitrate	6	5.0	10,000	0	0	5070 ± 818	49% ± 8%	84%	7.40
30,000 bicarbonate	5	5.0	10,000	30,000	0	6003 ± 318	58% ± 3%	73%	8.10
Chloride, nitrate	3	5.0	10,000	0	0	4757 ± 2255	46% ± 22%	87%	7.66
5,000 sulfate	3	5.0	10,000	0	5,000	4722 ± 2486	48% ± 25%	87%	7.29
10,000 sulfate	3	5.0	10,000	0	10,000	4988 ± 982	50% ± 10%	85%	7.34
15,000 sulfate	3	5.0	10,000	0	15,000	5336 ± 773	55% ± 8%	85%	7.70
20,000 sulfate	3	5.0	10,000	0	20,000	4093 ± 418	41% ± 4%	82%	7.44
25,000 sulfate	3	5.0	10,000	0	25,000	4584 ± 404	46% ± 4%	83%	7.39
30,000 sulfate	15	5.0	10,000	0	30,000	4153 ± 273	40% ± 2%	86%	7.54
Real Brine from WTP in Southern California									
Real Brine**	22	11.6	6,500	1,180	1,820	2056 ± 174	72% ± 3%	81% ± 11%*	8.50

* Confidence interval based on 5 points

** The real waste IX brine also contained 11.1 mg/L calcium, 3.14 mg/L magnesium, 2.94 mg/L phoshorous, 0.09 mg/L iron and 0.014 mg/L manganese.

A.5 IX Model Development - Parameter Optimization

Each ion selectivity coefficient for treatment breakthrough was initially determined individually by fitting the model to experimental results from Model Treatment Exp. 1-3, and this provided an initial starting point for model calibration. Then, all three ion selectivity coefficients and the resin capacity parameter were optimized simultaneously by minimizing the relative least squared error between model and experimental results from Model Treatment Exp. 4, where nitrate, chloride, sulfate and bicarbonate were simultaneously present in the feed solution. The "fsolve" function and "trust-region-dogleg" algorithm in MATLAB were used. A spatial discretization of 25 plates was used. During parameter fitting, a genetic algorithm was used to test numerous combinations of the three selectivity coefficients and resin capacity.

For the genetic algorithm, a set of "model creatures" was created, and each model creature contained a value for each of the four parameters. The model tested each model creature and then performed a relative least squares analysis of the model fits of the experimental data (Model Treatment Exp. 4) for chloride, nitrate, bicarbonate and sulfate. The last four nitrate points where weighted twice to bias the model fit to more accurately capture breakthrough, due to the importance of matching the nitrate breakthrough point around 44 mg/L. The influent water for these experiments was listed in Table 2.1. A preliminary "Best Creature" was identified from all model creatures based on the lowest relative least squares value.

After all model creatures were tested, they were treated as "parents." Next, a set number of couples were randomly chosen, and the parents' genes (parameters) were swapped in every possible combination; one resulting combination for each couple was chosen at random, and this was an "offspring." These offspring were then tested by the model and a new Best Creature was identified based on the lowest relative least squares value. Again, the last four nitrate points were weighted twice. After all offspring were tested, the Best Creature was assigned as the "best fit parameters." For the genetic algorithm fitting the treatment selectivity coefficients and resin capacity, 31 model creatures and 150 offspring were tested. The Best Creature for the treatment parameters was a resin capacity = 1,044 meq/L, K_C^N =3.52 ± 0.108, K_C^S =0.0056 ± 0.00023 and K_C^H =0.41 ± 0.0371.

Initially, fitting the regeneration parameters was accomplished using a single genetic algorithm with 70 model creatures and 400 offspring. The model results from each model creature were compared to four sets of experimental data simultaneously (Model Brine Exp. 1-4) in order to further constrain the model's results. The experimental results used for comparison included breakthrough curves of: 1) only nitrate, 2) nitrate and bicarbonate, 3) nitrate and sulfate,

and 4) chloride, nitrate, bicarbonate and sulfate. A composite non-weighted least squares value was summed after these comparisons and the lowest resulting least squares value identified the Best Creature. This fitting algorithm was run twice for the regeneration parameters: once with weights and once without weights. The non-weighted results were just as accurate as the weighted results (based on Best Creature confidence intervals), so the non-weighted results were used moving forward. Best Creatures were determined as described above. The Best Creature non-weighted parameters were: rK_C^N =22.2 ± 4.49, rK_C^S =0.45 ± 0.305, and rK_C^H =0.006 ± 0.00083. These results are listed in Table A.2 below.

Table A.2: Initial best-fit IX model parameters for treatment cycle condition (low ionic strength) and brine regeneration conditions (high ionic strength).

Initial Best Fit Parameters	
Resin Name: CalRes 2105	
Resin Type: SBA Cl^- form	
Resin Selectivity: Nitrate selective	
Resin Capacity: 1,096 meq/L	
Treatment Cycle	**Regeneration Cycle**
K_C^N = 3.52 ± 0.11	rK_C^N = 22.2 ± 4.49
K_C^S = 0.0056 ± 0.0002	rK_C^S = 0.45 ± 0.305
K_C^H = 0.41 ± 0.04	rK_C^H = 0.006 ± 0.0083

When the parameters listed in Table A.2 were used to predict the nitrate breakthrough during 2-Cycle treatment experiments, the nitrate breakthrough curve predicted for treatment cycle 2 provided a very poor match to experimental data during the second treatment cycle (Figure A.6a), predicting breakthrough more the 50 BV earlier than observed experimentally. This discrepancy was attributed to poor prediction of the spatial distribution of resin-loaded anion composition following brine regeneration. To demonstrate the sensitivity of breakthrough time on the spatial distribution of anions on the resin following regeneration, a sensitivity analysis was performed and results are shown in Figure A.5. Different regeneration parameters lead to different nitrate treatment breakthrough times in the second cycle. When the values of the regeneration selectivity coefficients are doubled, more nitrate is left on the resin during regeneration, leading to earlier nitrate breakthrough during treatment (red). Conversely, when regeneration selectivity values are halved, nitrate removal during regeneration is better, leading to a more regenerated resin, and a longer nitrate breakthrough time during the subsequent treatment cycle (blue).

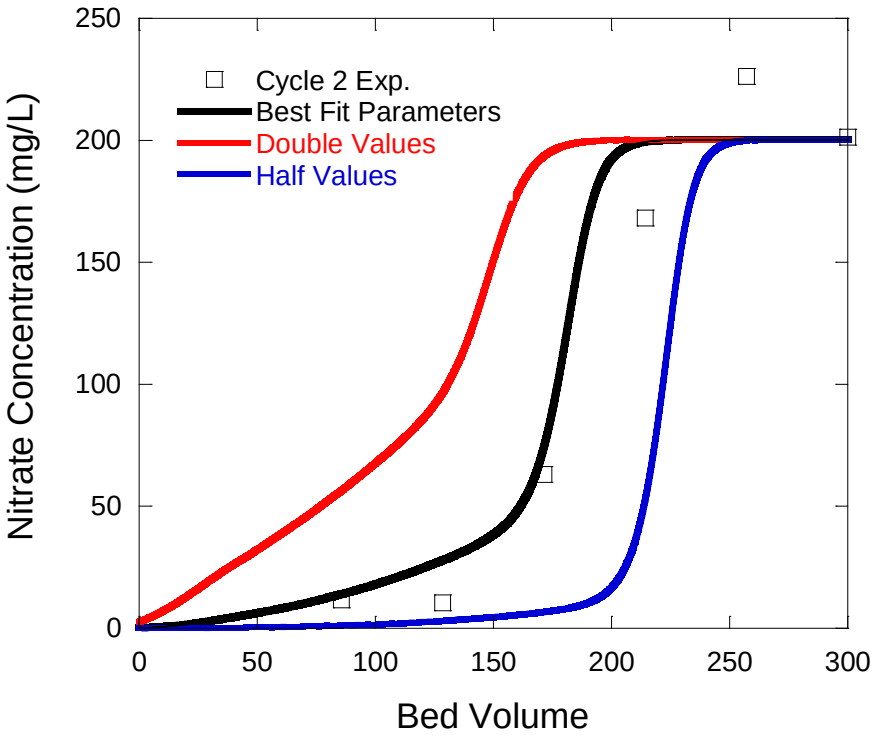

Figure A.5: Sensitivity analysis of nitrate breakthrough during treatment following regeneration using regeneration selectivity parameters from the best fit (black), values twice the best fit (red), and values half the best fit (blue).

To address this discrepancy, an alternative method was used to determine IX parameters for the regeneration cycle. A genetic algorithm with 15 model creatures and 100 offspring was used to fit nitrate breakthrough data in 2-Cycle Exp. 1. Treatment cycle (low ionic strength) parameters were fixed at those determined earlier, but regeneration cycle parameters were allowed to float during the fit. The first four nitrate points (versus the last four above from a different experiment) were weighted double to emphasize accuracy to breakthrough at 44 mg/L nitrate. The Best Creature non-weighted parameters for resin regeneration were: Resin

Capacity=1,096 meq/L, rK_C^N =12.0 ± 5.8, rK_C^S =0.15 ± 0.09, and rK_C^H =0.002 ± 0.001. These values are listed in Table 2.3. Using the new set of best fit parameters, the model was validated against results from 2-Cycle Exp. 2 – 6, which tested two different brine compositions (Figure 2).

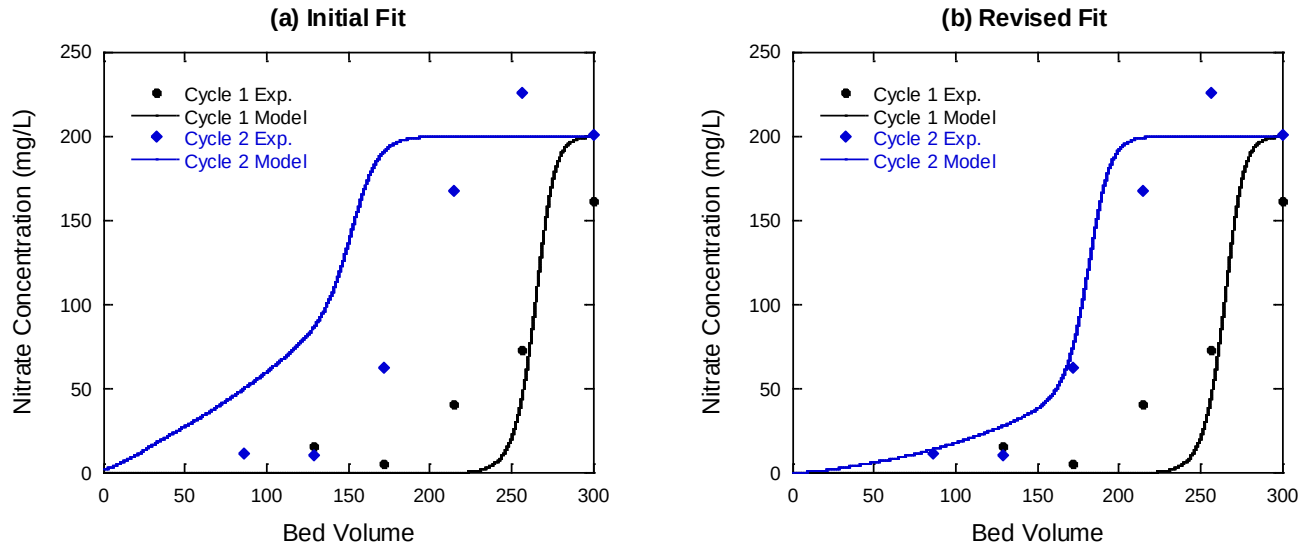

Figure A.6: Nitrate breakthrough curves during 2-Cycle Exp. 1 and (a) model predictions using the initial best-fit regeneration parameters listed in Table S.2, and (b) the revised best fit model parameters listed in Table 3.

A.6 IX Model Application

Table A.3: Multi-cycle model simulations used to evaluate the impacts of the waste brine volume used for regeneration and adding makeup NaCl to treated waste brine prior to reuse.

BV of Brine for each Regen Cycle	# Feed Cycles	Initial Resin Composition	Initial Brine Composition	Make-up NaCl in Brine ReUse?	Nitrate Left in Brine after Treatment
2 BV	10	100% Cl^-	10 wt% NaCl	No	1,500 mg/L
5 BV	10	100% Cl^-	10 wt% NaCl	No	1,500 mg/L
10 BV	10	100% Cl^-	10 wt% NaCl	No	1,500 mg/L
2 BV	10	100% Cl^-	10 wt% NaCl	Yes	1,500 mg/L
5 BV	10	100% Cl^-	10 wt% NaCl	Yes	1,500 mg/L
10 BV	10	100% Cl^-	10 wt% NaCl	Yes	1,500 mg/L

*All feed composition was: 70 mg/L Cl^-, 80 mg/L NO_3^-, 131 mg/L HCO_3^-, 48 mg/L SO_4^{2-}

**Model Parameters were those listed in Table 3